

Oligomer-Polymer Gel Spinning of High Performance Fibers

A Dissertation presented to

The Academic Faculty

By

Xudong Fang

In Partial Fulfillment of the
Requirements for the Degree of
PhD in the
School of Materials Science and Engineering
Georgia Institute of Technology

August, 2016

Copyright © 2016 by Xudong Fang

Oligomer-Polymer Gel Spinning of High Performance Fibers

Approved by:

Dr. Donggang Yao, Advisor
School of Materials Science and
Engineering

Georgia Institute of Technology

Dr. Meisha L. Shofner
School of Materials Science and
Engineering

Georgia Institute of Technology

Dr. Youjiang Wang
School of Materials Science and
Engineering

Georgia Institute of Technology

Dr. Karl I. Jacob
School of Materials Science and
Engineering

Georgia Institute of Technology

Dr. Yulin Deng
School of Chemical and Biomolecular
Engineering

Georgia Institute of Technology

Date Approved: 04/29/2016

To my five years' experience at Georgia Tech

Life is short. I need to hurry to pursue my dream.

Acknowledgments

I want to express my gratitude to my academic committee members, my family, my lab-mates, and friends for their continuous support. Without their persistent and sincere assistance in the past five years, I would not have been able to finish my doctoral work and make this accomplishment possible.

Firstly, I really need to express my appreciation to my Ph.D. Advisor, Prof. Yao. Without his patient direction, I cannot have the opportunity to continue my thesis work. In the first two years, most of my time was spent on coursework as I had no background relating to polymers. He spent huge amounts of time teaching me the knowledge and skills necessary for polymer processing. Besides technical knowledge, he also shared plenty of his life philosophy with me. What impresses me most is that “Make progress slowly every day, you will succeed one day”. I believe in this and have been practicing.

I also want to thank Prof. Shofner, Prof. Wang, Prof. Jacob, and Prof. Deng for their guidance in my research and kindness in sharing their research facilities. With their constructive suggestions, the quality and impact of this dissertation are significantly improved. I am also very grateful to Georgia Tech and the School of Materials Science and Engineering for their financial support and such an excellent Ph.D. program.

I owe favors to my previous and current lab-mates, including Tom Wyatt, Yifeng Hong, Sarang Deodhar, Ian Winter, Jing Shi and Adam Maffe for their support in my

research and life. Special thanks should be given to Tom. Without his assistance, I was not able to start my research work so quickly. He is a person with high ethical standards, whom I respect and learn from.

In the past five years staying at Georgia Tech, I also want to express my gratitude to all of my friends. They offered generous help and spiritual support when I was suffering. Among them, Mr. Liyi Li, Mr. Clive Liu, Dr. An-ting Chien and Dr. Jikun Wu should receive my special thanks. They provided great help and suggestions in my research work.

Lastly but most importantly, I should give credits to my family members, especially my wife and my son. They provide me the motivation and driving force to survive from the hard times and continue to the next target.

Table of Contents

Acknowledgments.....	iv
List of Tables	x
List of Figures	xi
List of Symbols	xvi
Summary	xvii
1. Introduction.....	1
1.1 High Performance Polymer Fibers.....	1
1.2 Fiber Spinning.....	4
1.3 Gel Spinning of UHMWPE Fibers	7
1.4 Oligomer-Polymer Spinning System	9
1.5 Challenges and Motivations.....	10
1.6 References.....	13
2. Gel Spinning of UHMWPE Fibers with Polybutene as a New Spin Solvent	
18	
2.1 Introduction	19
2.2 Experimental	22
2.2.1 Materials	22
2.2.2 Gel Spinning	23
2.2.3 Solvent Extraction.....	23

2.2.4 Hot Drawing.....	24
2.2.5 Characterization	25
2.3 Results and Discussions	26
2.3.1 PE/PB Gelation Properties	26
2.3.2 Extrusion of as-spun Fiber	31
2.3.3 Solvent Extraction	34
2.3.4 Hot Drawing.....	41
2.4 Phase Diagram of the “Oligomer-Polymer” Blend System	46
2.5 Recommendations and Outlook	53
2.6 Conclusions	53
2.7 References	55
3 Twist-Film Gel Spinning of Large-Size and High Performance UHMWPE	
Monofilaments	58
3.1 Introduction	59
3.2 Experimental	62
3.2.1 Mixing of the Blend	62
3.2.2 Gel Spinning of the Film.....	63
3.2.3 Twisting and Extraction of the Gel Film.....	64
3.2.4 Hot Drawing.....	65
3.2.5 Characterization	65

3.3	Results and Discussion.....	67
3.3.1	Extrusion of Film from a Slot Die.....	67
3.3.2	Effect of Mechanical Twisting on Solvent Removal	70
3.3.3	Effect of Twisting on Fiber Properties	73
3.3.4	Fiber Morphology and Strucutre	80
3.4	Conclusions	88
3.5	References	90
4	Gel Spinning of High Strength Polyoxymethylene Fibers	96
4.1	Introduction	97
4.2	Experimental	100
4.2.1	Materials.....	100
4.2.2	Gel Spinning.....	101
4.2.3	Spin Solvent Extraction.....	102
4.2.4	Hot-drawing	102
4.2.5	Characterization	103
4.3	Results and Discussion.....	104
4.3.1	Selection of Solvent for Gel Spinning	104
4.3.2	POM/Caprolactam Blend Properties	107
4.3.3	Gel Spinning of POM Fiber	111
4.3.4	Spin-Solvent Extraction	113

4.3.5 Hot Drawing.....	115
4.4 Recommendations and Outlook	124
4.5 Conclusion.....	125
4.6 References.....	126
5 Conclusions, Recommendations and Outlook.....	132
5.1 Conclusions.....	132
5.2. Recommendations.....	134
5.3 Outlook	136

List of Tables

Table 1.1 Properties of typical high performance polymer fibers.....	3
Table 1.2 Fiber prices (values given are typical starting prices for coarse yarns or rovings; finer deniers and special grades will be more expensive).....	4
Table 2.1. Weight of the gels of UHMWPE with solvents.....	28
Table 2.2. Orientation factors of gel spun UHMWPE fibers.....	39
Table 3.1. Orientation factors of UHMWPE filaments at different drawing stages...	85
Table 4.1. Orientation factors of POM fibers.....	121

List of Figures

Figure 1.1. Strength and modulus of high performance polymer fibers.....	2
Figure 1.2. Comparison of gel spinning with melt spinning.....	6
Figure 1.3. Specific strength vs specific modulus of various fibers.....	8
Figure 2.1. Process schematic for gel spinning of PE fibers: (A) gel spinning; (B) solvent extraction; (C) hot drawing.....	24
Figure 2.2. DSC of (A) neat PE powder and 2% PE/PB blend and (B) gel-spun PE fibers at various stages of processing. The DSC scans were conducted at 10°C/min heating rate in nitrogen atmosphere.....	30
Figure 2.3. Parallel plate rheometry: cooling from 150°C at 2°C/min to transition temperature.....	31
Figure 2.4. Linear viscoelastic behavior of the 2% PE/PB solution by frequency sweep at 150°C with a parallel plate rheometer.....	33
Figure 2.5. Rheological properties of the 2% PE/PB solution at 150°C obtained by capillary rheometry.....	34
Figure 2.6. Spin-solvent extraction comparison in n-hexane.....	36
Figure 2.7. TGA weight loss curves as a function of time. Fibers were heated to 350°C in nitrogen atmosphere for 50 min to evaporate PB. Neat PE and PB are included for reference.....	37
Figure 2.8. SEM images of gel-spun UHMWPE fibers: (A) precursor fiber; B) magnified surface morphology of the precursor fiber.....	39

Figure 2.9. WAXD patterns of gel-spun UHMWPE fibers at various draw ratios: (A) undrawn precursor fiber; (B) 30× drawn fiber at first stage; (C) 40× drawn fiber at first stage; (D) 120× total draw ratio fiber with 40× at first stage.....	40
Figure 2.10. SEM images of first-stage hot-drawn fibers: (A) 30× drawn; B) 40× drawn.....	42
Figure 2.11. Azimuthal integrations of the [110] and [200] diffractions of the gel spun UHMWPE fibers at various draw ratios.....	44
Figure 2.12. SEM images of the total 120× drawn fibers: (A) 30× drawn at the first stage; (B) 40× drawn at the first stage.....	45
Figure 2.13. Representative tensile stress-strain curves of UHMWPE fibers at maximum draw ratio and processed with different drawing conditions at the first stage: (A) total draw ratio 120× with the first-stage draw ratio of 30×; (B) total draw ratio of 120× with the first-stage draw ratio of 40×.....	45
Figure 2.14. The effect of k on dimensionless curves: (A) spinodal curve; (B) binodal curve.....	50
Figure 2.15. The effect of k on dimensionless phase diagrams.....	51
Figure 2.16. Variation of the dimensionless critical point when k is reduced from 1 to 0.01.....	52
Figure 2.17. Simulated spinodal curves of PE/PB solution and PE/paraffin oil solution.....	52
Figure 3.1. Schematic of twist-film gel spinning process.....	64

Figure 3.2. Frequency sweep of PEPB solutions with concentration of 2% and 4%.....	69
Figure 3.3. Gelation temperature of PEPB solutions with concentration of 2% and 4%.....	69
Figure 3.4. Weight percentage remaining as a function of the amount of twist applied.....	72
Figure 3.5. TGA weight loss curves as a function of time. Films heated to 300°C in nitrogen atmosphere for 240 min to fully remove polybutene. Neat polybutene is used as a reference.....	73
Figure 3.6. DSC endothermal melting peaks of UHMWPE/PB gel, extruded film and twisted-films with different TPMs.....	76
Figure 3.7. The effect of twisting on final fiber diameter and total draw ratio.....	78
Figure 3.8. The effect of twisting on final fiber tensile strength and Young's Modulus.....	79
Figure 3.9. Representative tensile strength vs tensile strain curves for large-size UHMWPE fibers obtained with three stages of hot drawing.....	79
Figure 3.10. Optical images of UHMWPE fibers obtained by twist-gel spinning process: (A) precursor; (B) 1 st stage with draw ratio $\times 7$; (C) 2 nd stage with draw ratio $\times 35$; (D) 3 rd stage with draw ratio $\times 94.5$	81

Figure 3.11. WAXD 2D patterns of UHMWPE filaments at different drawing stages: (A) twisted film precursor; (B) 1 st stage drawing 7×; (C) 2 nd stage drawing 35×; (D) 3 rd stage drawing 94.5×.....	83
Figure 3.12. Azimuthal integrations of UHMWPE filaments at different drawing stages: (A) [110] direction; (B) [200] direction.....	84
Figure 3.13. Wide-angle X-ray diffractograms of large-size UHMWPE monofilaments obtained by twist-film gel spinning process.....	85
Figure 3.14. Raman spectra of UHMWPE monofilaments at various drawing stages.....	88
Figure 4.1. DSC heating endotherms of (A) neat POM pellets and 20% POM/caprolactam blend and (B) gel-spun POM fiber at various stages of drawing. The DSC scans were conducted at 10 °C/min in nitrogen atmosphere.....	108
Figure 4.2. Temperature sweep of the POM/caprolactam blend cooling from 170°C by parallel plate rheometry.....	110
Figure 4.3. Viscoelastic properties of the 20% POM/caprolactam blend at 170°C: (A) linear viscoelastic region determination with strain sweep; (B) frequency sweep with strain of 2.5%.....	111
Figure 4.4. TGA curves of POM/caprolactam gel-fiber before and after extraction. TGA of pure caprolactam and neat POM pellets were included for reference. The samples were heated in nitrogen atmosphere to 400°C with rate of 20°C/min.....	114

Figure 4.5. SEM images of gel-spun POM fibers at various stages: (A) precursor after fully extraction; (B) 12.5× drawn first stage fiber; (C) 25× drawn second stage fiber; (D) ~40× drawn third stage fiber.....	115
Figure 4.6. WAXD patterns of gel-spun POM fiber at various drawing stages: (A) precursor after solvent extraction; (B) 12.5× drawn first stage fiber; (C) 25× drawn second stage fiber; (D) ~40× drawn third stage fiber.....	118
Figure 4.7. WAXD curves of gel-spun POM fibers at various stages.....	119
Figure 4.8. Relative intensity of the 100 as a function of the azimuthal diffraction angle for gel-spun POM fibers at various stages.....	121
Figure 4.9. Representative stress-strain curves of gel-spun POM fibers with total draw ratio of 40.....	122
Figure 4.10. Raman spectroscopy of the gel-spun POM fibers at various drawing stages.....	123

List of Symbols

ΔG_m	Gibbs free energy of mixing
R	Universal gas constant
T	Temperature
χ	Interaction parameter
ϕ_A	Volume fraction of oligomer
ϕ_B	Volume fraction of polymer
n_A	Degree of polymerization of oligomer
n_B	Degree of polymerization of polymer
k	$\left(\frac{n_A}{n_B} \right)^{\frac{1}{2}}$
ϕ_B^c	Volume fraction of polymer at the critical point
χ^c	Interaction parameter at the critical point
X	Dimensionless interaction parameter
Y	Dimensionless volume fraction of the polymer

Summary

High performance polymer fibers are playing an important role in various applications because of their outstanding properties such as ultra-high specific strength and modulus. However, high manufacturing cost and low production rate limit the production and market of such fibers. A major reason is the slow and expensive processes utilized. Gel spinning is one dominating process for producing high performance fibers by orientating disentangled molecular chains, which are maintained in the gel-like network during drawing. It has been successfully used for several polymers including polyethylene (PE), polypropylene (PP), polyvinyl alcohol (PVA), and polyacrylonitrile (PAN). However, the consumption of large amounts of solvent in gel spinning hinders the development of this process and results in high cost of the fibers. The major drawback of the gel spinning process is the solvent extraction stage. In this stage, the spin-solvent is extracted from the gel-fiber with a second solvent. As solvent extraction relies on diffusion, which is determined by concentration gradient and chemical interactions, it is a time-consuming process and the extraction solvent needs to be refreshed frequently to maintain a high diffusion rate.

The major task of this work is to reduce consumption of extraction solvents and improve the extraction efficiency in the gel spinning process. UHMWPE fiber, which shows the highest specific tensile strength among polymer fibers, is used as a case for investigation. By adopting an ‘oligomer-polymer’ blend system, a new spin solvent – polybutene – was discovered for gel spinning of UHMWPE. It is demonstrated that less extraction solvent is consumed compared to using paraffin oil, the most widely used spin

solvent for PE. The improvement results from stronger phase separation behavior of the PE/polybutene gel at ambient temperature. Meanwhile, experimental results show that the extraction speed of polybutene is considerably higher than paraffin oil, as polybutene is energetically less miscible with PE.

To further reduce consumption of extraction solvents, a mechanical twisting method was developed. It is found that a majority of the spin-solvent in the gel-fiber can be removed by applying twist to the fiber. Results showed that about 70% of the spin solvent can be removed by applying appropriate twists, while mechanical properties of the fiber can be maintained. Based on this innovation, a twist-film gel spinning process was developed to produce large-size and high strength UHMWPE filaments. Fibers with diameter of 80 μm and strength of 3.2 GPa are produced, which can be used as fish line or dental floss. For comparison, few conventional processes can produce such large-diameter high-strength fibers.

After the extraction issues were addressed with a new solvent and a new solvent-removal method, a second task of this work is to explore new high performance polymer fibers that can be produced by gel spinning. Polyoxymethylene (POM) is an important engineering thermoplastic with exceptional properties. It has wide applications and is commonly processed by injection molding and extrusion. However, the progress in development of strong POM fibers is rather slow although research has been conducted for decades. A major reason is that POM is insoluble in most solvents at room temperature and may decompose when temperature is above the melting point. Thus, it is difficult to obtain strong fibers with melt spinning or solution spinning. One contribution of this work is the development of a gel spinning process for POM. Caprolactam is

selected as the spin-solvent based on the ‘oligomer-polymer’ blend system and thermal stability of POM. The POM/caprolactam blend is a uniform solution at elevated temperature while forming a gel when quenched. Noticeable features of the obtained POM fibers are tensile strength of 2GPa and Young’s modulus of 40 GPa.

To summarize, the contribution of this thesis work includes optimization of the gel spinning process and extension of this process to produce new high performance polymer fibers. With discovery of a new spin-solvent and a new solvent-removal method, several issues of the current gel spinning process for UHMWPE are addressed by significantly reducing consumption of extraction solvents and improving the extraction efficiency. A concept of ‘oligomer-polymer’ blend system plays a key role in this process. The feature of this blend system is that it forms a homogeneous solution at elevated temperature while producing a gel with strong phase separation when quenched. Under guidance of this concept, POM fibers were successfully gel-spun to achieve high mechanical properties.

1. Introduction

1.1 High Performance Polymer Fibers

The precise definition of high performance polymer fibers is still controversial. High performance functionalities may include high strength, high stiffness, high damage tolerance, excellent durability, high dimensional stability and high flame resistance [1]. Among these properties, high strength and high modulus are critical for polymer fibers. Therefore, this work mainly focuses on fibers with high strength and modulus. In fact, consistent efforts have been made to improve the fiber strength since the beginning of the twentieth century to meet increasing requirements of engineering applications. Especially in the last quarter of the twentieth century, high performance fibers have experienced a stepped increase in strength and modulus, which can be used in various applications, as seen in Figure 1.1. One representative of them is ultra-high molecular weight polyethylene (UHMWPE) [1, 2]. Several other types of high performance polymer fibers were also developed and commercialized as shown in Table 1.1 [3]. With the introduction of such fibers, new applications have been or are being developed, particularly for various armor products and high-performance ropes.

To meet the requirements in the aforementioned applications, high performance fibers must have a sufficient number of chemical and physical bonds to transfer stress along the fiber and limit its deformation. The two main types of physical bonds are hydrogen bonds and van der Waals forces [4]. Compared to hydrogen bonds, van der

Waals forces are extremely weak. Both types of physical bonds have important effects on fiber spinning process and properties of the fiber. Spinning techniques must be developed based on the properties of the polymer, especially the physical bonds between the chains. The intermolecular and intramolecular interactions and the molecular structure of the polymer significantly affect the mechanical properties of fibers. For example, the high drawability of UHMWPE fibers depends to a large extent on the ability of the polyethylene molecules to slip past each other. This is possible because the only acting intermolecular force is the van der Waals force [5]. However, because of the weak chain-to-chain van der Waals force, polyethylene fibers undergo creep especially at high temperature [6]. Thus, full consideration needs to be given during fiber spinning and the application of fibers based on the property of the polymer.

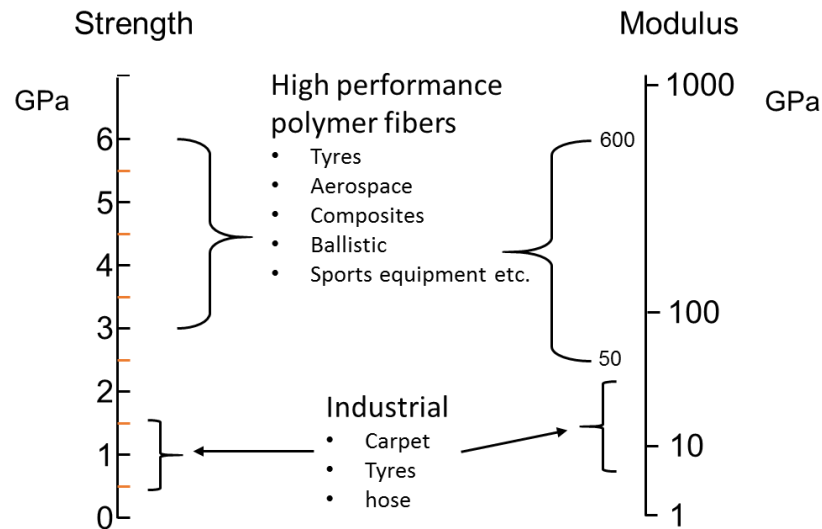


Figure 1.1. Strength and modulus of high performance polymer fibers [1, 7, 8].

Although several types of high performance fibers have been successfully developed, the production and market for them are limited due to high cost. They are

produced in relatively small quantities by several specialized companies. Niche markets willing to pay a high price for the superior properties must also be identified. Table 1.2 shows a general indication of the relative prices of several representative high strength fibers. One major reason for high pricing is the low productivity and cost-effectiveness of the spinning techniques currently used. High performance polymer fibers are usually obtained by solution spinning or gel spinning instead of melt spinning. Both processes are much slower and cost considerably more than melt spinning. Additional processing steps, such as heat treatment under tension, are frequently necessary to produce higher modulus fibers [9]. Therefore, to reduce the cost of the fibers, the spinning processes need to be optimized based on further fundamental understanding of the mechanism.

Table 1.1 Properties of typical high performance polymer fibers [1, 3, 7, 8, 10]

Polymer	Strength		Modulus	
	Commercialized	Lab achieved	Commercialized	Lab achieved
	value	value	value	value
	g/d	g/d	g/d	g/d
UHMWPE	30-40	72	1000-2000	2697
Polyamide-6	9.5	9.8	50	187
PPTA	18-28		400-1100	
POM	11.7		310	~400
PVA	11-17	44	230-387	1040
PAN	5-14	23	85	268

Table 1.2 Fiber prices (values given are typical starting prices for coarse yarns or rovings; finer deniers and special grades will be more expensive) [1]

High performance polymer fibers	US\$/kg
UHMWPE	25-40
Para-aramid	30-300
Meta-aramid	28-50
Zylon (PBO)	150-200

1.2 Fiber Spinning

To produce the high performance polymer fibers described in section 1.1, several types of spinning techniques have been developed in the past decades, including melt-spinning and solution-spinning. One special sub-type of solution spinning is gel spinning. Gel spinning is significant primarily because of thermo-reversible gels that can be formed [11]. With crystalline junctions supporting the network of polymer molecules, a lower

concentration of solution can be used for obtaining higher strength fibers. Among these spinning techniques, melt spinning is the most successful for commercialization because of low cost and high speed. However, the strength obtained from melt spinning is moderate due to entanglements between polymer chains [10]. Thus, to produce ultra-high strength fibers, an alternative way is to dissolve the polymer into a solvent to disentangle the molecular chains before spinning [12]. With a solution formed, ultra-high strength fibers can be obtained by solution spinning or gel spinning [13]. The comparison of gel spinning with melt spinning is shown in Figure 2. In the gel spinning process, solidified fibers can be collected due to formation of gels after the solution is extruded. Compared to melt spinning, lower jet stretch is applied in the extrusion stage [2, 14]. The precursors obtained by fully removing the spin solvent is hot drawn to a high ratio to extend the chains. With highly orientated chains, the fiber shows high strength and high crystallinity [15-17]. For polymers that cannot be melt spun, solution spinning is a possible way to obtain fibers.

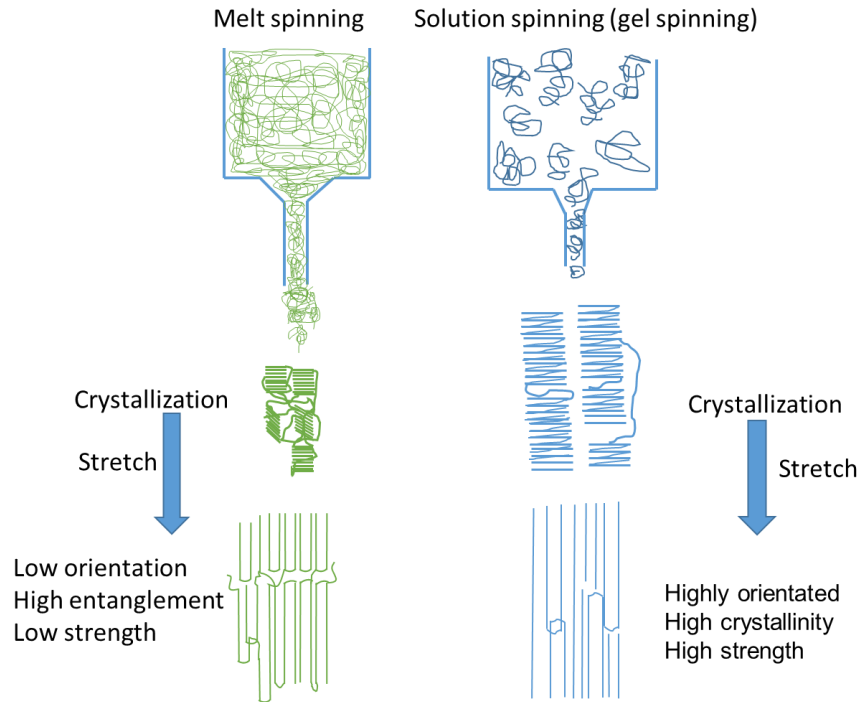


Figure 1.2. Comparison of gel spinning with melt spinning

Even though high performance fibers can be obtained, solution spinning and the sub-type gel spinning process have limitations for commercialization. One common problem arises from huge amounts of solvents consumed, which hinders wide applications of such processes in industry. In the solution formation stage, considerable solvents (spin solvents) are used to form a solution with the polymer. For solution spinning, the concentration of solution is usually 20-30% [3, 9, 12, 13, 18], whereas for gel spinning the concentration is usually in the range of 5-10% [19, 20]. A second type of solvent is also needed for extraction after the solution is extruded from the spinneret. This solvent is used for fully removing the spin solvent to obtain precursor fibers [21, 22]. The extraction process is usually slow and extensive solvents are used. Due to the large quantity of solvents consumed in the process and relatively low speed of spinning, the fibers produced are quite expensive and are only available in comparatively small quantities [1, 23]. More

work needs to be done for wide application of the processes in producing high performance fibers. In this section, the pros and limitations of the current spinning processes are compared. One or more types of the processes can be used according to the properties of the polymer and the required fiber performance.

1.3 Gel Spinning of UHMWPE Fibers

As introduced in section 1.2, gel spinning is a method used to produce high strength fibers by utilizing an intermediate gel-like state. It became well-known in the fiber industry due to the success of the UHMWPE fiber development. This process has been studied by researchers from various countries since the 1970s [3]. Stages in the process include preparation of spin dope, fiber spinning, gelation, solvent extraction and hot drawing. To obtain high strength UHMWPE fiber, various solvents have been used for the spin dope such as tetralin, decalin, naphthalene and paraffin oil [12, 24, 25]. After a homogenous spin dope is obtained, the solution can be spun from an extruder. In this stage, one major technical challenge is to adjust the spinning speed to remove defects. The extruded solution is substantially cooled by a gas or a liquid medium, and crystallization occurs. During the crystallization process, the solution is solidified into a rigid gel structure with dispersed crystallites connected by a small amount of entanglements. The spin solvent contained in the gel fiber needs to be extracted before drawing. As shown in the literature, the drawability of the fiber is poor without extraction of the spin solvent [12, 18, 26]. The drawability in the last stage determines the final properties of the fiber. For UHMWPE, the most effective method of hot drawing is two-stage drawing [27]. The first stage is done at a relatively low temperature around 100°C to orientate most of the amorphous fibers [13,

28, 29]. Then the fibers are drawn at a higher temperature during a second stage drawing to increase their crystallinity and strength.

Gel-spun UHMWPE fibers exhibit ultra-high strength, high modulus, and good chemical and wear resistance. Owing to low density and good mechanical properties, these fibers are highly desirable for use in applications such as cut-proof protective gear and marine ropes [30, 31]. Figure 1.3 shows specific strength versus specific modulus and illustrates why UHMWPE fibers have authentic high performance [32]. The UHMWPE used has extremely long chains with molecular weight usually over one million. The chains can transfer load effectively to the polymer backbone by strengthening intermolecular interactions, resulting in a tough material with high strength.

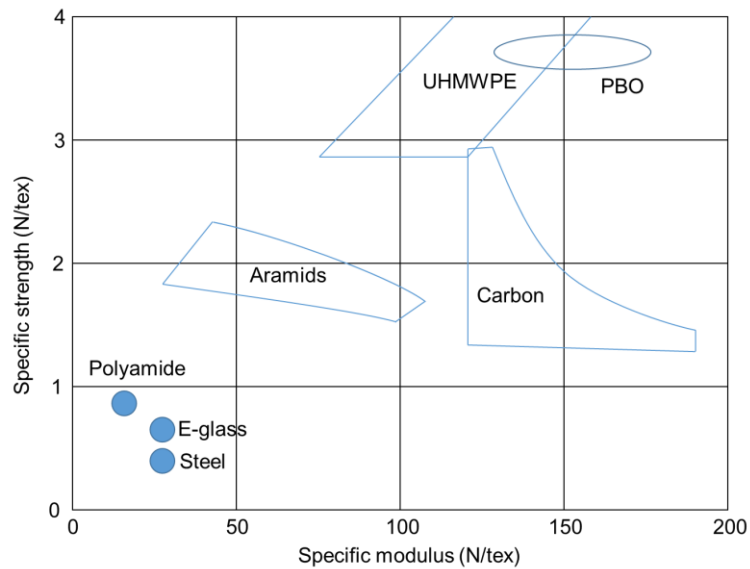


Figure 1.3. specific strength vs specific modulus of various fibers [33]

Gel-spinning of UHMPWPE high strength fibers has been quite successful but there is still large space for improvement. The fibers are mainly produced by three companies with the following trade names: Dyneema by DSM High Performance Fibers

in the Netherlands and the joint venture DSM/Toyobo in Japan, and Spectra by Honeywell in the USA [34]. Since the start of commercial production, performance of the fibers has been improved considerably. The gel-spun fibers are characterized by a high degree of chain extension, an orientation factor larger than 0.95 and a high level of crystallinity (up to 0.85) [35]. However, due to consumption of large quantities of solvents, the gel spinning process still needs to be optimized to reduce fiber cost.

1.4 Oligomer-Polymer Spinning System

With progress of research on the gel spinning process, more work has been performed on preparation of spin dope, focusing primarily on solvents used for dissolving polymers. A new concept of oligomer-polymer spinning has been introduced [36]. An optimal blend for gel spinning is obtained when the oligomer and the polymer have identical or similar repeat units. It has been demonstrated that the gel spinning process of UHMWPE fibers benefits from this concept. Meanwhile, the strongest poly(ethylene oxide) (PEO) fiber was obtained through the application of this concept by using polyethylene glycol (PEG) as the spin solvent for gel spinning [24]. This oligomer-polymer spinning system is quite useful and may help develop more high performance fibers with the gel spinning process.

The oligomer-polymer spinning system is beneficial for preserving disentanglements of polymer chains during gel spinning. The system exhibits solution-like behavior at elevated temperature and displays a distinct gelation behavior when quenched to low temperature. The solution is quenched so that favorable disentangled morphology can be preserved. This is critical to successfully drawing the fibers to a large ratio in the

solid state. The disentangled morphology in the semi-dilute solution is preserved by partial crystallization of the solute when the solution is extruded to form a solid-like gel. The morphology can be maintained even when the spin solvent is completely removed as long as the fiber is not heated to the melting temperature. Because of the preserved morphology, the fiber can be effectively orientated in solid state. Furthermore, the orientation can be maintained as relaxation time of molecules is long in the solid-like gel network.

Mechanism of the oligomer-polymer system and benefits to the gel spinning process need to be further investigated. The fundamental mechanism of this system is still obscure and poorly understood [37]. Feasibility tests were completed for only several cases. More work must be completed to better understand the underlying mechanism and benefits gained in solvent extraction and hot drawing stages.

The concept of oligomer-polymer spinning system can be applied to gel spinning of other high performance polymer fibers. Success of a system containing identical repeat units has been demonstrated using paraffin oil with UHMWPE and PEG with PEO. In fact, it may also be effective for systems with similar repeat units, especially when the oligomer with exact repeat unit matching the polymer is not easily obtained. If a system with similar repeat unit works, more high performance polymer fibers can be obtained with the gel spinning process. One task in this work is related to studying the system and extending its application in gel spinning of other polymer fibers.

1.5 Challenges and Motivations

Gel spinning of UHMWPE fibers has been developed for decades, but more work still needs to be done. The consumption of large amounts of solvents is still a huge problem

limiting growth of this application in industry. To produce high strength fibers, the concentration of spin dope is usually lower than 10%. Additionally, a large quantity of a second-type solvent is consumed to completely remove the spin solvent before hot drawing the fiber [38, 39]. Actions need to be taken to reduce the consumption of solvents and improve the process efficiency.

The extraction process in gel spinning of UHMWPE fiber needs to be optimized. Besides consumption of huge amounts of solvents in the extraction process, efficiency also needs to be improved. Currently most of the extraction process is completed by soaking the gel fiber in a solvent, like hexane, for a certain amount of time. The extraction time needs to be shortened for improved efficiency. Besides reducing soaking time, it will be beneficial to explore new and efficient extraction methods.

The application of gel spinning in producing high performance polymer fibers needs to be extended. According to the literature, this process is only suitable for several types of flexible polymers, including polyethylene (PE), polypropylene (PP), polyvinylalcohol (PVA), polyacrylonitrile (PAN), and poly(ethylene oxide) (PEO) [40]. This process must be further developed in order to be considered as an effective method of disentangling molecular chains, deriving inspiration from the new concept of “oligomer-polymer spinning”.

To address the above issues, in this thesis work, a new spin solvent polybutene was proposed to improve extraction efficiency and reduce the cost for gel spinning of UHMWPE fiber. This solvent was discovered based on the concept of oligomer-polymer spinning. It has been validated that polybutene forms a gel with UHMWPE, which can be used for spinning high strength fibers. Furthermore, it was demonstrated that the gel formed

with polybutene showed stronger phase separation behavior when quenched in air than that formed with paraffin oil. Extraction solvents can be saved by using polybutene as the spin solvent. More work was completed to test and compare the extraction efficiency of the two types of fibers with hexane. Considering the feasibility tests data, it is highly possible that polybutene can be applied as a spin solvent for large scale production of high strength UHMWPE fibers.

Based on the comparison of extraction efficiency of paraffin oil and polybutene, the phase diagram of “oligomer-polymer” was investigated. A critical parameter in the “oligomer-polymer” blend is the ratio of repeat units between the oligomer and the polymer. Dimensionless numbers were defined for volume fraction of the polymer and the interaction parameter based on the ratio of repeat units. With such parameters defined, governing equations were obtained for the spinodal curve and the binodal curve. The effect of the ratio of repeat units on geometry of the two curves was numerically studied. The numerical results for phase separation of PE with polybutene and paraffin oil were consistent with the experimental results, which demonstrated polybutene is more effective for gel spinning of UHMWPE fibers.

Besides development of the gel spinning process with a new spin solvent, a new extraction process was proposed and a feasibility study was completed. Compared to the conventional way of extracting with solvents, the new process uses mechanical force to remove the spin solvents. With this extraction process, a new twist-film gel spinning process for large diameter PE monofilaments was developed.

Another area of work in this dissertation research was the extension of gel spinning to polyoxymethylene (POM) fibers. A feasibility study has been completed, and high

strength POM fiber was obtained. The resulting process is environmentally friendly without using toxic solvents. The extraction process is also cost-effective by using green extraction solvent. Three stages of hot drawing were applied to the precursor fiber with a total draw ratio of 40. The resulting final fiber shows tensile strength of 2 GPa and Young's modulus of 40 GPa.

1.6 References

1. Hearle, J.W., *High-performance fibres*. 2001: Elsevier.
2. *HIGH-STRENGTH POLYETHYLENE FIBERS DEVELOPED*. Chemical & Engineering News, 1984. **62**(8): p. 37-37.
3. Barham, I.P. and A. Keller, *High-strength polyethylene fibres from solution and gel spinning*. Journal of materials science, 1985. **20**(7): p. 2281-2302.
4. Cayrol, B. and Peterman, J., *ELASTIC HARD POLYETHYLENE FIBERS*. Journal of Polymer Science Part B-Polymer Physics, 1974. **12**(10): p. 2169-2172.
5. Sikkema, D.J., M.G. Northolt, and B. Pourdeyhimi, *Assessment of new high-performance fibers for advanced applications*. MRS bulletin, 2003. **28**(08): p. 579-584.
6. Lai, J. and A. Bakker, *Analysis of the non-linear creep of high-density polyethylene*. Polymer, 1995. **36**(1): p. 93-99.

7. Afshari, M., R. Kotek, and P. Chen, *High performance fibers*. High Performance Polymers and Engineering Plastics, 2011: p. 269-340.
8. Mera, H. and T. Takata, *High - Performance Fibers*. Ullmann's Encyclopedia of Industrial Chemistry, 1989.
9. Zwick, M.M., *Spinning of Fibers from Polymer Solutions Undergoing Phase Separation. I. Practical Considerations and Experimental Study*. Fiber spinning and drawing, 1967(6): p. 109.
10. Takajima, T., *Advanced fiber spinning technology*. 1994: Woodhead Publishing.
11. Fukae, R., A. Maekawa, and O. Sangen, *Gel-spinning and drawing of gelatin*. Polymer, 2005. **46**(25): p. 11193-11194.
12. Smith, P. and P.J. Lemstra, *Ultrahigh - strength polyethylene filaments by solution spinning/drawing, 2. Influence of solvent on the drawability*. Die Makromolekulare Chemie, 1979. **180**(12): p. 2983-2986.
13. Smith, P. and P.J. Lemstra, *Ultra-high-strength polyethylene filaments by solution spinning/drawing*. Journal of Materials Science, 1980. **15**(2): p. 505-514.
14. Abbott, L.E. and J.L. White, *Melt spinning of low-density and high-density polyethylene fibers - development of orientation and crystallinity and mechanical properties of spun fiber*. Abstracts of Papers of the American Chemical Society, 1972. **164**(AUG-S): p. 41.
15. Hoogsteen, W., et al., *Gel-spun polyethylene fibres*. Journal of materials science, 1988. **23**(10): p. 3459-3466.
16. Ward, I.M., *Developments in Oriented Polymers—2*. 2012: Springer Science & Business Media.

17. De Vries, A., C. Bonnebat, and J. Beautemps. *Uni - and biaxial orientation of polymer films and sheets*. in *Journal of polymer science: Polymer symposia*. 1977. Wiley Online Library.
18. Smith, P., et al., *Ultrahigh-strength polyethylene filaments by solution spinning and hot drawing*. Polymer Bulletin, 1979. **1**(11): p. 733-736.
19. Yasuda, H., K. Ban, and Y. Ohta, *Gel spinning processes*. Advanced Fiber Spinning Technology, 1994: p. 172.
20. Yufeng, Z., et al., *Study on gel - spinning process of ultra - high molecular weight polyethylene*. Journal of applied polymer science, 1999. **74**(3): p. 670-675.
21. Lemstra, P., et al., *High-strength/high-modulus structures based on flexible macromolecules: Gel-spinning and related processes*, in *Developments in Oriented Polymers—2*. 1987, Springer. p. 39-77.
22. Hoogsteen, W., G. Ten Brinke, and A. Pennings, *The influence of the extraction process and spinning conditions on morphology and ultimate properties of gel-spun polyethylene fibres*. Polymer, 1987. **28**(6): p. 923-928.
23. Salem, D.R., *Structure formation in polymeric fibers*. 2001: Hanser Verlag.
24. Wyatt, T.P., et al., *Development of a gel spinning process for high - strength poly (ethylene oxide) fibers*. Polymer Engineering & Science, 2014. **54**(12): p. 2839-2847.
25. Shi, X., et al., *Gelation/crystallization mechanisms of UHMWPE solutions and structures of ultradrawn gel films*. Polymer journal, 2014. **46**(1): p. 21-35.

26. Smook, J., M. Flinterman, and A. Pennings, *Influence of spinning/hot drawing conditions on the tensile strength of porous high molecular weight polyethylene*. Polymer Bulletin, 1980. **2**(11): p. 775-783.
27. Ohta, Y., H. Murase, and T. Hashimoto, *Effects of spinning conditions on the mechanical properties of ultrahigh - molecular - weight polyethylene fibers*. Journal of Polymer Science Part B: Polymer Physics, 2005. **43**(19): p. 2639-2652.
28. Smith, P. and P.J. Lemstra, *Ultra-high strength polyethylene filaments by solution spinning/drawing. 3. Influence of drawing temperature*. Polymer, 1980. **21**(11): p. 1341-1343.
29. Capaccio, G., T. Crompton, and I. Ward, *The drawing behavior of linear polyethylene. I. Rate of drawing as a function of polymer molecular weight and initial thermal treatment*. Journal of Polymer Science: Polymer Physics Edition, 1976. **14**(9): p. 1641-1658.
30. Prevorsek, D.C., Y.D. Kwon, and H.B. Chin, *Analysis of the temperature rise in the projectile and extended chain polyethylene fiber composite armor during ballistic impact and penetration*. Polymer Engineering & Science, 1994. **34**(2): p. 141-152.
31. Lee, B., J. Song, and J. Ward, *Failure of Spectra® polyethylene fiber-reinforced composites under ballistic impact loading*. Journal of Composite Materials, 1994. **28**(13): p. 1202-1226.
32. Qian, D., et al., *Fiber-reinforced polymer composite materials with high specific strength and excellent solid particle erosion resistance*. Wear, 2010. **268**(3): p. 637-642.

33. VAN DINGENEN, J., *Gel-spun high-performance polyethylene fibres*. High-performance fibres, 2001: p. 62.
34. Berger, L., H. Kausch, and C. Plummer, *Structure and deformation mechanisms in UHMWPE-fibres*. Polymer, 2003. **44**(19): p. 5877-5884.
35. Van Dingenen, J., *Gel-spun high-performance polyethylene fibres*. High Performance Fibres, 2001: p. 62-92.
36. Yao, X.F.T.W.Y.H.D., *Gel Spinning of UHMWPE Fibers with Low Molecular Weight Polybutene as a New Spin Solvent*, in *SPE Annual Technical Conference Proceedings*2015: Orlando, FL. p. 2771-2775.
37. Delisi, C., *Statistical thermodynamics of oligomer-polymer interactions*. Biopolymers, 1974. **13**(11): p. 2305-2314.
38. Xiao, C., et al., *Investigation on the thermal behaviors and mechanical properties of ultrahigh molecular weight polyethylene (UHMW - PE) fibers*. Journal of applied polymer science, 1996. **59**(6): p. 931-935.
39. Wyatt, T., Y. Deng, and D. Yao, *Fast solvent removal by mechanical twisting for gel spinning of ultrastrong fibers*. Polymer Engineering & Science, 2015. **55**(4): p. 745-752.
40. Fang, X., et al., *Gel spinning of UHMWPE fibers with polybutene as a new spin solvent*. Polymer Engineering & Science, 2016.

2. Gel Spinning of UHMWPE Fibers with Polybutene as a New Spin Solvent

ABSTRACT

Gel spinning of UHMWPE fibers using a low molecular weight polybutene (PB) as a new spin solvent was investigated. A 98/2 wt% PB/UHMWPE gel exhibits a melting temperature around 115°C and shows large-scale phase separation upon cooling the solution to room temperature. The resulting precursor fiber from this gel was hot-drawn to a ratio of 120 yielding a fiber with tensile strength of 4 GPa and Young's modulus of over 150 GPa. Wide-angle x-ray diffraction indicates good molecular orientation along the fiber axis. The results also demonstrate the potential to further improve the mechanical properties. With respect to the gel spinning industry, this new solvent has a number of advantages over paraffin oil and decahydronaphthalene, and holds a promise of greatly improving the process efficiency.

Keywords: gel spinning, UHMWPE, fiber, polybutene, high strength

2.1 Introduction

High performance polyethylene (PE) fibers continue to replace conventional materials in many military and civilian applications such as composites, ropes, and textiles. The success of these fibers owes largely to their exceptional specific strength and modulus, coupled with excellent chemical resistance and low moisture absorption. Over the years, various processes have been proposed to produce high performance PE fibers [1]. The gel-spinning process, invented in the late 1970s, proves to be the most effective and industrially feasible method. In this process, a gel-fiber is formed from a semi-dilute solution, resulting in a lower density of chain entanglements relative to melt spinning which promotes greater drawability in the hot drawing stages [2]. A PE chain with ultra-high molecular weight (UHMW) is allowed to become highly oriented along the fiber direction to obtain high tensile strength [3]. The UHMWPE fiber is typically processed by dissolution in a large volume of solvent so that the viscosity is low enough to spin fibers [4, 5]. The fiber properties and the corresponding gel properties depend on factors such as the solvents used, the polymer concentration, and the processing temperatures [6]. Various solvents have been attempted to form gels with polyethylene to obtain high strength fibers [5, 7-9]. Dodecane, naphthalene, p-xylene, 1, 2, 4-trichlorobenzene, kerosene and camphene have been used to dissolve UHMWPE [7, 10-16]. These UHMWPE solutions exhibit a thermo-reversible gelation behavior due to crystallization of polyethylene upon cooling; however, fibers obtained by gel spinning with the aforementioned solutions exhibit tensile strength usually less than 3 GPa. Accordingly, such solvents are not preferred for gel spinning of PE fibers by industry. Among the solvents studied for gel-spinning UHMWPE fiber, paraffin oil and decahydronaphthalene

(also known as decalin) are arguably the most successful spin-solvents used in industrial manufacturing. Furthermore, the strongest UHMWPE fibers reported were obtained using one of these solvents; the strength of which is higher than 4 GPa [12, 17-20].

Despite the success with paraffin oil and decalin, both of these solvents have limitations. Paraffin oil, due to its low volatility and low flammability, is commonly used to form strong PE fibers, but the concentration is limited to higher values. When the concentration is too low, the gel-network is too weak to form a coherent fiber during the spinning process. This restricts the production of high strength fibers since lower concentrations have been shown to yield higher tensile strengths from the reduced entanglements in more dilute solutions. A second limitation of the paraffin oil spin-solvent is from process efficiency and cost. Since paraffin oil is non-volatile, it must be extracted from the gel-fiber using a second (volatile) solvent and dried, before hot drawing to a large ratio to obtain high strength fiber. Common extraction solvents for paraffin oil include n-hexane, diethyl ether, n-pentane, methylene chloride, trichlorotrifluoroethane (TCTFE), dioxane and toluene [11]. Typically n-hexane is used as an effective extraction solvent for achieving high strength [4, 6, 18]. Since UHMWPE and paraffin oil have identical chemical repeat units, the interaction between paraffin oil and polyethylene is strong requiring more time to extract paraffin oil from the fiber with n-hexane [9]. The extraction process can take hours or even days depending on the extraction conditions [21]. In a continuous process of fiber production, the extraction solvent should be continuously replaced with fresh extraction solvent to accelerate the process [22]. Under typical conditions, the concentration of UHMWPE solution for gel-spinning is about 5-10 wt%. In such a range of spinning concentration, a large amount of

hexane is consumed for extracting. The concentration limit and the extraction cost can negatively impact the effectiveness and economics of the overall process.

Limitations also exist for decalin as a spin solvent. For decalin, the spin dope concentration can be lower, reaching 2% due to rapid evaporation that occurs immediately upon extrusion [5, 9]. With such a low concentration, super strong UHMWPE fibers can be obtained [18, 20]. Since decalin is volatile at the typical spinning temperatures, a second extraction solvent is not necessary. However, decalin is highly flammable and toxic, leading to a more dangerous and environmentally unfriendly process. Besides, time and efforts have to be spent in optimization of the processing conditions if decalin is used as the solvent. As is reported, high strength fiber is usually obtained at a low spinning speed [18, 23]. However, as decalin is highly evaporative, skin-core inhomogeneous ‘shish-kebab’ structure is formed at low spinning speeds, which will affect the drawability of the final fiber and the strength [24-26]. An intermediate value for spinning speed is consequently needed for obtaining high strength fiber. The environmental concerns and competing effects of spinning speed on fiber strength limit wide application of decalin in gel spinning. Therefore, a need emerges to develop/determine new environmentally friendly solvents that can form spinnable gels in a large concentration range.

In the present work, polybutene (PB) is investigated as a new spin-solvent for gel-spinning high-strength PE fiber. The PB described in this study is a liquid oligomer (or multimer), and is similar to paraffin oil in that it is non-volatile, non-toxic, and non-flammable. It will be shown that PB behaves similar to paraffin oil during gel-spinning, achieving similar tensile properties in the final fiber. The key benefit of PB compared to

paraffin oil for gel-spinning lies in its phase separation behavior. Since paraffin oil and PE have identical chemical repeat units, there is a stronger interaction between them which causes the extraction to be more difficult than extraction of PB. PB has a slightly different chemical repeat unit so its interaction should be reduced. In present investigation, PB will be shown to be fully miscible with PE at elevated temperature, yet have significantly higher phase separation from the gel-fiber upon quenching than paraffin oil. This larger phase separation significantly reduces the amount of extraction solvent required for gel-spinning while simultaneously accelerating the extraction process due to the weaker interaction of PB with PE in the gel-fiber state.

2.2 Experimental

2.2.1 Materials

The UHMWPE used is a Ticona (Celanese) GUR resin, in powder form, with weight-average molecular mass about 4 million Da. Polybutene with trade name Indopol PB L-6 and number-average molecular mass 280 was supplied by INEOS Oligomers Inc. The Indopol PB L-6 has a viscosity of 7 cSt at 40°C. The spin dope was prepared by combing UHMWPE powder with PB at 20°C and stirring the mixture in a beaker while heating to 150°C. The mixture was then poured into a preheated batch mixer (C.W. Brabender Prep-Center fitted with twin roller blades) and mixed for 20 min at 150°C to obtain a homogenized solution. After the solution was cooled to room temperature in the mixer, a gel of UHMWPE with PB was obtained. For comparison, PE gels were also prepared using paraffin oil and decalin as a spin solvent. Hydrobrite 550 PO white paraffin oil with number-average molecular mass of 541 Da was supplied by Sonneborn Inc. The

paraffin oil has a viscosity of about 100 cSt at 40°C. Decalin (cis+trans, 98%) was supplied by Alfa Aesar. The gels of PE with paraffin oil and decalin were prepared with the same method as that with PB.

2.2.2 Gel Spinning

The schematic of the gel spinning process of PE fibers is shown in Figure 2.1A. The process was performed through an Alex James and Associates piston extruder with a 2.54 cm bore diameter and 150 mL capacity. The homogenized PB/UHMWPE solution was quickly transferred into the bore (preheated to 150°C) of the extruder and allowed to equilibrate for 20 min. The solution was then extruded through a 1 mm die orifice with an aspect ratio of ~15:1 maintained at a temperature of 150°C. The fiber extrusion speed was set to ~1 m/min. The UHMWPE fiber solution was freely extruded into a 1 cm air-gap and quenched into ethanol at 20°C. The quenched gel-filaments were transferred from the ethanol bath to storage under ambient conditions until needed for experiments.

2.2.3 Solvent Extraction

The extraction of PB was performed by winding the gel-fiber onto a 1 inch diameter polytetrafluoroethylene (PTFE) rod. Both ends of the gel-fiber were fixed to maintain constant fiber length. The rod as prepared was submerged into an agitated bath of n-hexane at ~20°C for 60 min, as shown in Figure 2.1B. The PTFE rod containing the extracted gel-fiber was removed from the hexane bath and dried under forced air convection while maintaining fixed fiber ends.

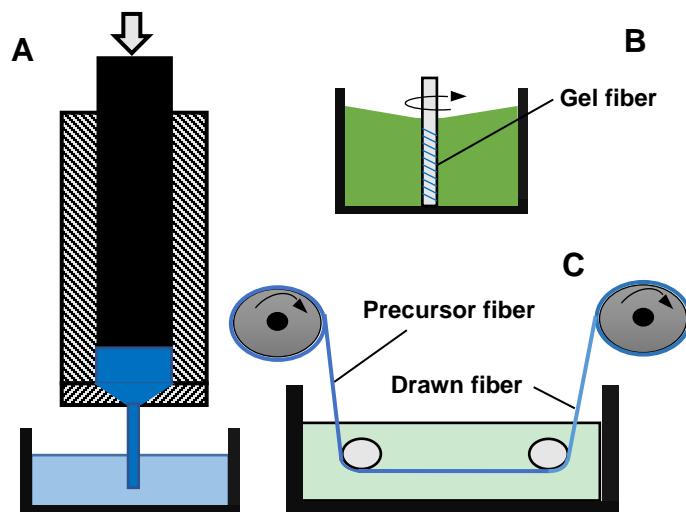


Figure 2.1. Process schematic for gel spinning of PE fibers: (A) gel spinning; (B) solvent extraction; (C) hot drawing.

2.2.4 Hot Drawing

Hot drawing was performed with two stages through heated polyethylene glycol (PEG) as shown in Figure 2.1C. The total path length through the hot bath was kept at 0.8 m in the two stages. The first stage drawing was performed at 120°C with a feeding speed of approximately 0.5 m/min. To study the effect of processing conditions on the fiber property, a collection speed of 15 m/min (draw ratio=30) and 20 m/min (draw ratio=40) was attempted in the first stage. Draw ratio as used in this paper is defined as the ratio of the collection roller speed to the feed roller speed. The weight induced stretch in the air-gap region was relatively small and neglected compared to the large draw ratio during hot-drawing since a small air gap of 1 cm was used. The second stage drawing was performed at 130°C with a feeding speed of 0.5 m/min and a collection speed controlled incrementally from a minimum of 1 m/min to a maximum limited by the drawability of the fiber. The

maximum draw ratio was determined by stepwise increasing the second stage collection speed at appropriate time intervals until fiber breakage. Fibers were drawn at each incremental ratio to obtain samples at least 6 m long for testing.

2.2.5 Characterization

The instrument used for obtaining differential scanning calorimetry (DSC) data was a TA Q200 DSC unit (TA Instruments). Samples were sealed in hermetic aluminum pans. Nitrogen atmosphere and a heating rate of 10°C/min were used for all samples. Thermal gravitational analysis (TGA) was performed using a TA TGA5000 (TA Instruments). Samples were heated to 350°C in nitrogen atmosphere and held at this temperature until the weight change approached a steady value. The rheological data were collected with a TA AR2000EX parallel-plate rheometer (TA Instruments). The rheological behavior in the spinning process was also tested with a Dynisco LCR7001 capillary rheometer (Dynisco). Scanning electron microscopy (SEM) images were collected with a LEO 1550.

The diameter of fibers was measured by weighing a known length of fiber and calculating the cross-sectional area. Before weighing, the hot-drawn fibers were briefly rinsed with ethanol to remove residual PEG from the hot-drawing stage and dried with forced air convection.

The tensile properties of fibers were measured using an Instron 5566 universal testing machine. Fiber samples were wound onto wooden rods approximately 2 mm in diameter and super-glued over the wound fiber ends. Crosshead speed was 100 mm/min with a gauge length of ~10 cm. All tensile tests were performed under ambient conditions (40-60% relative humidity at 20-22°C). Four samples from each type of fiber were tested and averaged.

Wide angle x-ray diffraction (WAXD) data were collected on a Rigaku Micro Max 002 (Cu K α radiation, $\lambda=0.154$ nm) operating at 45 kV and 0.65 mA using an R-axis IV++ detector. Exposure time was 30 min for all samples. The crystalline orientation factor was calculated with the method developed by Wilchinsky [27]. The 110 and 200 equatorial diffractions were used to determine the orientation factor based on the orthorhombic UHMWPE unit cell [28].

2.3 Results and Discussions

2.3.1 PE/PB Gelation Properties

Selection of an appropriate spin-solvent is critical for the gel spinning process of PE as the gelation properties greatly affect the fiber performance. It is reported that the gels of UHMWPE exhibit excellent spinnability and the fibers obtained by drawing of the gels generally have high strength and modulus [7]. The conversion of the polymer solution to a gel results from the formation of crystalline junction points in the gel. For the gels of PE with paraffin oil and decalin, the structural features and the gelation mechanism on cooling have been studied by Jen et al [7, 8]. It is demonstrated that the gelation of UHMWPE from the two solutions is attributed to liquid-liquid phase separation driven by concentration fluctuations. The fluctuation is determined by the crystallization of PE when the solution is being cooled. For the gels with decalin, solvent flows out of the gels and syneresis occurs during crystallization. However, no significant syneresis happens for the gels with paraffin oil. As little information about the gels of PB/UHMWPE can be found, the gelation properties of PE with PB were examined in this study.

The gels of PB/UHMWPE with different concentrations were prepared, tested and compared with the gels of paraffin oil/UHMWPE and decalin/UHMWPE which served as controls. First, the phase separation behavior between the solvents and UHMWPE was studied. Each type of solvent and PE were mixed and cooled down to room temperature in the batch mixer to form gels. The gels from the three types of solvents were collected, wiped off solvents and weighed for comparison. The results are summarized in Table 2.1. At a concentration of around 3.3 wt% (2 g/60 ml), decalin showed the strongest phase separation and least solvent remained inside the gel. The phase separation between paraffin oil and UHMWPE was weak with most of the solvent being held inside the gel. Weak separation is consistent with the argument that paraffin oil has better affinity with UHMWPE than decalin because paraffin and PE have identical alkyl main chains, but only different chain lengths [8]. The phase separation behavior between PB and UHMWPE was intermediate, suggesting PB is less compatible with PE at room temperature than paraffin oil. Thus, it is deduced in order to gel-spin relatively low concentrations of UHMWPE, solvents with less interactions at room temperature are needed so that the polymer chains have a higher probability to contact with each other during gelation and form physical crosslinks. This deduction is especially important for gel spinning of fibers at relatively low concentration since the polymer chains have less entanglements which is beneficial for improvement of strength [7]. With a less compatible solvent, the polymer can quickly form a gel for spinning continuous fibers. If the solvent is too favorable to the polymer chains, it will take a longer time for the polymer chains to diffuse and form crystalline crosslinks. To validate this argument, lower concentration of solutions were prepared for gelation. The results are given in Table 2.1. For PB, a ~2% (1.2 g/60 ml) gel was obtained and only

around 55% of the solvent was preserved in the gel. While for paraffin oil, at the same concentration, a coherent gel network was not formed. From this point of view, it is possible to obtain high strength fibers by gel spinning of low concentration PB/UHMWPE solution.

Table 2.1. Weight of the gels of UHMWPE with solvents.

PE Weight (g)	Solvent Type	Solvent Volume (ml)	Gel Weight (g)
2.00±0.01	Paraffin oil	60	41.26±1.18
2.00±0.01	PB	60	35.68±1.20
2.00±0.01	Decalin	60	25.60±0.19
1.20±0.01	PB	60	30.40±0.82
1.20±0.01	Paraffin oil	60	No self-standable gel

The thermal and rheological properties of PB/UHMWPE gels were studied to provide a reference for gel spinning process parameters. The DSC thermogram of a PB/2%UHMWPE gel is shown in Figure 2.2A. The blend shows single melting and crystallization peaks at reduced temperature compared to the neat UHMWPE, suggesting complete miscibility and similarity to paraffin oil/UHMWPE [29]. The similarity is

supported by the solubility parameters of the materials, which are 7.9, 7.5 and 8.05 (cal/cm³)^{1/2} for PE, paraffin oil and PB, respectively [30]. According to Flory-Huggins' theory, PE can be miscible in the two solvents. Thus, this gel also benefits from the polymer/oligomer blend with solution-like behavior [29]. The melting temperature of neat UHMWPE is reduced from ~140°C to 115°C after mixing 2% wt. UHMWPE with PB.

One important parameter that needs to be tested is the transition temperature of viscous solution to solid gel. It can be inferred from a sharp viscosity increase approaching infinity as measured by parallel plate rheometry in an oscillation temperature ramp mode with 1% strain at a frequency of 10 rad/s. Complex viscosity of the 2 wt% PE/PB blend gradually increased when it was cooled from 150°C to ~100°C, where the viscosity increased rapidly indicating a transition from solution to solid gel, as shown in Figure 2.3. The formation of this solid structure is consistent with the crystallization temperature measured by DSC for the same 2% PE/PB gel; therefore, the solid structure formed during quenching of the PE/PB fiber should be consistent with a network of polymer molecules swollen in solvent and mechanically supported by crystalline regions, which behave like physical crosslinks [29].

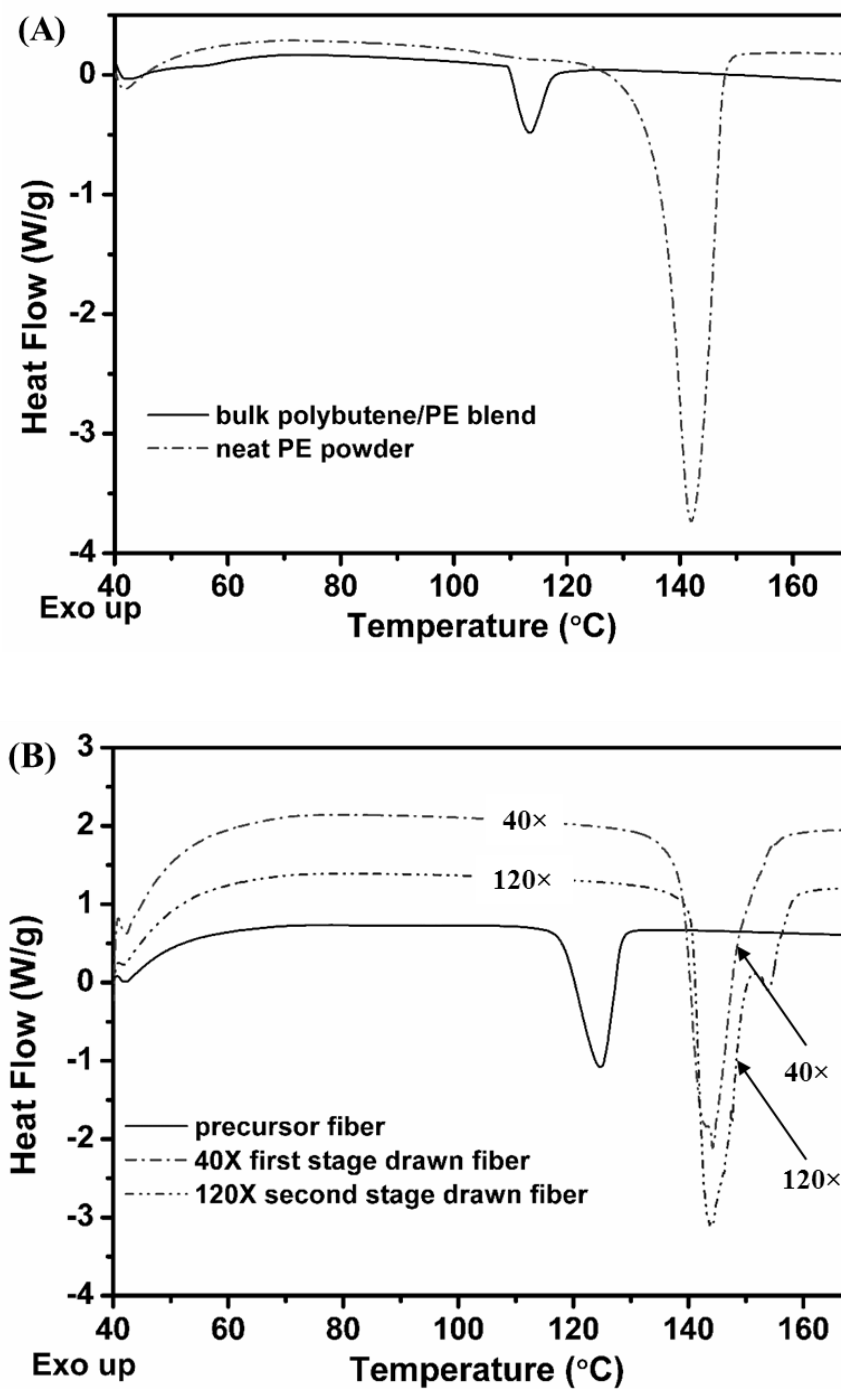


Figure 2.2. DSC of (A) neat PE powder and 2% PE/PB blend and (B) gel-spun PE fibers at various stages of processing. The DSC scans were conducted at 10°C/min heating rate in nitrogen atmosphere.

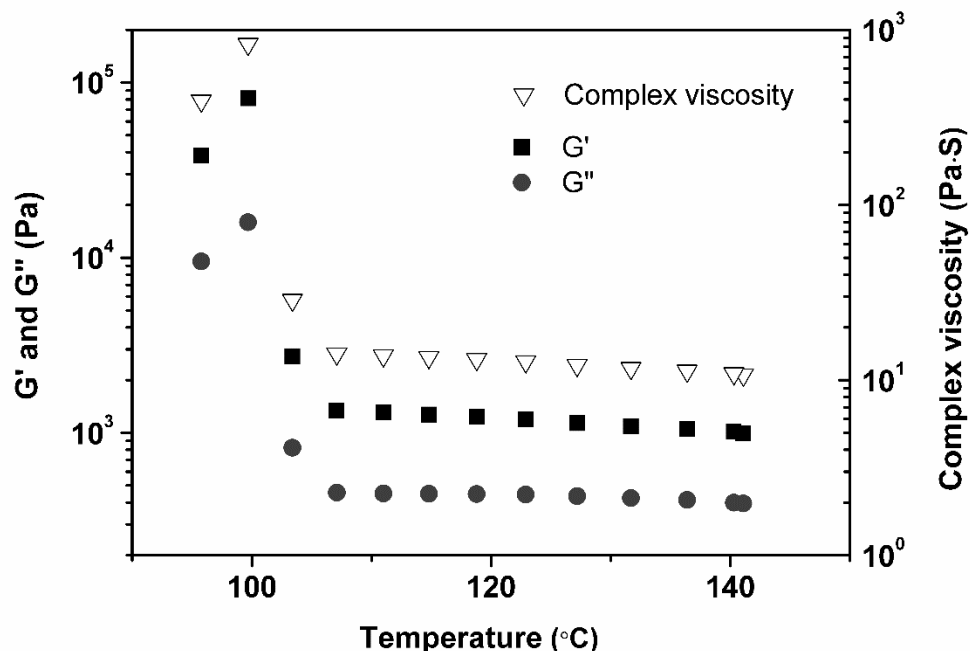


Figure 2.3. Parallel plate rheometry: cooling from 150°C at 2°C/min to transition temperature.

2.3.2 Extrusion of as-spun Fiber

Continuous production of UHMWPE fibers by gel spinning requires continuously pumping and extruding the gel solution through a spinneret. Several conditions can affect the property of the fiber including spinning temperature, spinning speed and jet stretch ratio. As PB is quite stable up to 350°C, the extrusion temperature can be adjusted over a wide range in order to obtain a uniform fiber extrudate. In this study, an operating temperature of 150°C was able to produce and maintain uniform fibers. According to the literature, too much jet stretch can be destructive to the fiber property [6]. Thus, no jet stretch is applied to the fiber in this study. As a result of using extremely long chain molecules for generating strong fibers, the solution is highly elastic and can easily incur

flow instabilities such as secondary flow vortices, elastic turbulence, pulsing flow and draw resonance [31]. Stretching of the viscoelastic solution beyond a critical value of the deformation rate may readily lead to brittle fracture of the spinline as a result of storage of part of the deformation energy. The resulting fiber has considerably poor mechanical properties [23]. The rheological behavior of the gel solution determines the spinnability of the gel solution [32]. Based on the rheological property of the solution, it is important to use an appropriate spinning speed for generation of strong fiber.

A suitable spinning speed can be determined with a series of rheological tests. The fundamental rheological behavior of UHMWPE solutions have been reported in several papers, and non-Newtonian flow behavior including shear thinning occurs during the process [33-35]. For the new PB/UHMWPE solution and gel, both parallel-plate rheometry and capillary rheometry were conducted to study the flow behavior. Figure 2.4 shows frequency sweep of the 2% PE/PB solution at a constant temperature of 150°C with constant strain of 1% and 5%. It can be seen that at low frequency (<1 Hz), the loss modulus (G'') is larger than the storage modulus (G'). The solution is dominated by viscous behavior instead of elasticity. It can be deduced that the solution should be spinnable in this region by suppressing the elasticity to obtain high strength fiber. For the region at high frequency (>1 Hz), the storage modulus (G') is higher than the loss modulus (G''), which means elasticity is dominating the solution. If the solution is spun in this region, notable die swell will happen and fibers obtained will have more defects. Figure 2.5 shows shear viscosity versus shear rate obtained from capillary rheometry. It can be seen that the PB/UHMWPE solution is highly shear-thinning and its viscosity to shear rate relation fits well to the classical power-law model. An appropriate extruding

rate can be obtained by combining the data in Figure 2.4 and Figure 2.5. According to the Cox-Merz rule, a correlation between the complex viscosity in an oscillatory frequency sweep and the stationary viscosity from continuous shear can be established [36]. This means that viscous behavior would dominate at a shear rate less than 1 s^{-1} . A suitable spinning speed for reducing die swell and flow instability was therefore estimated to be $\sim 0.5 \text{ m/min}$, corresponding to this shear rate region.

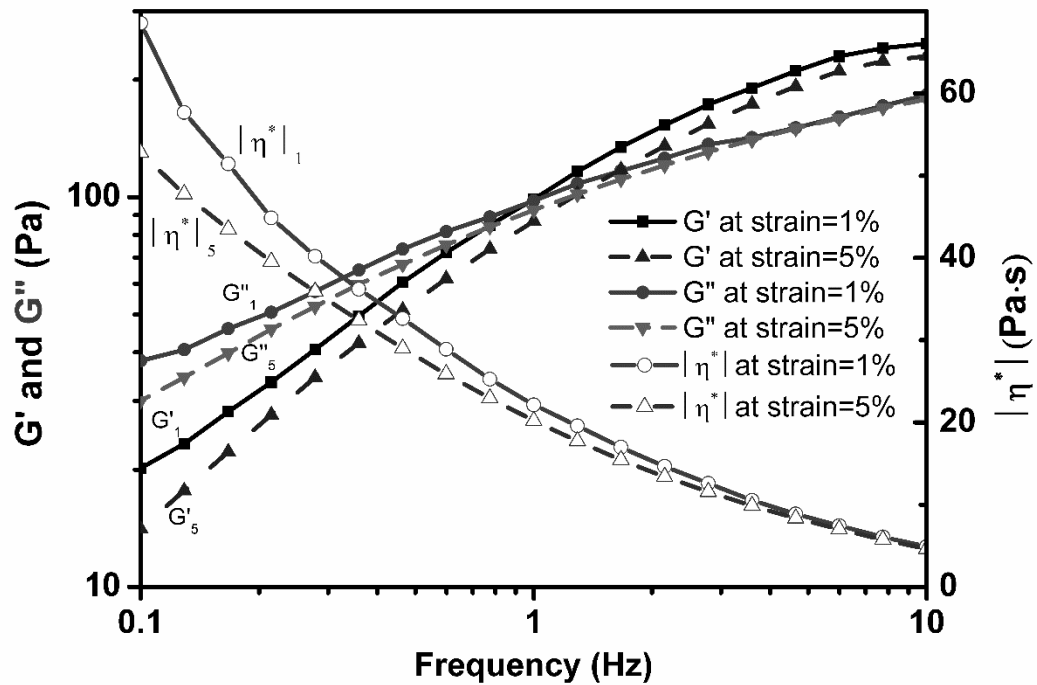


Figure 2.4. Linear viscoelastic behavior of the 2% PE/PB solution by frequency sweep at 150°C with a parallel plate rheometer.

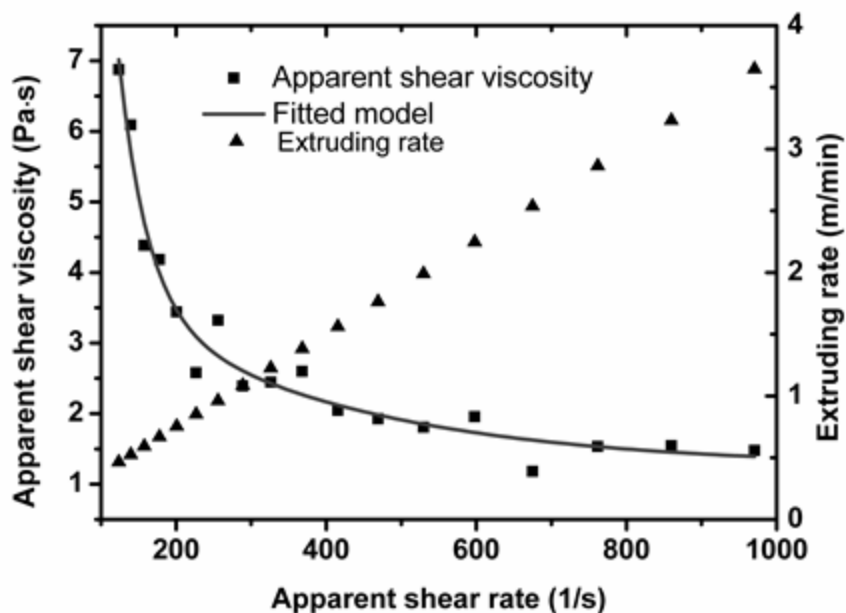


Figure 2.5. Rheological properties of the 2% PE/PB solution at 150°C obtained by capillary rheometry.

2.3.3 Solvent Extraction

Solvent extraction is a key factor affecting the efficiency of the process and the drawability of the UHMWPE fibers [21]. In this study, hexane was used as an extraction solvent, and extraction was conducted using a setup shown in Figure 2.1B. As much solvent has been separated from the as-spun gel fibers when quenched to room temperature, only residual PB in the gel fiber is extracted to obtain precursor fibers. The volume of hexane in the extraction bath was ~5000 larger than the volume of the gel-fiber in order to maintain a maximum concentration gradient throughout the extraction process.

The extraction of PB can be quantitatively analyzed using the weight loss of fiber and compared to that of paraffin oil. The gel fibers of weight (W_0) were extracted in hexane for different time with agitation, and the extracted fibers were then fully dried with forced air convection to remove residual hexane and weighed. The sample weight (W_t) was measured at several time intervals until no weight change occurred as hexane has been completely evaporated from the fiber. After extracting in hexane for sufficient time, an equilibrium state was obtained with the final sample weight W_1 . With W_0 and W_1 determined, the initial concentration of the gel fiber was calculated to be 21.3% UHMWPE and 78.7% PB. The initial concentration of the gel fiber was much higher than the spin dope concentration 2% due to strong phase separation as described previously. The solvent extraction ratio (E_s , %) can be calculated simply by

$$E_s = \frac{W_0 - W_t}{W_0 - W_1} \times 100\% . \quad (1)$$

The solvent extraction ratios of PB and paraffin oil are compared in Figure 2.6. As show in the figure, PB can be extracted fast and an equilibrium is reached in about 2 min. The extraction process of PB is more efficient than that of paraffin oil. PB can be extracted much faster even with a higher ratio of solvent in the gel fiber. About 82% solvent is removed in the fiber when extracting for 1 min. The percentage of solvent extracted increases to 98% in 2 min and then quickly increases to more than 99%. Instead, for paraffin oil, about 92% solvent can be extracted in 1 min, but the percentage of solvent extracted can only reach 95% at 2 min. Moreover, it takes more than 10 min to reach 98% solvent extraction, which is much slower than that of PB.

TGA scans were performed on pure PB, pure UHMWPE, and the PE/PB gel fiber before and after extraction to verify the extraction analysis. The gravimetric losses are shown in Figure 2.7. The pure PB spin-solvent evaporates almost completely after 20 min at 350°C in nitrogen atmosphere. A similar TGA scan on the undrawn, solvent-rich gel fiber showed a weight reduction of 78.2% in 50 min which was assumed to result from evaporation of the PB component. This corresponds to 78.2% PB in the gel fiber, and this value is consistent with the calculated one obtained using the procedure by Eq. (1). As predicted, the fiber after extraction in hexane showed no significant weight loss, as shown in Figure 2.7, suggesting the extraction process was sufficient to obtain an UHMWPE fiber, nearly free of the PB spin-solvent.

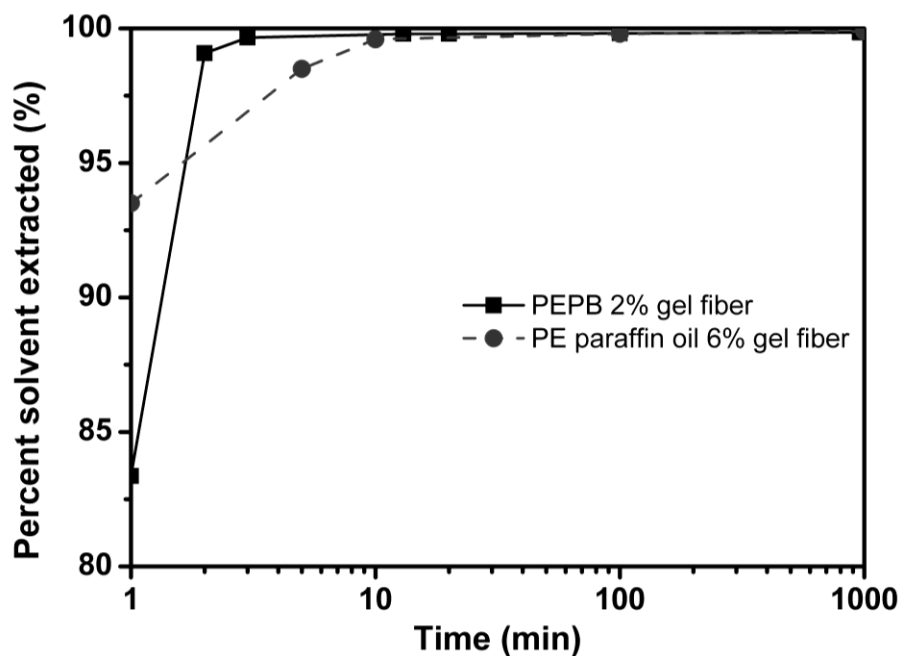


Figure 2.6. Spin-solvent extraction comparison in n-hexane.

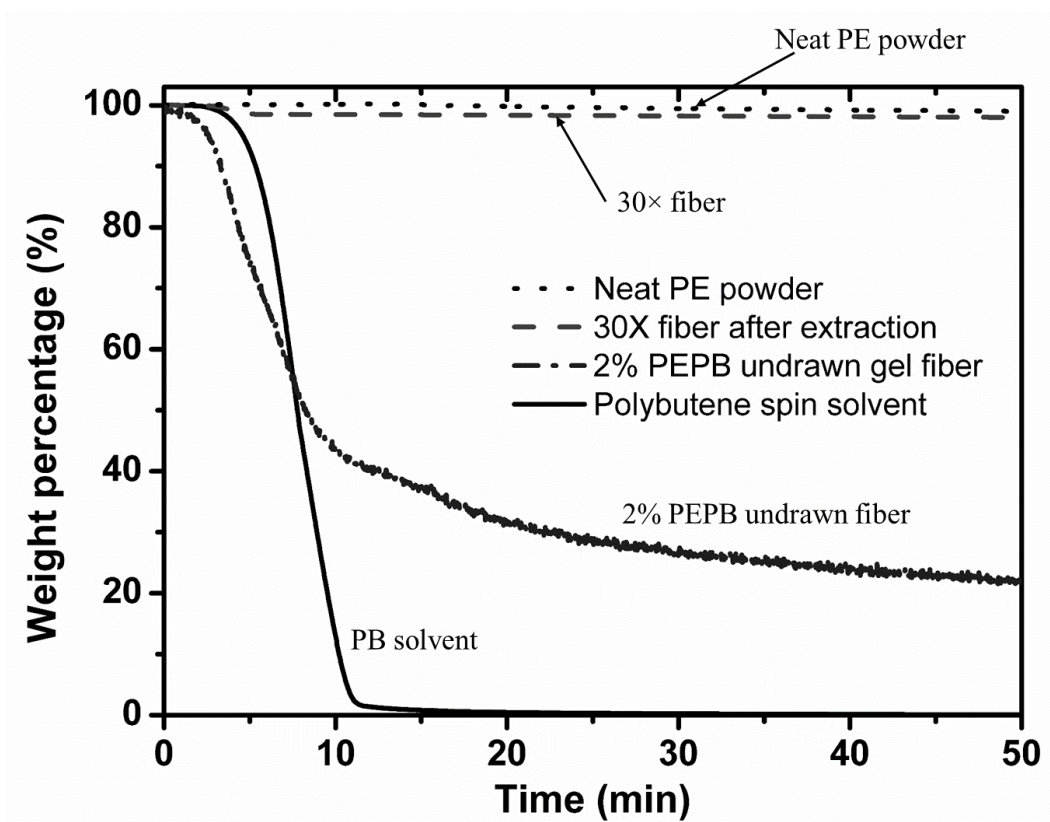


Figure 2.7. TGA weight loss curves as a function of time. Fibers were heated to 350°C in nitrogen atmosphere for 50 min to evaporate PB. Neat PE and PB are included for reference.

The above results show that PB is easier to be extracted from the gel fiber than paraffin oil. This can be attributed to the poor interaction between PB and UHMWPE in the gel fiber, as shown by the large degree of phase separation in the bulk gel. Due to phase separation during cooling and gelation, a large amount of PB is leached out from the bulk gel. Table 2.1 shows the change of weight after gelation. The separated solvent was allowed to flow out and stabilize before taking measurements. The gel with PB shows more weight loss due to phase separation than the gel with paraffin oil after being

cooled to room temperature in air. The actual weight percentage of UHMWPE in the bulk gel of the PB/2% UHMWPE solution is ~4%. In the fiber form, the phase separation is more intensive; the actual weight percentage of UHMWPE in the gel fiber of the PB/2% UHMWPE solution is ~20%. The comparison indicates that most solvent after phase separation is still trapped in the bulk gel while in the fiber form with small diameter and large surface area, mechanical separation between PB and the gel network takes place more readily. All these results indicate that for gel spinning of UHMWPE fiber with PB as the spin-solvent, less extraction solvent is needed due to strong phase separation during quenching of the gel and the extraction process is also faster.

Precursor fibers obtained after extraction were hot-drawn with different draw ratios. SEM micrographs of the precursor fiber are shown in Figure 2.8. Relatively smooth surface is obtained. However, non-uniformity can be observed from the magnified surface. It is mostly caused by the shrinkage in the radial direction in the extraction process when the ends were fixed. The WAXD pattern of the precursor fiber (Figure 2.9A) shows a nearly unoriented crystalline structure. The corresponding orientation factor is given in Table 2.2. The lack of C-axis orientation of the precursor fiber is anticipated due to free falling without jet stretch of the gel fiber. The negative small orientation factor may infer some small vertical orientation, as also seen in previous studies [29]. The peak melting temperature of the precursor fiber is ~124°C, determined from the corresponding DSC thermogram in Figure 2.2B. The melting temperature of the bulk gel is ~113°C (determined from Figure 2.2A), considerably lower than that of the precursor fiber.

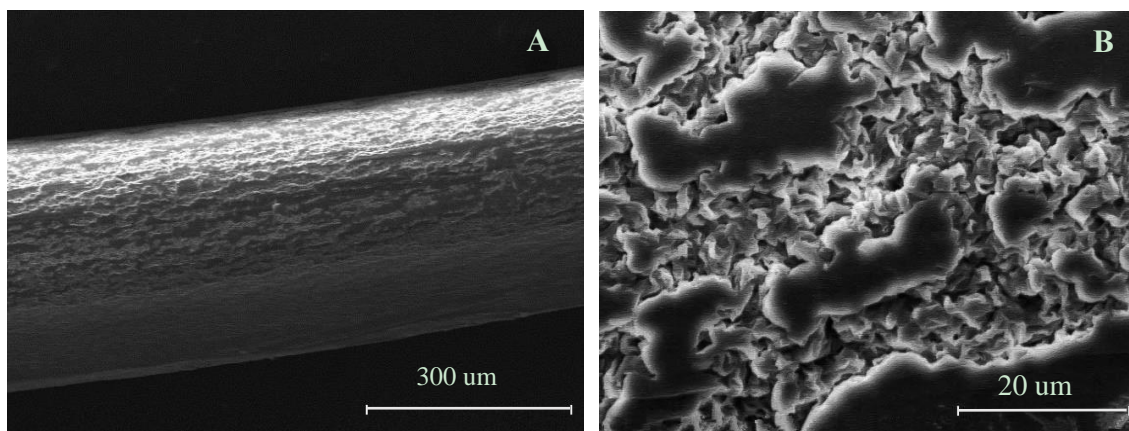


Figure 2.8. SEM images of gel-spun UHMWPE fibers: (A) precursor fiber; (B) magnified surface morphology of the precursor fiber.

Table 2.2. Orientation factors of gel spun UHMWPE fibers.

Fiber type	Orientation factor
Precursor	-0.263
30× drawn first stage fiber	0.8826
40× drawn first stage fiber	0.8936
120× drawn final fiber	0.8996

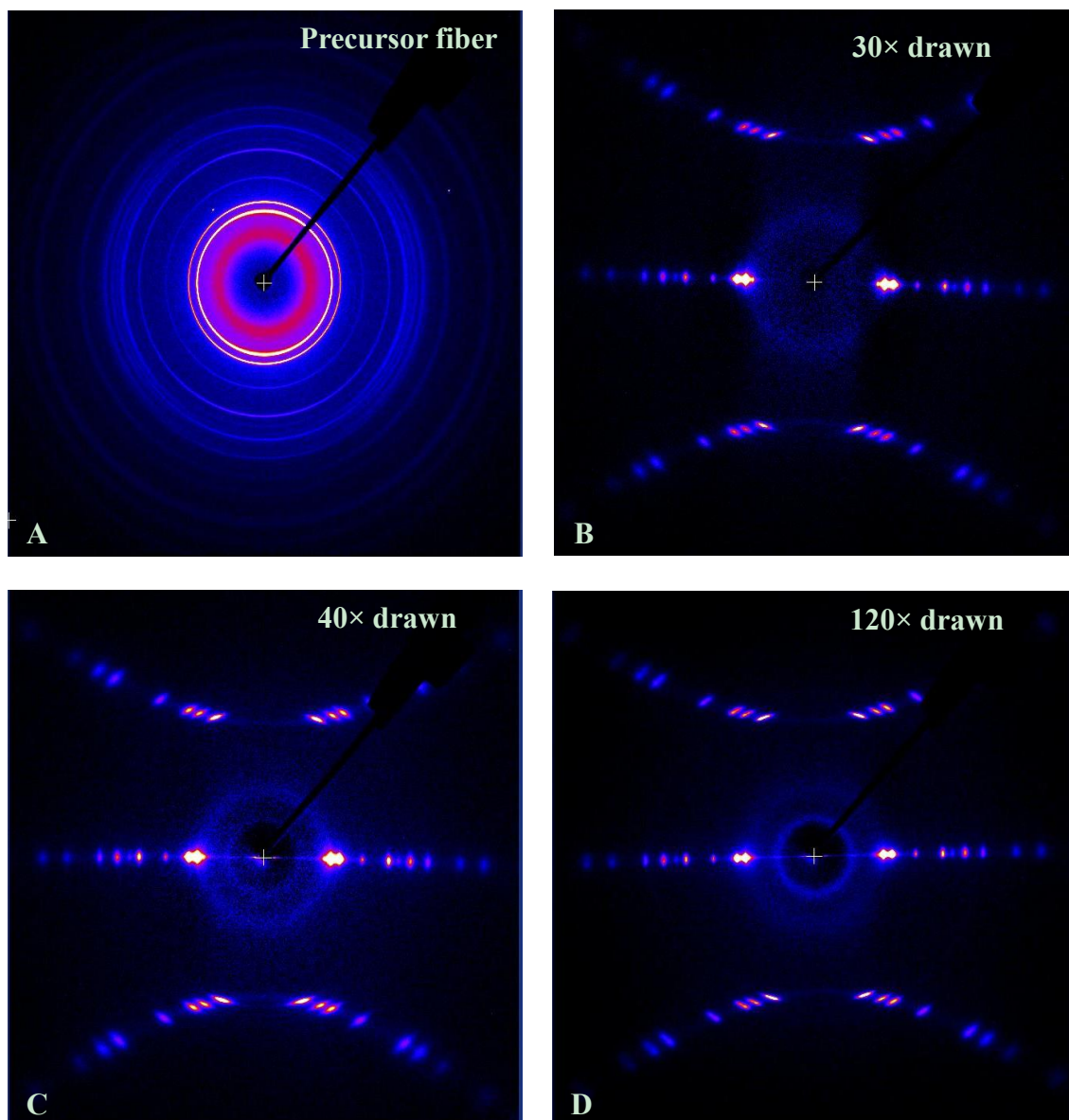


Figure 2.9. WAXD patterns of gel-spun UHMWPE fibers at various draw ratios: (A) undrawn precursor fiber; (B) 30× drawn fiber at first stage; (C) 40× drawn fiber at first stage; (D) 120× total draw ratio fiber with 40× at first stage.

2.3.4 Hot Drawing

It is known that with hot drawing, the shish-kebab structure developed in both the as-spun and drawn fibers can be transformed continuously into the micro-fibril structure composed mostly of the shish structure [24]. The chains in the kebabs are incorporated into the shishes and consumed to extend the longitudinal dimension of the shishes during the drawing process. The fiber diameter becomes smaller with the structural transformation by hot drawing. It is also noted that the tensile strength and modulus generally increase with the decrease of fiber diameter. Hence, the objective of the hot drawing process is to achieve a large draw ratio and obtain fibers with the possibly smallest diameter. In the previous studies of gel spun PE fibers with paraffin oil and decalin [29], drawing in two stages seems to be especially effective to obtain high draw ratios compared with other methods. Thus, in this study, the PE fibers spun with PB were also drawn in two stages using the same hot drawing conditions.

The processing conditions such as drawing temperature and draw ratio at each stage are critical to the tensile properties of the fibers. The temperature should be set high enough to enable long-range molecular rearrangements of polymer chains but lower than the melting temperature of the fiber being drawn to avoid fiber break. For gel spun UHMWPE fibers, the favorable drawing temperatures were in the range of 80-148°C [29]. If the temperature is too low, the molecular chains cannot be drawn enough to reach high strength, while at high temperature the fiber may be melted.

The drawing temperature and draw ratio for the first stage can be determined from the material property of the precursor fiber. The drawing temperature was set to be 120°C, 4°C lower than the melting temperature of the precursor fiber, for the first stage to obtain

sufficient molecular mobility but not to melt the fibers. The typical draw ratio reported in the literature is about 30 \times . In this study, two levels of first-stage draw ratio were tested: 30 \times and 40 \times . The appearance of the fibers obtained after the first stage with the draw ratio of 30 \times and 40 \times is shown in Figure 2.10. It can be observed the fibers show similar shape with different diameters.

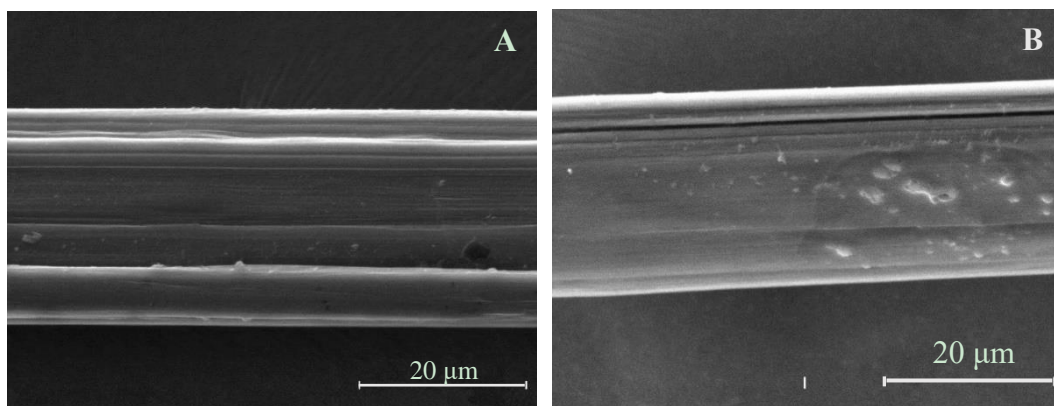


Figure 2.10. SEM images of first-stage hot-drawn fibers: (A) 30 \times drawn; B) 40 \times drawn.

The structure of the first-stage drawn fibers was examined with X-ray. The WAXD pattern of the 30 \times drawn fiber in Figure 2.9B is similar to that of the 40 \times drawn fibers in Figure 2.9C. As anticipated, the process of uniaxial extension is accompanied by orientation of the C-axes of the crystallites along the drawing direction. The fibers at both draw ratios showed significant orientation. Their azimuthal integrations of the [110] and [200] diffractions are plotted in Figure 2.11. The azimuthal width of each direction decreases appreciably after first-stage drawing. By comparing the intensities of the drawn fibers with different draw ratios, it can be seen that the intensity was mainly increased at the [110] diffraction with the increase of draw ratio. The intensity at [200] diffraction did

not significantly change. It can be inferred that, in the first stage of drawing, the fiber is mainly orientated with [110] diffraction when the draw ratio is increased. The orientation along [200] is only slightly increased when the draw ratio is larger. The crystallite orientation factor (Table 2.2) calculated in accordance with Herman's method increased from 0.8826 to 0.8936 when the draw ratio was changed from 30× to 40×. The peak melting temperature of the 40× drawn fiber is 144°C (determined from the DSC thermograph in Figure 2.2B), much higher than that of the precursor fiber.

The fibers obtained in the first stage need to be orientated further at a higher temperature to improve performance. According to the peak melting temperature of the 40× drawn fiber and the reported drawing temperature for the second stage in the literature [6,9,19,29], the temperature for the second stage was set to be 130°C in this study. The maximum total draw ratio was found to be 120× for both the 30× and 40× drawn fiber. SEM images of the final 120× drawn fibers are shown in Figure 2.12. The final fibers have smaller diameter and relatively smoother surface than the first-stage drawn fibers. The representative tensile stress-strain curves of the final fibers are shown in Figure 2.13. The maximum strain for both the two types of fibers is less than 5%. For the fibers 30× drawn at the first stage, the tensile strength and Young's modulus of the final fiber are 3.62 ± 0.28 GPa and 124.73 ± 14.32 GPa, respectively. The fibers 40× drawn at the first stage show better performance, with tensile strength and Young's modulus of 4.07 ± 0.19 GPa and 155.83 ± 28.29 GPa, correspondingly. The orientation factors of these fibers are provided in Table 2. It can be seen that the orientation factor only increased slightly from 40× to 120×. The peak melting temperature of the drawn fibers with draw ratios of 40× and 120× are

also similar, both about 144°C. It can be inferred that orientation of the fibers is mainly completed in the first stage of drawing.

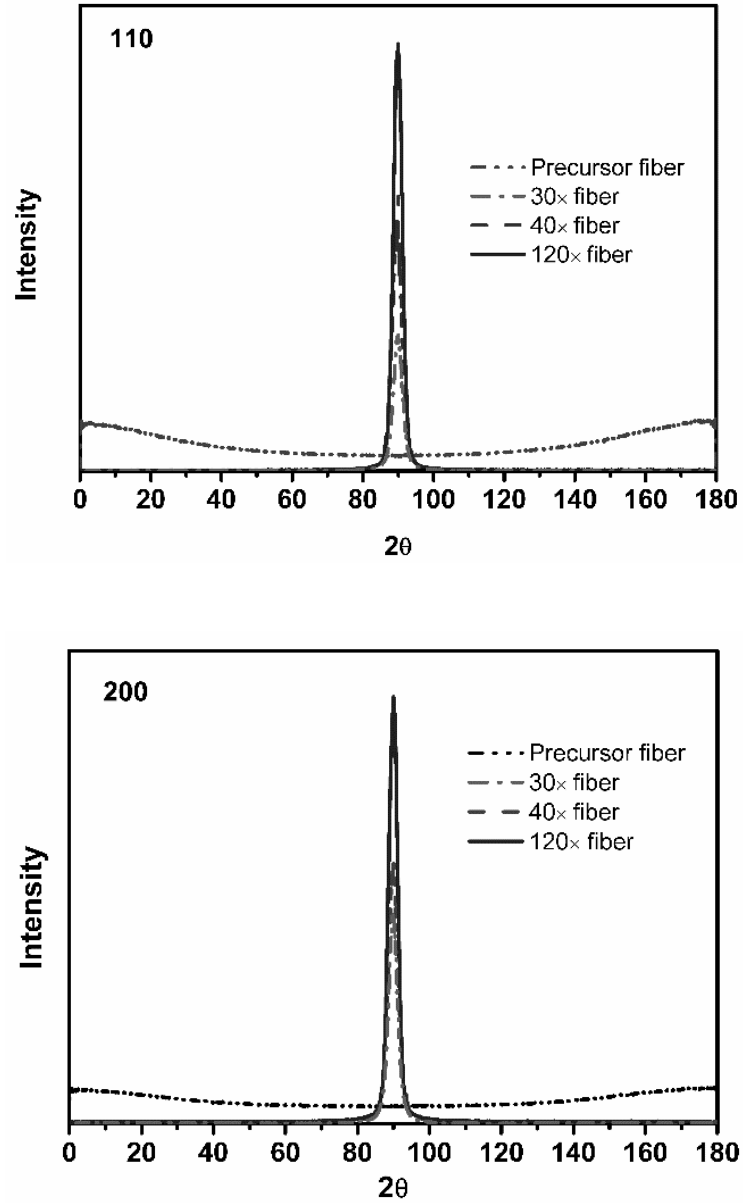


Figure 2.11. Azimuthal integrations of the [110] and [200] diffractions of the gel spun UHMWPE fibers at various draw ratios.

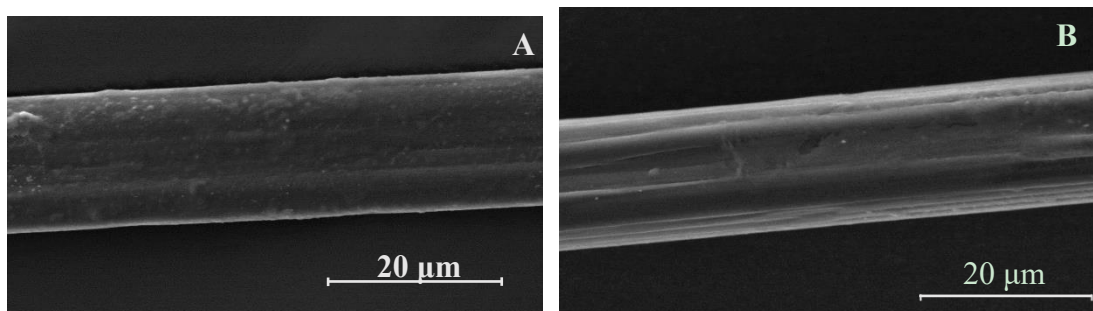


Figure 2.12. SEM images of the total 120 \times drawn fibers: (A) 30 \times drawn at the first stage;
(B) 40 \times drawn at the first stage.

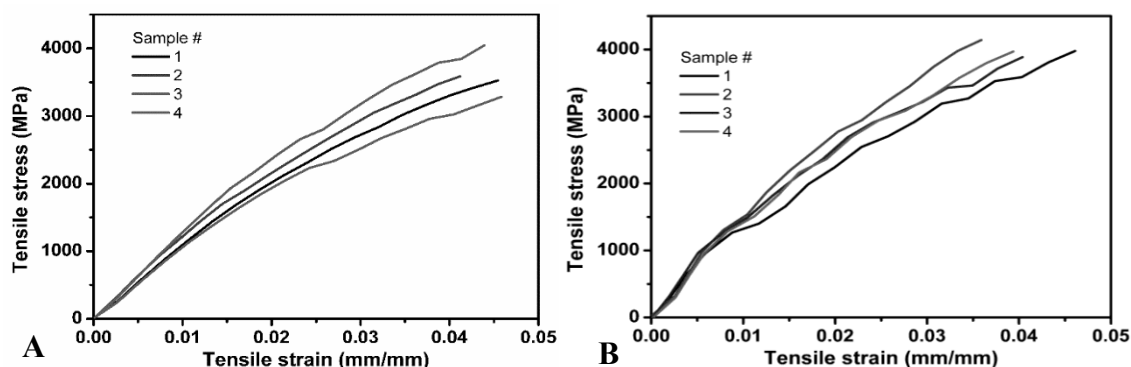


Figure 2.13. Representative tensile stress-strain curves of UHMWPE fibers at maximum draw ratio and processed with different drawing conditions at the first stage: (A) total draw ratio 120 \times with the first-stage draw ratio of 30 \times ; (B) total draw ratio of 120 \times with the first-stage draw ratio of 40 \times .

In the hot drawing stages, chain extension and the ultimate draw ratio substantially depend on the number of intermolecular entanglements initially present in the fiber. The intermolecular entanglements appear to be affected by the nature of the solvent, the

polymer concentration and the spinning conditions [19]. In this study, PB is verified as an effective solvent for preparing spin dope for UHMWPE and low concentration of solution can be gel spun under the spinning conditions. It can be deduced low intermolecular entanglements are formed in this system, resulting in relatively high drawability of the precursor fiber. The mechanism of the high orientation factor and the high strength of the fiber can be explained using known theory of crystallization under extension. In the hot drawing process, long straightened segments of chains can penetrate the amorphous interlayers and coherently link adjacent crystallites to one another. As drawing continues, both the concentration and degree of orientation of the continuous intrafibrillar chains increase due to the conversion of convoluted conformers into straight conformers [37]. This in turn increases the length of the crystallinities and causes the crystallization front to move deep into the amorphous interlayers. When the fibers are drawn to a high ratio, most of the UHMWPE chains undergo crystallization.

2.4 Phase Diagram of the “Oligomer-Polymer” Blend System

The “oligomer-polymer” blend system has been demonstrated as an effective method for preparation of spin dopes for gel spinning. The system shows viscous solution behavior when temperature is above the melting point of the polymer. When the temperature is decreased to a certain value, phase separation will occur and gels will be formed afterwards. With formation of gels, the disentangled morphology in the polymer chains can be maintained even after the solvent is completely extracted, unless the gel is reheated to a high temperature. Thus, gelation is a distinct benefit of the “oligomer-polymer” blend system. Besides, the strong phase separation behavior is also favored by

gel spinning as it can significantly improve the extraction efficiency and reduce consumption of the extraction solvent. As described in this chapter, the phase separation behavior of polybutene is much stronger than that of paraffin oil. However, the mechanism about phase separation in the “oligomer-polymer” system is still unclear. In this section, Flory-Huggins theory is used to build the phase diagram of this system.

The free energy of mixing for the “oligomer-polymer” blend can be expressed as:

$$\Delta G_m = RT\chi\phi_A\phi_B + RT\left(\frac{\phi_A}{n_A}\ln\phi_A + \frac{\phi_B}{n_B}\ln\phi_B\right) \quad (1)$$

In Eq. (1), ϕ_A and ϕ_B are volume fractions of the two components, n_A and n_B are degrees of polymerization. To obtain phase diagram of the blend system, three derivatives of the free energy of mixing are needed. Assuming χ is just a function of T , and independent of ϕ_B , the first derivative is

$$\frac{\partial \Delta G_m}{\partial \phi_B} = RT\chi(1 - 2\phi_B) - \frac{RT}{n_A}[1 + \ln(1 - \phi_B)] + \frac{RT}{n_B}(1 + \ln\phi_B) \quad (2)$$

The second derivative is

$$\frac{\partial^2 \Delta G_m}{\partial \phi_B^2} = -2RT\chi + \frac{RT}{n_A} \cdot \frac{1}{1-\phi_B} + \frac{RT}{n_B} \cdot \frac{1}{\phi_B} \quad (3)$$

The third derivative is

$$\frac{\partial^3 \Delta G_m}{\partial \phi_B^3} = \frac{RT}{n_A}(-1)(1 - \phi_B)^{-2} + \frac{RT}{n_B} \cdot \phi_B^{-2} \quad (4)$$

At the critical point of upper critical solution temperature (UCST), set equation (4) to be zero, the volume fraction at the critical point can be obtained.

$$\left(\frac{\phi_B}{1-\phi_B}\right)^2 = \frac{n_A}{n_B} \quad (5)$$

Set $\sqrt{\frac{n_A}{n_B}} = k$, the volume fraction of the polymer at the critical point can be calculated as

$$\phi_B^c = \frac{k}{k+1} \quad (6)$$

The interaction parameter χ at the critical point can be calculated as

$$\chi^c = \frac{1}{2} \left(\frac{1}{n_A(1-\phi_B)} + \frac{1}{n_B} \cdot \frac{1}{\phi_B} \right) \quad (7)$$

Substituting k into Eq. (7),

$$\chi^c = \frac{1}{2} \left(\frac{1}{n_A(1-\phi_B)} + \frac{1}{n_B} \cdot \frac{1}{\phi_B} \right) \quad (8)$$

The following dimensionless numbers are defined

$$\chi^c \cdot n_B = \frac{1}{2} \left(\frac{k+1}{k} \right)^2 \quad (9)$$

To obtain the spinodal decomposition curve, set the second derivative Eq. (3) to be zero, the relationship between volume fraction and the interaction parameter can be obtained as

$$\frac{1}{n_A} \frac{1}{(1-\phi_B)} + \frac{1}{n_B} \frac{1}{\phi_B} = 2\chi \quad (10)$$

Dimensionless interaction parameter and volume fraction of the polymer are defined as

$$X = \frac{\chi}{\chi_c} \quad (11)$$

$$Y = \frac{\phi_B}{\phi_B^c} \quad (12)$$

With such dimensionless numbers, Eq. (8) can be simplified as

$$XY^2 + \left[\frac{1}{k^2} - 1 - X \left(\frac{k+1}{k} \right)^2 \right] \cdot \frac{k}{k+1} Y + 1 = 0 \quad (13)$$

Eq. (13) is the governing equation for spinodal master curve. With similar method, the governing equation for binodal master curve can be obtained by setting Eq. (2) to be zero.

$$\frac{X}{2} \left(\frac{k+1}{k} \right)^2 \left(1 - \frac{2k}{k+1} Y \right) - \frac{1}{k^2} \left[1 + \ln \left(1 - \frac{k}{k+1} Y \right) \right] + 1 + \ln \left(\frac{k}{k+1} Y \right) = 0 \quad (14)$$

Eq. (14) is the governing equation for binodal master curve. The boundary conditions for the governing equations Eq. (13) and Eq. (14) are

$$X \in [1, +\infty);$$

$$Y \in (0, 1+1/k);$$

$$k \in (0, 1].$$

The governing equations can be numerically solved to analyze the effect of k on phase diagrams. It can be observed from Figure 2.14 that the ratio of degree of polymerization of oligomer to polymer significantly affects the geometry of both the spinodal and binodal curves. The ideal condition is mixing polymers with identical number of repeat units, where k equals 1. With decrease of k from 1, the spinodal curve becomes wider. It means for mixing of the polymer with an oligomer of lower molecular weight, the dimensionless interaction parameter is less sensitive to the change of dimensionless volume fraction. For the binodal curve, it shows a similar trend that the dimensionless interaction parameter is stable in a broader range of dimensionless volume fraction. The effect of k on the phase diagram is shown in Figure 2.15. It can be obtained that with decrease of k , the cross-point of spinodal curve with binodal curve shifts to a smaller dimensionless volume fraction. This means, for an oligomer with lower molecular weight, the critical volume fraction becomes smaller. When phase separation starts, the volume fraction of the polymer in one phase will be very small, which means that phase is almost pure oligomers. This can assist in explaining the strong phase separation behavior of the oligomer-polymer blend. The defined dimensionless numbers also show a similar trend with change of k from 1 to 0.01 as shown in Figure 2.16. To

demonstrate the feasibility of this work, the conventional phase diagrams of the PEPB blend and PE/paraffin oil blend are calculated and shown in Figure 2.17. In the figure, both blends start phase separation at around 140°C. In one phase, the volume fraction of PE is close to zero, which can be assumed as pure liquid oligomers. While in the second phase, the volume fraction of PE shows significant difference. Before the blends are cooled to ~50°C, the PE/paraffin oil blend shows stronger phase separation with a larger volume fraction of PE in the second phase. However, when the blends are cooled to room temperature, the phase separation behavior of the PE/PB blend is much stronger. The results of the simulated phase diagrams are consistent with the experimental data in comparison of the bulk gel properties.

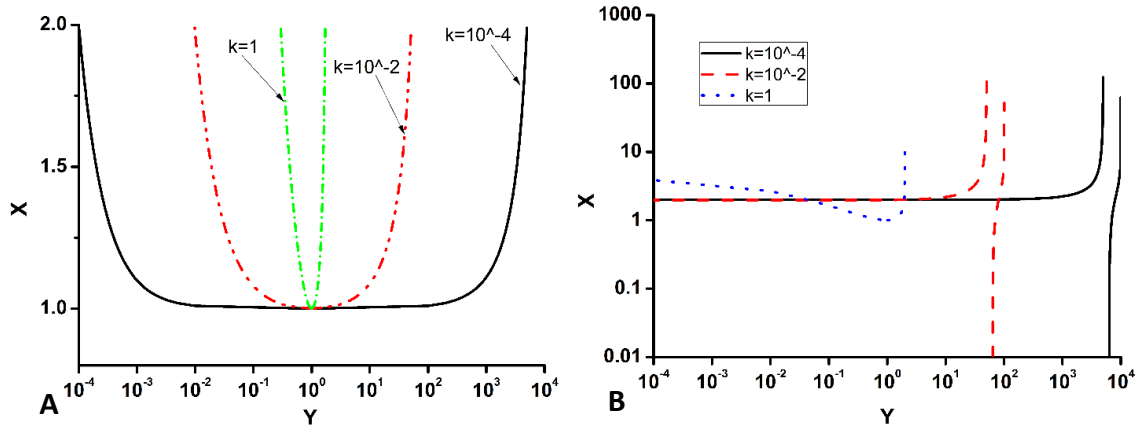


Figure 2.14. The effect of k on dimensionless curves: (A) spinodal curve; (B) binodal curve

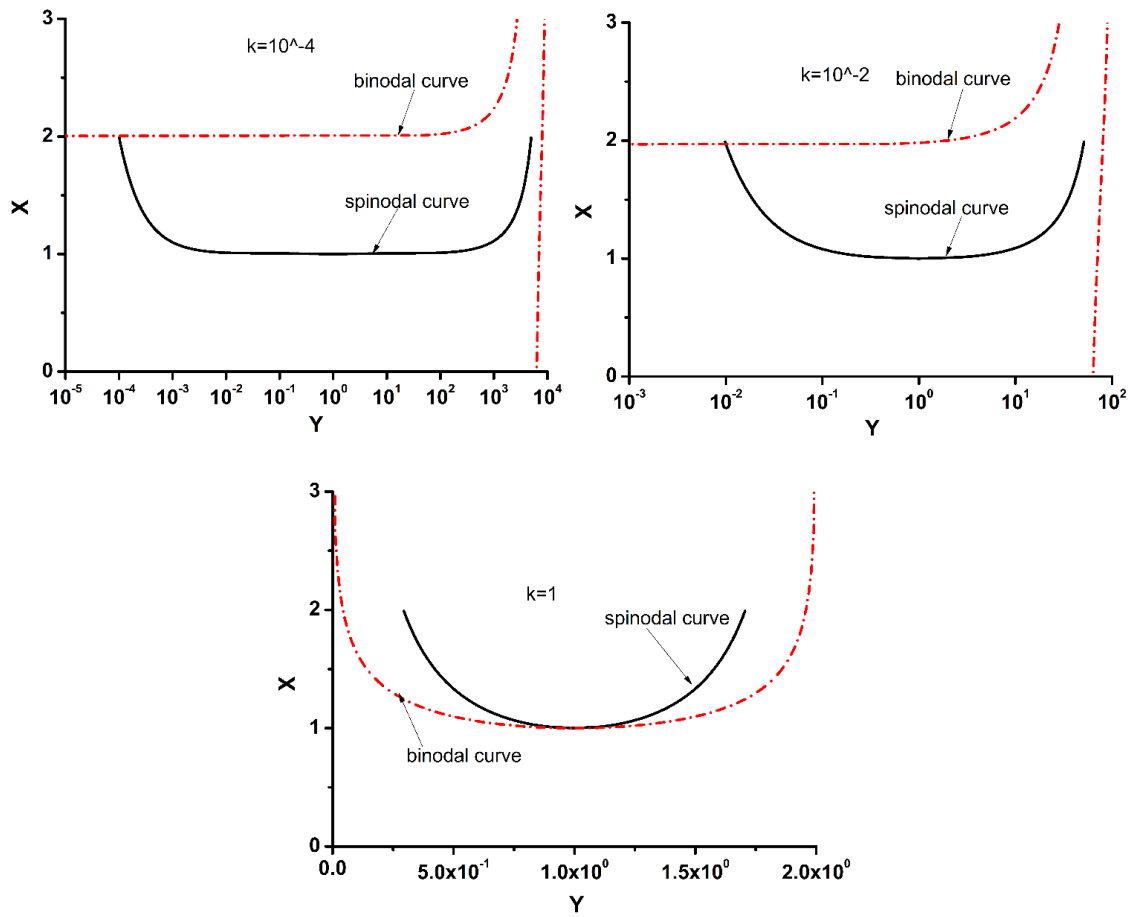


Figure 2.15. The effect of k on dimensionless phase diagrams

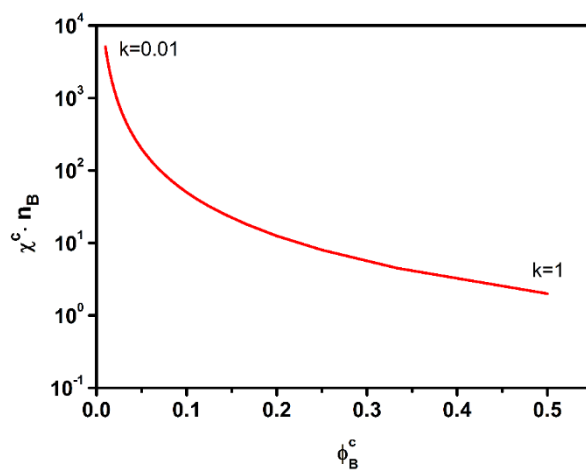


Figure 2.16. Variation of the dimensionless critical point when k is reduced from 1 to 0.01

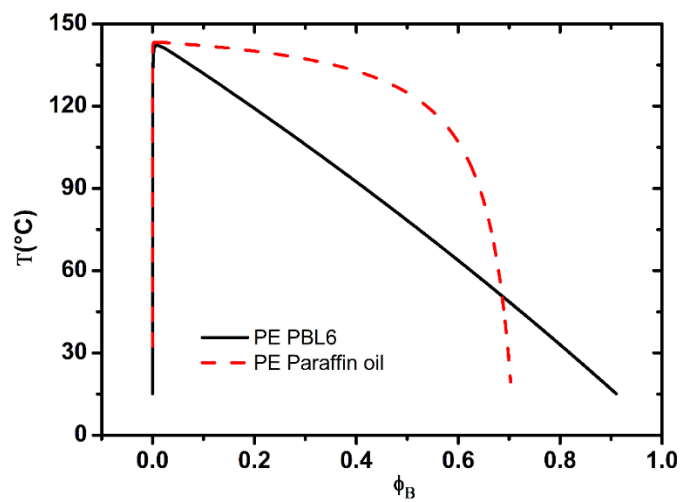


Figure 2.17. Simulated spinodal curves of PE/PB solution and PE/paraffin oil solution

2.5 Recommendations and Outlook

In this study, gel spinning of high strength UHMWPE fibers with PB as a new spin solvent was demonstrated. The concept of oligomer/polymer blend was used to explain the gelation behavior of PB/UHMWPE. The PB/UHMWPE gels show stronger phase separation than the paraffin oil/UHMWPE gel, and lower concentration can be used to create spinnable solution. This suggests that it should be possible to spin the PB/UHMWPE gel at a lower concentration and possibly improve the tensile properties. This paper only provides an initial study for feasibility demonstration. As PB is stable in a broad range of temperature, it is highly possible to optimize the process windows to further improve the mechanical properties. The improved phase separation in the gel, as compared to that in the paraffin gel, may also help develop more effective solvent extraction methods and improve the overall process efficiency.

2.6 Conclusions

In this study, PB was introduced as a new solvent for gel spinning of high strength, continuous UHMWPE fibers. The gelation behavior of PB/UHMWPE was investigated and compared with gels of paraffin oil/UHMWPE. It is found that the gels of PB/UHMWPE show larger phase separation at a low concentration than the gels of paraffin oil/UHMWPE. Particularly, this is supportive to the concept of oligomer/polymer blend. UHMWPE was mixed with PB, an oligomer with similar repeating units to form the gel for spinning fibers. With A 98/2 wt% of PB/UHMWPE gel, PE fibers with strength of 4 GPa can be obtained. DSC and rheological measurements were used to determine suitable extrusion and drawing

conditions. The results show that the blend is miscible, having a single melting peak under the fiber extrusion condition. It is also demonstrated that tensile strength and Young's modulus increase with increasing draw ratio at the first stage when the total draw ratio is maintained. The high strength fibers show a highly orientated crystalline structure, verified by WAXD.

2.7 References

1. C.R. Choe, K.H. Kim, and K.H. Lee, *Polymer Bulletin*, **22**, 293 (1989).
2. P. Smith, P.J. Lemstra, J.P.L. Pijpers, and A.M. Kiel, *Colloid and Polymer Science*, **259**, 1070 (1981).
3. Smith, P. and P.J. Lemstra, *Journal of Materials Science*, **15**, 505 (1980).
4. A. Pennings, R. Van Der Hooft, A. Posterma, W. Hoogsteen, and G. Ten Brinke, *Polymer Bulletin*, **16**, 167 (1986).
5. P. Smith and P.J. Lemstra, *Die Makromolekulare Chemie*, **180**, 2983 (1979).
6. P.J. Barham and A. Keller, *Journal of Materials Science*, **20**, 2281 (1985).
7. H.K. Jen, W.L. Chen, Y.M. Chang, and C.T. Ke, *Journal of Materials Science*, **32**, 3607 (1997).
8. X.M. Shi, Y. Bin, D. Hou, Y. Men, and M. Matsuo, *Polymer Journal*, **46**, 21 (2014).
9. T. Wyatt, Y. Deng, and D. Yao, *Polymer Engineering & Science*, **55**, 745 (2015).
10. Y. Zhang, C. Xiao, G. Jia, and S. An, *Journal of Applied Polymer Science*, **74**, 670 (1999).
11. A.P. De Boer and A. Pennings, *Journal of Polymer Science: Polymer Physics Edition*, **14**, 187 (1976).
12. P. Smith and P.J. Lemstra, *Polymer Bulletin*, **1**, 733 (1979).

13. C. Anton, M. Mackley, and S. Solbai, *Polymer Bulletin*, **17**, 175 (1987).
14. T. Kunugi, S. Oomori, and S. Mikami, *Polymer*, **29**, 814 (1988).
15. C. Sawatari and M. Matsuo, *Polymer*, **30**, 1603 (1989).
16. M.M. Zwick, *Fiber spinning and drawing*, **6**, 109 (1967).
17. J. Smook, M. Flinterman, and A. Pennings, *Polymer Bulletin*, **2**, 775 (1980).
18. A. Pennings, M. Roukema, and A. Van der Veen, *Polymer Bulletin*, **23**, 353 (1990).
19. B. Kalb and A. Pennings, *Journal of Materials Science*, **15**, 2584 (1980).
20. A.V. Savitsky, I.A. Gorshkova, I.L. Frolova, G.N. Shmikk, and A.F. Ioffe, *Polymer Bulletin*, **12**, 195 (1984).
21. M. Xiao, J. Yu, J. Zhu, L. Chen, J. Zhu, and Z. Hu., *Journal of Materials Science*, **46**, 5690 (2011).
22. Z. Maghsoud and H. Moaddel, *Iranian Polymer Journal*, **16**, 363 (2007).
23. W. Hoogsteen, G. Ten Brinke, and A. Pennings, *Polymer*, **28**, 923 (1987).
24. Y. Ohta, H. Murase, and T. Hashimoto, *Journal of Polymer Science Part B: Polymer Physics*, **48**, 1861 (2010).
25. Y. Ohta, H. Murase, and T. Hashimoto, *Journal of Polymer Science Part B: Polymer Physics*, **43**, 2639 (2005).
26. M. Kakiage, T. Tamura, S. Murakami, H. Takahashi, T. Yamanobe, and H. Uehara, *Journal of Materials Science*, **45**, 2574 (2010).

27. Z.W. Wilchinsky, *Journal of applied physics*, **30**, 792 (1959).
28. Z.W. Wilchinsky, *Journal of Polymer Science Part A-2: Polymer Physics*, **6**, 281 (1968).
29. T.P. Wyatt, A.T. Chien, S. Kumar, and D. Yao, *Polymer Engineering & Science*, **54**, 2839 (2014).
30. G. Wypych, *Handbook of Plasticizers*, Chem. Tech. Publishing, Toronto, Canada, p. 46, 2004.
31. D. Paul and J. Southern, *Journal of Applied Polymer Science*, **19**, 3375 (1975).
32. T. Jian, W.D. Shyu, Y.T. Lin, K.N. Chen, J.T. Yeh, *Polymer Engineering & Science*, **43**, 1765 (2003).
33. A. Zhang, K. Chen, H. Zhao, and Z. Wu, *Journal of Applied Polymer Science*, **38**, 1369 (1989).
34. H.T. Chiu and J.H. Wang, *Journal of Applied Polymer Science*, **70**, 1009 (1998).
35. Y. Ohta, H. Murase, H. Sugiyama, and H. Yasuda, *Polymer Engineering & Science*, **40**, 2414 (2000).
36. W. Cox and E. Merz, *Journal of Polymer Science*, **28**, 619 (1958).
37. V. Galitsyn, E. Ro, Y.S. Koval, A. Genis, N. Machalaba, P. Pakhomov, S. Khizhnyak, and E. Antipov, *Fibre Chemistry*, **43**, 33 (2011).

3 Twist-Film Gel Spinning of Large-Size and High Performance UHMWPE Monofilaments

ABSTRACT

A novel twist-film gel spinning process was developed for large-size and high performance ultra-high molecular weight polyethylene (UHMWPE) monofilaments. In this process, twisting is demonstrated as an effective way to significantly reduce consumption of extraction solvent by more than 70%. Applying twisting to the gel film makes conventional solvent extraction proceed significantly faster. Besides solvent extraction efficiency is greatly improved, UHMWPE monofilaments can be obtained with diameter about 80 μm while tensile strength is still over 3.2 GPa, which cannot be completed with conventional processes. Compared to the conventional ones, this process is more efficient and cost-effective for commercialization of high performance and large-size UHMWPE monofilaments. It is expected to promote broad expansion of such monofilaments into various applications.

Key words: twist, film, gel spinning, UHMWPE, fiber, high strength

3.1 Introduction

UHMWPE fibers have been investigated for decades to meet requirements of various high-performance applications. Generally UHMWPE fibers are produced in small diameter about 20 μm with high strength of 3 GPa or above using the gel spinning process [1]. Nonetheless, large-diameter monofilaments with shapes of ribbon, strips or tapes are also essential in industry. They can be used for composites, dental floss, fish line, and other line products [2, 3]. For example, oriented monofilaments with high stiffness and strength can be used as reinforcements in single-polymer polyethylene composites [4] suitable for protective and ballistic applications [5]. In this case, large-diameter monofilaments have incomparable benefits over small ones. They do not need to be made into yarns and the possibility of interfacial defects is reduced [6]. However, large-diameter polyethylene monofilaments produced by traditional processes typically have low mechanical properties and this greatly hinders their use in high-performance applications. In the past decades, a considerable amount of work has been done to improve the strength of such filaments.

Different processing techniques have been attempted to make high-strength polyethylene filaments with large diameters. Improvement of strength has been achieved over decades. In the 1950s, melt extrusion was initially used to obtain polyethylene tapes [7]. By melt extrusion and jet stretching, tapes with thickness greater than 5 mm can be produced. Continuous lengths of polyethylene tapes with uniform cross-sectional thickness can be produced at relatively low temperature, but the strength of such extruded tapes is low due to the lack of orientations [8]. Calendering has also been reported for making large-size polyethylene ‘threads’ or filaments [2, 9]. UHMWPE powders were

fed between a combination of endless belts disposed in an up and down opposing relationship. The powders were compression molded at a temperature below melting point between the endless belts and then rolled and stretched into an oriented profile. Slitting of the resulting tapes, sheets, films or filaments with a heated knife can obtain items of a particular size that can be applied in a specific application. One major processing limitation with this process is that either the thermomechanical history needs to be precisely regulated or the production line is quite long with endless rollers. Furthermore, strength of the monofilaments obtained with this powder-calendering process is still quite limited. The reason might be high concentration of entanglements limiting orientation of polymer chains [10], as well as the lack of strong fusion bonding between powders.

In the 1970s, gel spinning was developed as a special solution spinning process for making high-performance UHMWPE fibers. This process has also been attempted to obtain high-strength large-diameter UHMWPE monofilaments [11-14]. However, application of the standard gel spinning process for making large-diameter monofilaments is limited for the following reasons. First, solvent extraction becomes extremely slow for large-diameter filaments, making the standard process uneconomical and essentially impractical. For instance, it may take hours or even days to satisfactorily remove spin-solvent in a gel fiber with diameter larger than 1 mm. Second, large heat-transfer gradient in the radial direction during quenching of the large-diameter gel-fiber increases defects and structural non-uniformity. Skin-core effect is more significant and the resulting fiber has much reduced tensile strength [15, 16].

Even though conventional gel spinning is not effective, processes using its mechanism were developed to obtain large-diameter UHMWPE fibers. In one representative process, extruded UHMWPE tapes or filaments were swollen with a suitable solvent like paraffin oil at high temperature, and then gel was formed by quenching. The solvent was extracted with a second type of solvent or removed by evaporation. High-strength tapes or filaments were obtained by hot drawing the dried gels [3, 17, 18]. Such processes were effective in improving tensile strength of extruded filaments/profiles, achieving strength in the range of 1.2-1.6 GPa. This strength, however, is still quite low compared with those of directly gel-spun fibers. The process is also relatively complex and the solvent extraction/removal stage is subject to similar disadvantages as experienced by conventional gel spinning [10]. Modifications were made recently by eliminating the solvent removal step. The ‘plasticizer’ was kept inside the tape or filament [17]. This somewhat simplifies the process but does not effectively improve the strength.

Several other processes have also been tried to obtain high-strength large-diameter monofilaments. One process is based on the concept of single-polymer composites by selectively melting the surface portion of bundled fibers to bind the filaments together followed by compression of the fiber bundle to form a large-diameter monofilament [19]. In this method, however, it is difficult to precisely control the processing temperature and time in order to achieve partial melting of the fiber surface. The fibers are also severely annealed at elevated temperature, leading to greatly reduced mechanical properties. To improve the strength and modulus, a modified process was proposed. High-strength multi-filament yarns with c-axis orientation factor over 0.96

were compressed and drawn in several temperature zones with accurate control of tension force to obtain monofilaments [20]. With this modification, strength as high as 2 GPa can be achieved. Nevertheless, this method is compromised by complicated drawing procedures in multi-temperature zones. If the yarns are produced at high cost, this method is not suitable for producing monofilaments to a large scale.

From the literature survey, it can be seen that few processes are available for producing large-diameter high-strength monofilaments. The strength of such monofilaments, in general, is much lower than those of gel spun fibers. Therefore, there is a large impetus to develop new, more enabling process to fill this technical gap.

In the current work, a new twist-film gel spinning process was developed for making large-diameter high-strength UHMWPE monofilaments. This new process is an extension of the standard gel spinning process, with key features added to enable fabrication of large-diameter filaments. Instead of standard circular fibers, films are first extruded out of a UHMWPE solution. Mechanical twisting is then applied to the film to remove most of the spin solvent and form a helical precursor. After additional solvent extraction, the precursor is drawn in multiple stages to obtain a high-strength monofilament with diameter of approximately 80 μm and strength of 3.2 GPa.

3.2 Experimental

3.2.1 Mixing of the Blend

The oligomer-polymer blend of UHMWPE with polybutene was used for gel spinning of film. The UHMWPE used is a Ticona (Celanese) GUR resin, in powder form,

with weight-average molecular mass about 4 million Da. The polybutene with trade name Indopol PB L-6 and number-average molecular mass 280 was supplied by INEOS Oligomers Inc. The Indopol PB L-6 has a viscosity of 7 cSt at 40°C. The spin dope was prepared by combining UHMWPE powder with PB at 20°C and stirring the mixture in a beaker while heating to 150°C. The mixture was then poured into a preheated batch mixer (C.W. Brabender Prep-Center fitted with twin roller blades) and mixed for 20 min at 150°C to obtain a homogenized solution as shown in Figure3.1 (I).

3.2.2 Gel Spinning of the Film

The schematic of the film gel spinning process for UHMWPE is shown in Figure3.1 (II). Spinning was completed through an Alex James and Associates piston extruder with a 2.54 cm bore diameter and 150 mL capacity. The homogenized PB/UHMWPE solution was quickly transferred into the bore (preheated to 150°C) of the extruder from the batch mixer and allowed to equilibrate for 20 min. The solution was then extruded through a slot die with dimension of 10 mm×1mm as shown in Figure3.1 (II), which was maintained at a temperature of 150°C. The film extrusion speed was set to ~0.5 m/min. The UHMWPE film was freely extruded into a 4 cm air-gap and quenched into ethanol at 20°C. The quenched gel-film was transferred from the ethanol bath to storage under ambient conditions until needed for further processing.

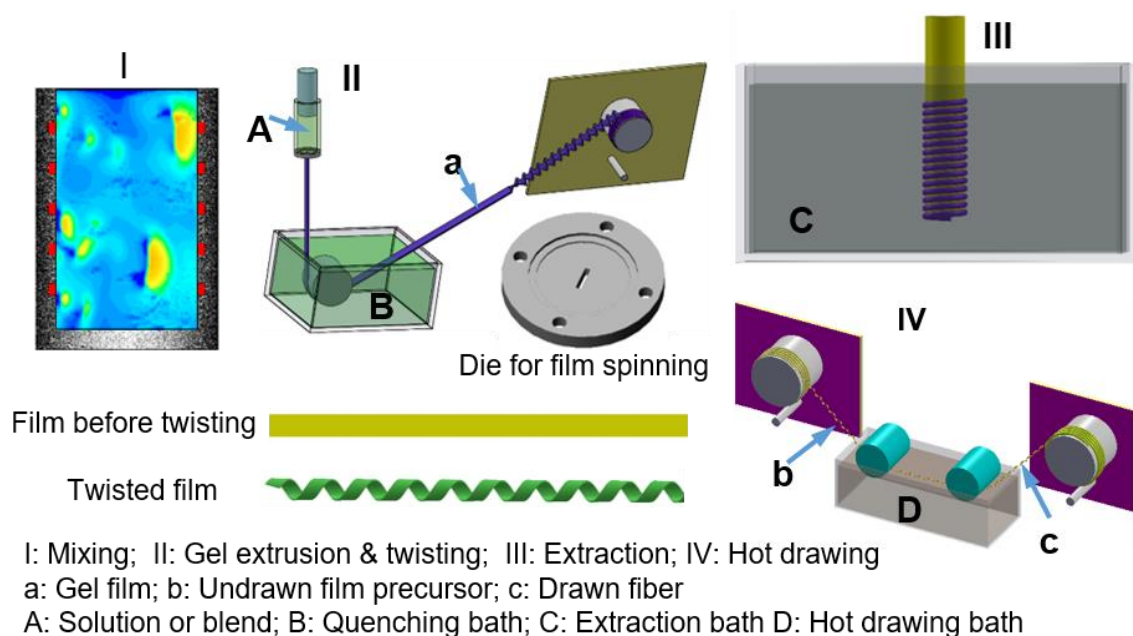


Figure 3.1. Schematic of twist-film gel spinning process

3.2.3 *Twisting and Extraction of the Gel Film*

Solvent removal is a critical stage for gel spinning process. The gel fibers/films need to be fully extracted before drawing to achieve high strength. For the gel-spun films, most of the solvent PB was removed by mechanical twisting, and the residue was extracted with the setup as shown in Figure 3.1 (III). The twisted gel-film was wound onto a 1 inch diameter polytetrafluoroethylene (PTFE) rod and both ends of the film were fixed to maintain constant length. The rod with wound films was submerged into an agitating bath of n-hexane at ambient temperature for 120 min. Subsequently, they were removed from the hexane bath and dried under forced air convection while fixed film ends were maintained.

3.2.4 Hot Drawing

Hot drawing is an indispensable stage for orientating the twisted-film precursor to reach high mechanical strength. It was performed with three stages through heated polyethylene glycol (PEG) as shown in Figure 3.1 (IV). The total path length through the hot bath was kept at 0.8 m in each stage. The first stage drawing was performed at 90°C with a feeding speed of approximately 0.6 m/min. A collection speed of 4.2 m/min (draw ratio=7) was attempted in the first stage. Draw ratio as used in this paper is defined as the ratio of the collection roller speed to the feed roller speed. The weight induced stretch in the air-gap region was relatively small and neglected compared to the large draw ratio during hot-drawing. The second stage drawing was performed at 110°C with a feeding speed of 1 m/min and a collection speed of 5 m/min (draw ratio=5). For the third stage of drawing, the temperature was set at 130°C. A feeding speed of 1 m/min and a collection speed controlled incrementally from a minimum of 1.2 m/min to a maximum limited by the drawability of the fiber. The maximum draw ratio was determined by stepwise increasing the third stage collection speed at appropriate time intervals until fiber breakage. Fibers were drawn at each incremental ratio to obtain samples at least 6 m long for testing.

3.2.5 Characterization

The diameter of fibers was measured by weighing a known length of fiber and calculating the cross-sectional area. Before weighing, the hot-drawn fibers were briefly rinsed with ethanol to remove residual PEG from the hot-drawing stage and dried with forced air convection.

The tensile properties of fibers were measured using an Instron 5566 universal testing machine. Fiber samples were wound onto wooden rods approximately 2 mm in diameter and super-glued over the wound fiber ends. Crosshead speed was 100 mm/min with a gauge length of ~10 cm. All tensile tests were performed under ambient conditions (40-60% relative humidity at 20-22°C). Four samples from each type of fiber were tested and averaged.

The instrument used for obtaining differential scanning calorimetry (DSC) data was a TA Q200 DSC unit (TA Instruments). Samples were sealed in hermetic aluminum pans. Nitrogen atmosphere and a heating rate of 10°C/min were used for all samples. Thermal gravitational analysis (TGA) was performed using a TA TGA5000 (TA Instruments). Samples were heated to 350°C in nitrogen atmosphere and held at this temperature until the weight change approached a steady value. The rheological data were collected with a TA AR2000EX parallel-plate rheometer (TA Instruments). Fiber surface and appearance were observed by an optical microscope (Olympus BX51 optical microscope installed with an Olympus UC30 digital camera).

Wide angle x-ray diffraction (WAXD) data were collected on a Rigaku Micro Max 002 (Cu K α radiation, $\lambda=0.154$ nm) operating at 45 kV and 0.65 mA using an R-axis IV++ detector. Exposure time was 120 min for all samples. Diffraction patterns were analyzed with AreaMax V1.00 and MDI Jade 6.1. The crystalline orientation factor was calculated with the method developed by Wilchinsky [21]. The 110 and 200 azimuthal diffractions were used to determine the orientation factor based on the orthorhombic UHMWPE unit cell [22]. Raman spectra of the twisted-film precursor and fibers obtained at various drawing stages were obtained using a 785 nm laser on a Raman microscope system from

HORIBA Scientific. For Raman spectroscopy, the fiber samples were mounted onto metal tabs and fixed with cyanoacrylate adhesive at both ends. Raman spectra were taken in the VV mode, and the fiber samples were aligned parallel to the polarizer and analyzer. PeakFit software was used to analyze the acquired Raman spectra with Gaussian-Lorentzian curve fitting.

3.3 Results and Discussion

3.3.1 Extrusion of Film from a Slot Die

In this work, large-size monofilaments were obtained by hot-drawing of twisted-films extruded from a slot die. The die size is 10 mm×1 mm. The geometry of the die is rectangular instead of a circular shape to reduce the effect of core-shell structure on final fiber strength and drawability [15,16,23]. It is seldom reported to obtain high strength large-size monofilaments directly by drawing extrudates from a circular die.

Concentration of the spin dope is one of the critical parameters that need to be determined to obtain high performance filaments. To obtain high strength PE filaments with gel spinning process, a low concentration spin dope is generally preferred to reduce entanglements between polymer chains [10]. However, the concentration is also limited by factors including the dimension of the die, spinning temperature etc. Continuous filaments cannot be formed at low concentrations due to the low viscosity of the solution under these conditions. In this work, the spinning temperature was set as 150°C, which is slightly higher than the melting peak of PE to assure using the lowest concentration spin dope while the viscosity is above the lower limit. If the temperature was set to a higher value, the viscosity

of the low concentration solution would be below the critical point. An appropriate concentration was determined based on rheological tests of the spin dope. Frequency sweeps of 2% (w/v) and 4% (w/v) PE/PB solutions at a constant temperature of 150°C and constant strain of 1% are shown in Figure 3.2. It can be seen that the storage modulus (G'), loss modulus (G'') and complex viscosity ($|\eta^*|$) for concentration of 4% are much higher than that of 2%. It is demonstrated that continuous and stable film can be spun with 4% spin dope while no stable films can be obtained with the 2% spin dope. Thus, 4% spin dope was selected for the experimental demo. The rheological data can also provide reference for spinning films with this die for other types of materials. It can be experimentally demonstrated that at low frequency (<0.3 Hz), the loss modulus (G'') is larger than the storage modulus (G'). The solution is dominated by viscous behavior instead of elasticity. It can be deduced that the solution should be spinnable in this region by suppressing the elasticity to obtain high strength fiber. For the region at high frequency (>0.3 Hz), the storage modulus (G') is higher than the loss modulus (G''), which means elasticity is dominating the solution. If the solution is spun in this region, notable die swell will occur and fibers obtained will have more defects. Other parameters such as air gap and quench bath can also be determined based on rheological properties of the spin dope. For example, the gelation temperature of the PEPB solution is obtained from parallel plate rheometry, as shown in Figure 3.3. It can be observed that the gelation point is around 110°C, which provides reference for setting air gap and selection of quench bath to quickly obtain gel film/fiber when the solution is extruded out.

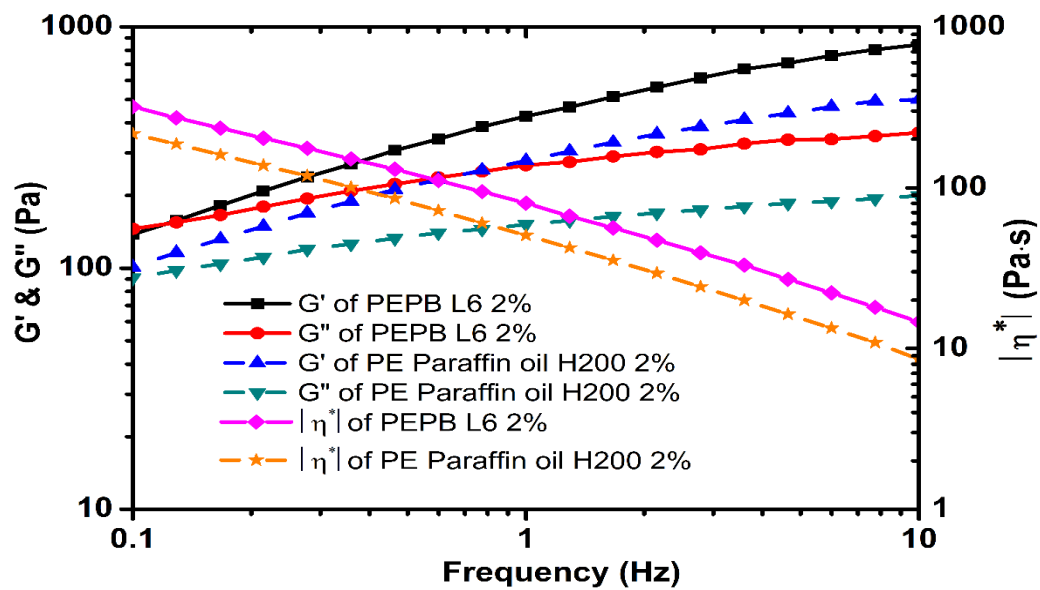


Figure 3.2. Frequency sweep of PEPB solutions with concentration of 2% and 4%

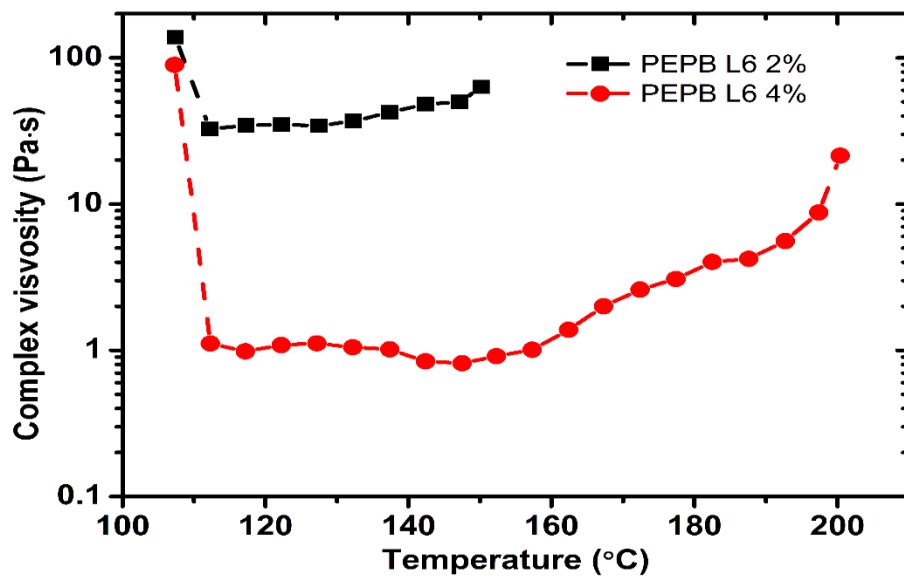


Figure 3.3. Gelation temperature of PEPB solutions with concentration of 2% and 4%

3.3.2 *Effect of Mechanical Twisting on Solvent Removal*

Solvent removal has been a big issue for gel spinning process, which greatly affects manufacturing cost and process efficiency. The conventional methods for removing spin solvents from the gel fiber are typically evaporation and extraction. Evaporation is mainly used for the solvents with high vapor pressure, like decalin. It is so volatile that it is easily volatilized far below its boiling point [24]. However, evaporation cannot be widely applied in industrial manufacturing. One reason is environmental issues. The volatile solvents are usually toxic and cannot be directly emitted into atmosphere, which need complex procedures to recycle. Another reason is that long ovens are indispensable for hot drawing the corresponding fibers to fully evaporate the volatile solvents, which increases manufacturing cost of the final fiber [25, 26]. For nonvolatile spin solvents such as paraffin oil, extraction with a second type of solvent is commonly used. The extraction technology is a key parameter to improve process efficiency and drawability of the UHMWPE gel fibers. Amounts of study have been done for improving extraction efficiency for certain types of spin solvents. The effect of paraffin oil concentration on the extraction time has been investigated to prove that the extraction solvent needs to be continuously replaced by pure solvent in a continuous process of fiber production [27]. The solvent separation and extraction dynamics of different concentration solutions were also studied [28]. It was indicated that the phase separation of different concentration UHMWPE gel fibers were only severe in the first hour and several days were needed to reach an equilibrium state. The root reason for low efficiency is that extraction is based on diffusion which is limited by concentration gradient and chemical interaction etc. [29]. Typically, the concentration of UHMWPE solution for gel spinning is about 6-8 wt%. Under such conditions, 12-15

times amount of spin solvent and around 1000 times or more extraction solvent will be used for producing 1 unit of UHMWPE fibers. Some spin solvent and extraction solvent will be inevitably wasted during the solvents' recycling processes, which will cause environmental issues and increase cost of the final fibers. Thus, an alternative way for fast extraction of solvents is urgently needed to improve process efficiency and reduce manufacturing cost.

In this work, mechanical twisting was introduced as an effective way for fast solvent removal. It is nontoxic and nonflammable with minimal generation of solvent by-product while simultaneously increasing the process efficiency. A majority of spin solvent from the gel film was removed by mechanical twisting. To quantitatively study the effect of twisting on solvent removal, the mechanical solvent removal was performed by fixing one end of the gel film and attaching the other end to a motor with adjustable rotations per minute (rpm). After twisting, a soft tissue was used to gently remove any residue solvent droplets from the bottom of the film. The amount of mechanical twisting applied to the gel film is defined as turns per mm (TPMM) given by

$$TPMM = \frac{t \cdot rpm}{L} \quad (1)$$

Where L is the length between the two ends of the film in mm, t is the time for twisting in minutes, and rpm is the rotations per minute. A TPMM from 0 to 3 was applied to the gel film by varying the removal time, and the resultant mass loss from the gel film was measured. The weight percentage remaining (W_r , %) is assumed to be entirely from removal of the spin solvent, which can be calculated simply by

$$W_r = \frac{W_{after}}{W_{before}} \times 100\% \quad (2)$$

The values W_{before} and W_{after} are the gel film weight before and after twisting, respectively. The weight percentage remaining as a function of TPMM is plotted in Figure 3.4. As shown in the figure, the gel film weight can be reduced to ~35% by twisting to ~3 TPMM. Further increase in TPMM does not significantly increase solvent removal; however, excess deformation of the gel film occurring at higher TPMM leads to instability of the process and may reduce mechanical performance of the final hot drawn fiber. A majority of the spin solvent is removed in the initial stage of twisting when TPMM ranges from 0 to 1.

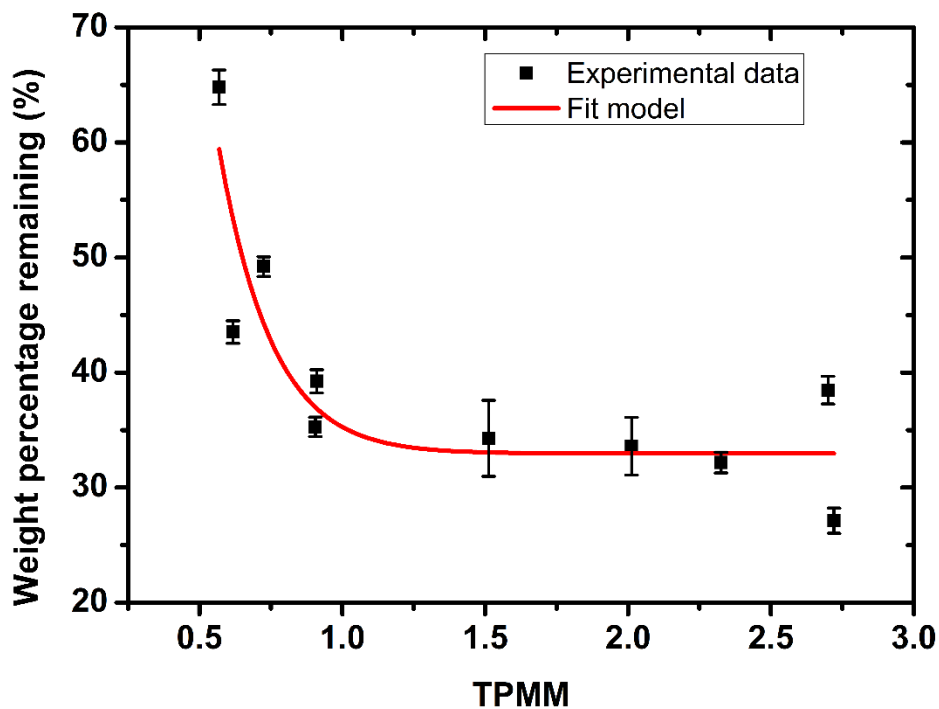


Figure 3.4. Weight percentage remaining as a function of the amount of twist applied.

The polybutene residue in the gel films after twisting was also measured by TGA, as shown in Figure 3.5. The neat polybutene is completely gone in about 25 minutes while neat UHMWPE remains about 100% under such conditions [10]. The gel film has

about 80% of spin solvent inside instead of 96% in the spin dope, which results from simultaneous phase separation at room temperature. With twisting applied, the concentration of spin solvent in the gel film decreases. It can be seen that the concentration of spin solvent reduces to ~30% when TPMM=1. The results are consistent with that in twisting experiments and validate that a majority of the spin solvent in the gel film can be removed by mechanical twisting.

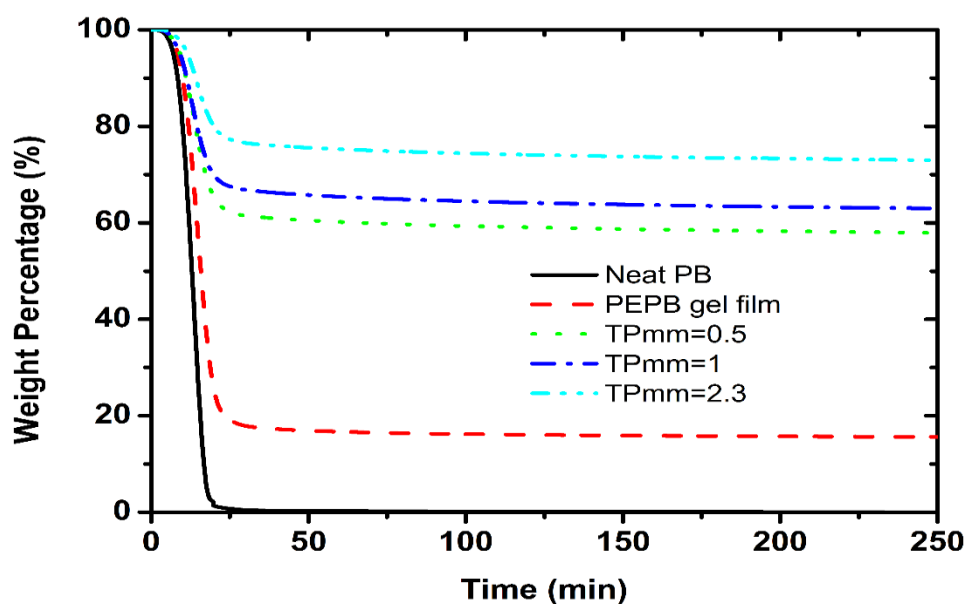


Figure 3.5. TGA weight loss curves as a function of time. Films heated to 300°C in nitrogen atmosphere for 240 min to fully remove polybutene. Neat polybutene is used as a reference.

3.3.3 Effect of Twisting on Fiber Properties

As demonstrated, mechanical twisting plays a significant role in removing spin solvents from the gel film. However, the effect of twisting on the properties of the final

fiber still needs to be investigated. It was reported that, for melt-spun PE fibers, twisting either as-spun or drawn fibers decreased the axial orientation, modulus, tensile strength and also the elongation to break [30]. The changes in these properties increased with twist angle. However, as shown in our previous work, for small-size gel-spun UHMWPE fibers, the effect of twisting on fiber properties was quite different [29]. It was demonstrated that twisting largely enhanced solvent extraction effectiveness while the fiber properties were not reduced. As little information about twisting of large-size gel-film can be found, the effect of twisting on gel-spun film and the final hot drawn fiber was investigated in this study.

The effect of twisting on as-spun UHMWPE/PB gel films was studied with DSC. As shown in Figure 3.6, the melting peak of the twisted films shifts to higher temperature with increase of TPMMs. One possible reason is the increased polyethylene concentration in the gel film after removing a portion of the spin solvent. With reduction of the compatible component PB, the melting peak of the gel film shifts to that of neat PE. Another possible reason is that twisting causes transformation of a small fraction of the film to the monoclinic form of polyethylene [30]. With comparison of the melting peaks, it can be found that the melting peak continuously increases from the bulk gel to the film with TPMM of 1. It can be inferred that the film is slightly oriented both in the extrusion stage and the twisting process. However, the melting peaks do not have significant variation among the films from TPMM of 1 to TPMM of 2.7. This has similar trend as the effect on solvent removal. With a certain degree of twisting, a majority of the spin solvent can be removed and the film can be moderately orientated. Over-twisting does not show a significant impact on improving solvent removal and orientation of the as-spun film.

Besides the impact on as-spun gel film, more concern is about the effect of twisting on performance of the final fiber. This was investigated based on optimized hot drawing conditions. For gel spinning of small-size UHMWPE fibers, hot drawing was usually completed in two stages to convert the ‘shish-kebab’ structure to ‘shish’ to achieve high strength by drawing to a large ratio [10]. As no reports are available for hot drawing of the twisted-films, trials were done with the conditions of small-size UHMWPE fiber as a reference. The drawing temperature, stages of drawing and the draw ratio at each stage are critical to tensile properties of the fibers. The temperature at each stage should be set appropriately to avoid melting the fiber while enabling long-range molecular rearrangements of polymer chains. For gel spun UHMWPE fibers, the favorable drawing temperatures were in the range of 80-148°C [31]. It was demonstrated with trials that three stages of drawing were an optimal condition for obtaining high strength final fibers. The drawing temperature at each stage was 90, 110 and 130°C, respectively.

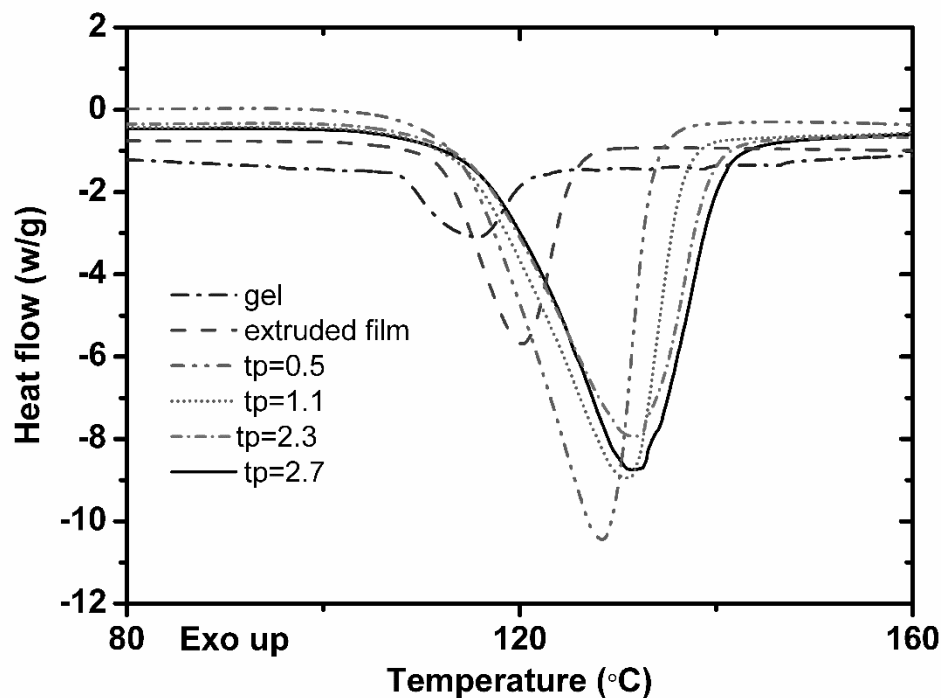


Figure 3.6. DSC endothermal melting peaks of UHMWPE/PB gel, extruded film and twisted-films with different TPMs.

The effect of twisting on final fiber properties was examined by hot drawing the twisted precursor films in three stages with optimized draw ratios to achieve the highest strength. In order to hot draw effectively, the spin solvent should be almost completely removed from the twisted-gel film before hot drawing. Excessive spin solvent residue in the gel film suppresses the melting temperature, thereby reducing the maximum drawing temperature that the film can undergo. If the twisted film precursors are oriented at relatively low temperatures, the tensile strength can be significantly reduced due to creation of defects [32]. Thus, the twisted gel films were soaked in agitated hexane for 2 hrs while maintaining fixed length for complete extraction before hot drawing.

After hot drawing the twisted gel films with optimized drawing ratios to reach high strength, the effect of twisting on final fiber diameter and total draw ratio can be obtained. As shown in Figure 3.7, the final fiber diameter increases from $\sim 65\ \mu\text{m}$ to $\sim 100\ \mu\text{m}$ when TPMM is applied from 0 to ~ 3 . Correspondingly, the total draw ratio decreases from ~ 135 to ~ 60 with the increase of TPMM. One possible reason for the reduced draw ratio at high TPMM is the low efficiency in heat transfer with large amounts of helical patterns. The nonuniformity of heat distribution from surface to core limits drawability of the whole film precursor. Hence, the diameter of the final hot-drawn fiber is much larger due to low draw ratio. While for the precursor films with low TPMM, they can be heated fast to be drawn to a large ratio. However, the films directly drawn to a large ratio may have 'slit film fiber' or 'fibrous film', which is detrimental to their mechanical performance [33].

The effect of twisting on mechanical properties of final hot-drawn fibers is also obtained based on the optimized drawing ratios. As shown in Figure 3.8, the tensile strength increases to $\sim 3.2\ \text{GPa}$ when twisting is applied at TPMM of 1. However, with continuous increase of TPMM, the tensile strength decreases significantly. The effect of twisting on Young's modulus of the final fiber shows a similar trend. The Young's modulus reaches a maximum value of $\sim 140\ \text{GPa}$ when TPMM equals 1. Thus, the optimal twisting condition for obtaining high strength fiber from the gel-film precursor is TPMM of 1. After being twisted, the film precursor is hot drawn for three stages at 90, 110 and 130°C , with draw ratio of $\times 7$, $\times 5$ and $\times 2.5$ at each stage, respectively. The ultimate tensile strength of the final fiber is $3.184 \pm 0.059\ \text{GPa}$ and the Young's modulus is $144.3 \pm 12.5\ \text{GPa}$. Representative tensile curves of the final hot-drawn fibers are shown in Figure 3.9. The size of the final fiber is around $\sim 80\ \mu\text{m}$ in diameter. The results demonstrate that large-size

and high performance UHMWPE monofilaments can be obtained with twist-film gel spinning process. With a certain amount of twists applied, a majority of spin solvents can be removed while maintaining high mechanical property of the final filaments.

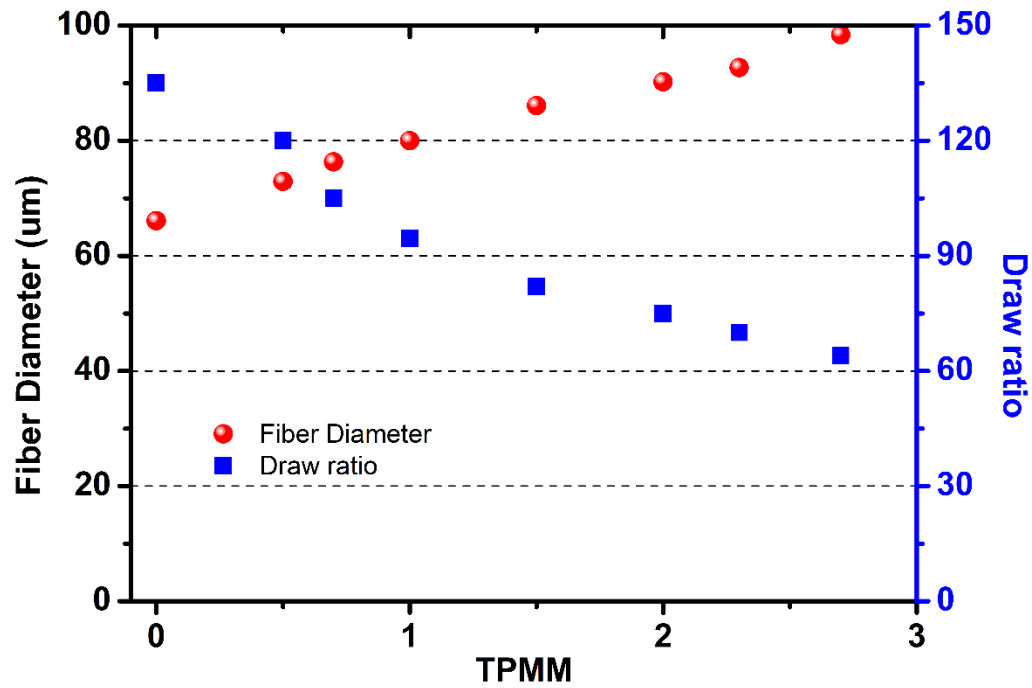


Figure 3.7. The effect of twisting on final fiber diameter and total draw ratio

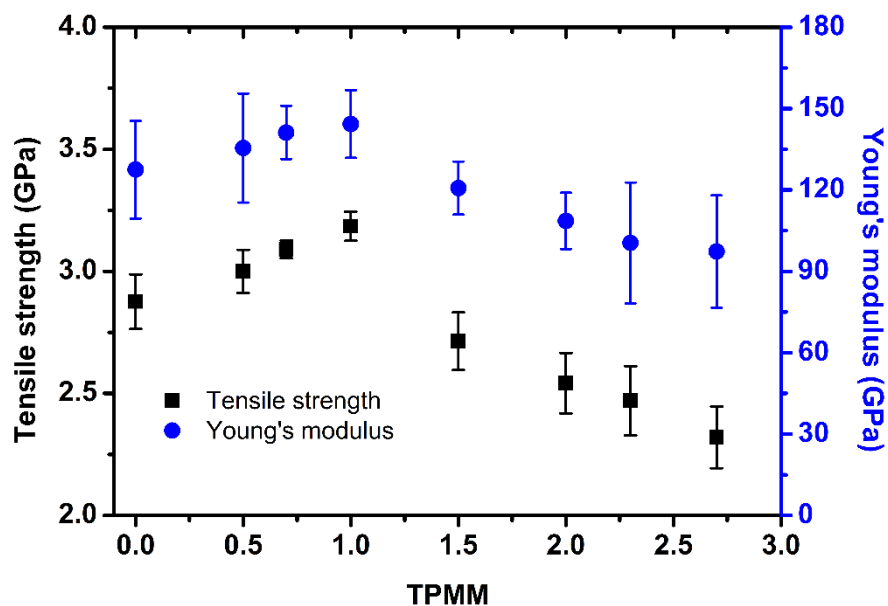


Figure 3.8. The effect of twisting on final fiber tensile strength and Young's Modulus

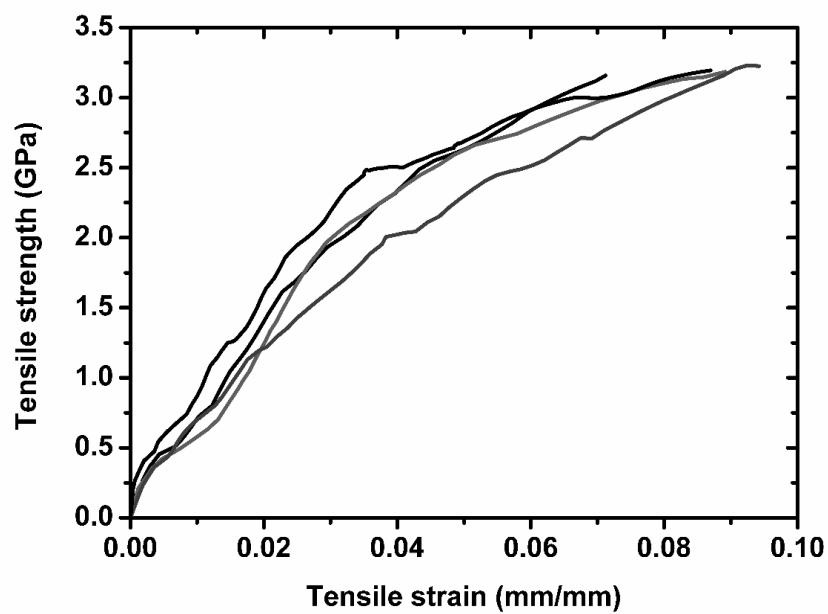


Figure 3.9. Representative tensile strength vs tensile strain curves for large-size UHMWPE fibers obtained with three stages of hot drawing.

3.3.4 *Fiber Morphology and Structure*

The surface appearance of the twisted film precursors, and fibers hot drawn at each stage was examined. The twisted precursors were prepared by applying the desired amount of twisting (TPMM=1) and then extracting with hexane to fully remove residue at fixed length. The fiber samples were collected by hot-drawing the precursors. Optical images of the precursor and fibers at each stage are shown in Figure 3.10. From Figure 3.10 (A), the helical appearance indicates the twist applied becomes visible at a TPMM of 1. Meanwhile, it also indicates that the twist applied was well preserved through extraction in hexane and drying, and the TPMM applied to the gel films can be considered permanent after drying. The dried twisted film precursors did not show an obvious tendency to unwind even when unconstrained. With increase of drawing, the helical patterns on the fiber surface are less as shown in Figure 3.10 (B)-(D). The final drawn fibers do not show obvious helical appearance but some marks, which may be formed by the helical patterns during drawing. The helical patterns are hard to observe at a hot-draw ratio of 35 as shown in Figure 3.10 (C). This observation is understandable as the film precursor has been extended for 35 times, so the initial TPMM has been decreased by a factor of 35. For the initial TPMM of 1, the net TPMM after 35 times drawing is approximately 0.03. With such a low TPMM, the helical patterns should only appear every 33 mm; hence, with the current length scale under the microscope, the twisting effect is difficult to be noticed. At the final stage of hot drawing, the actual TPMM becomes 0.01. Therefore, the twisted film precursors after three stages of hot drawing have almost the same surface appearance on a length scale of around 100 mm compared to that without twisting except the marks left in drawing stages.

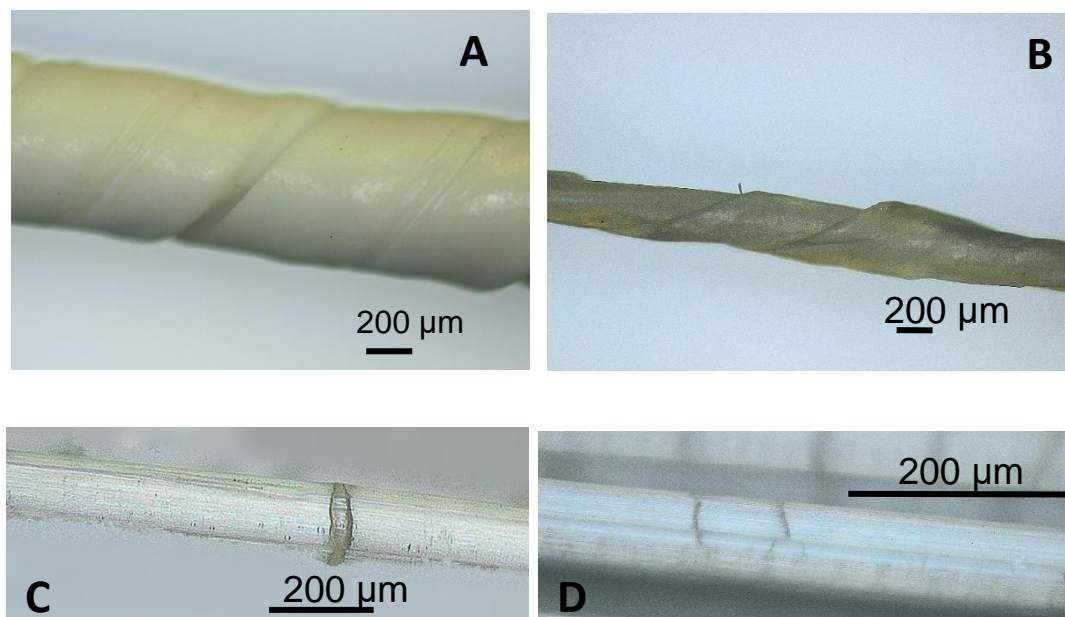


Figure 3.10. Optical images of UHMWPE fibers obtained by twist-gel spinning process: (A) precursor; (B) 1st stage with draw ratio $\times 7$; (C) 2nd stage with draw ratio $\times 35$; (D) 3rd stage with draw ratio $\times 94.5$

The structure of the fibers at each drawing stage was examined with X-ray. The WAXD patterns are shown in Figure 3.11. In Figure 3.11 (A), the twisted film precursor shows diffractions along the equator and meridian indicating crystalline orientation parallel and perpendicular to the fiber axis. The perpendicular orientation is typical for polyethylene gel fibers spun and extracted with solvents [34]. It can be deduced that the orientation along the equator mostly is caused by twisting. With hot drawing, it can be observed that the C-axes of the crystallites is orientated along the drawing direction in each stage. The diffractions along meridian gradually disappears. Particularly, the fibers at second stage and third stage show significant orientation parallel to the fiber axis while almost no orientation in perpendicular direction. To quantitatively describe the orientation

development in the drawing stages, azimuthal integrations along specified crystallization directions are obtained. The azimuthal integrations of the [110] and [200] diffractions are plotted in Figure 3.12. The azimuthal width of each direction decreases significantly when the fiber is drawn into the next stage. While the intensities at both directions increase greatly with the increase of draw ratio. Based on the data of these two directions, the orientation factor for orthorhombic UHMWPE crystallite can be calculated with Herman's method as shown in Table 3.1. The orientation factor keeps increasing with progress of hot drawing. By comparing the orientation factors, it can be inferred that the orientation mainly occurs in the first and second stage, as the orientation factor shows only slight increase in the third stage.

In the calculation of orientation factor, it is found the structure of these large-size and high-performance UHMWPE monofilaments is different from the small-size ones. As shown in the publications, orientation of UHMWPE fibers by hot drawing is mostly in the [110] and [200] directions [10, 29, 34]. However, the filaments obtained by twist-film gel spinning process are different, as shown in Figure 3.13. In the total integrations of intensity with diffraction angles, a peak at $\sim 40.4^\circ$ corresponding to the crystallite direction [011] appears and becomes comparable to the peak of [200] when hot drawing is completed [69]. By comparing the relative intensities of the three major peaks, it can be inferred that orientation is mainly focused on [110] and [200] direction in the precursor film and the first stage fiber. While in the second and third stages, orientation of the fiber is more likely to happen in [200] and [011] direction. One possible reason for the fiber inclined to orientate in [011] direction is the twist applied before hot drawing.

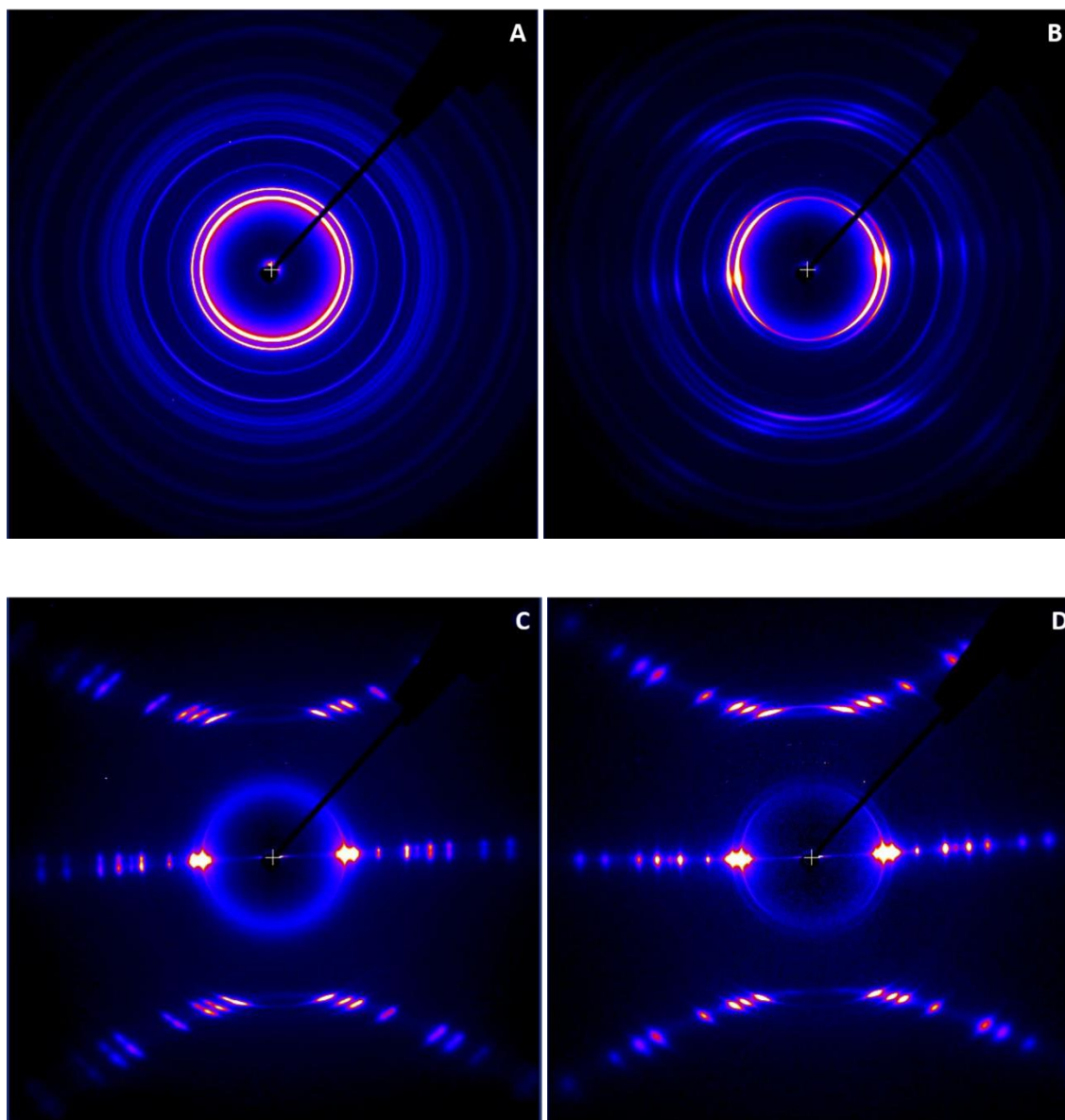


Figure 3.11. WAXD 2D patterns of UHMWPE filaments at different drawing stages: (A) twisted film precursor; (B) 1st stage drawing 7 \times ; (C) 2nd stage drawing 35 \times ; (D) 3rd stage drawing 94.5 \times .

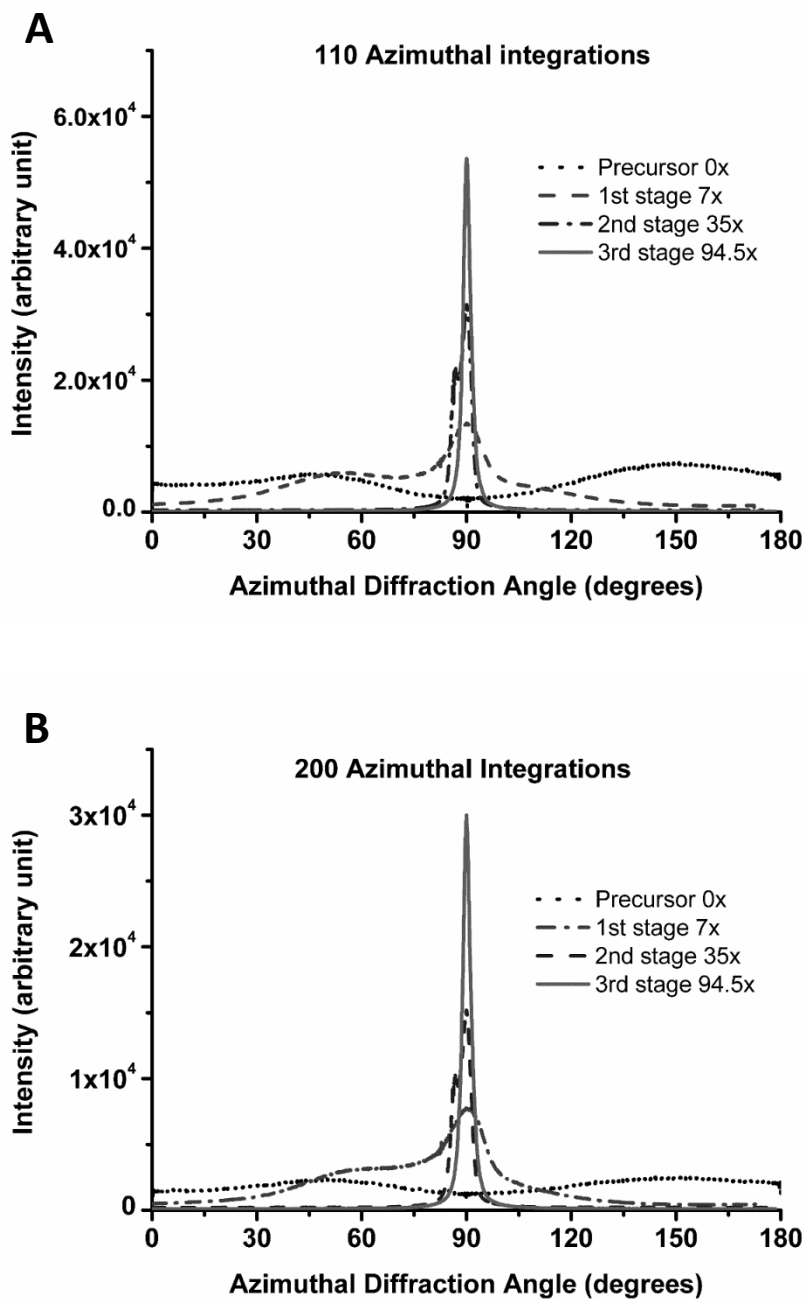


Figure 3.12. Azimuthal integrations of UHMWPE filaments at different drawing stages:

(A) [110] direction; (B) [200] direction

Table 3.1. Orientation factors of UHMWPE filaments at different drawing stages

Fiber type	Orientation factor
Precursor	-0.0902
1 st stage 7x	0.4334
2 nd stage 35x	0.8093
3 rd stage 94.5x	0.8985

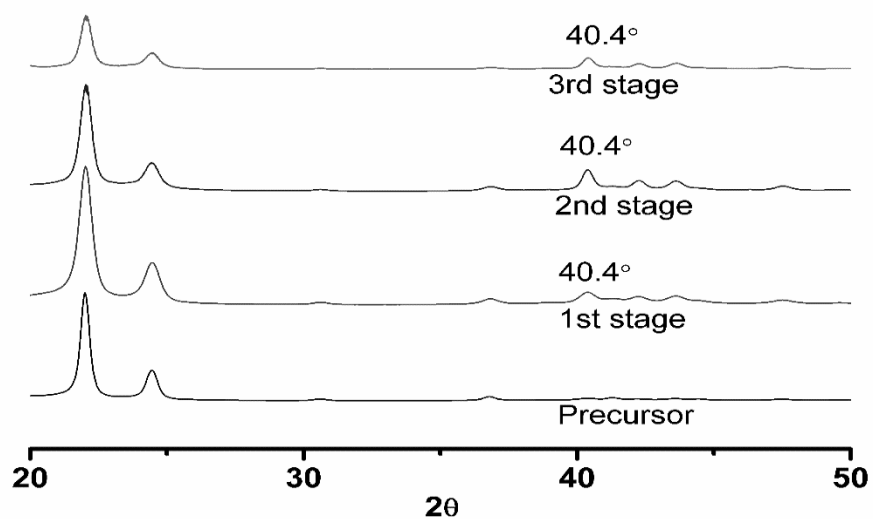


Figure 3.13. Wide-angle X-ray diffractograms of large-size UHMWPE monofilaments obtained by twist-film gel spinning process

The structure of the fibers was also examined with Raman spectroscopy. Figure 3.14 shows the Raman spectra of UHMWPE filaments at different drawing stages. It can provide consistently reliable information about structural and morphological changes in the fibers. With the well established assignments of the observed vibration bands in the wavenumber region $900\text{--}1500\text{ cm}^{-1}$, crystallinities of the fibers can be calculated [36-38]. From the method proposed by Strobl and Hagedorn, it is possible to estimate the relative amounts of the orthorhombic crystalline phase [39]. For the crystalline fraction, the integrated intensity of the 1416 cm^{-1} band (assigned to CH_2 bending) is used. It can be observed that with further drawing, the relative intensity of this band compared to the largest peak at 1125 cm^{-1} keeps increasing, which infers the crystallinity of the fiber is improved by orientation. Meanwhile, by comparing the spectra of the twisted precursor and the first stage fiber, it is found the bands 1024 cm^{-1} (assigned to CC stretching) and 1270 cm^{-1} (assigned to CH_2 twisting) are diminished, which represents a majority of the amorphous phase [40]. This is consistent with WAXD measurements that the fiber is orientated and crystallized by hot-drawing to convert amorphous regions into lamellae [41]. By hot-drawing from the first stage to the third stage, the peak around 1060 cm^{-1} continues to diminish while the peak around 1416 cm^{-1} increases, which can support the selected orientations at such stages in WAXD measurements. For the band around 1300 cm^{-1} , which is assigned as interphase between crystalline and amorphous, almost no change is observed in the first stage while a huge decrease is obtained in the second stage. This phenomenon has not been reported before, which needs further investigation.

With analysis of the morphology and structure of the filaments during hot drawing, it seems the effects of twisting are clearer. First, in the process of solvent removal by

mechanical twisting, a polymorphic transformation is induced through slip or shear mechanism to yield a small amount of new crystalline phase, presumably the monoclinic polyethylene [42]. The monoclinic crystalline phase is supported by the WAXD pattern of orientated precursors and the broad peak around 1416 cm^{-1} in Raman spectra. The crystalline induced by twisting is maintained until the filament is drawn at 90°C for the first stage. Hot drawing increases the perfection and periodicity of the stacking of lamellar crystals, and causes the monoclinic polyethylene to transform to the orthorhombic crystal. Thus, with further drawing in the second stage and third stage, the orientation of filaments is continuously improved and more orthorhombic crystals are obtained. The effect of twisting on fiber morphology and structure is gradually diminished by hot drawing to a large ratio. With three stages of hot drawing, helical patterns are hardly observed on the fiber surface and the crystalline phase is orthorhombic. Tensile strength and Young's modulus of the fibers are significantly increased but the elongation to break is decreased.

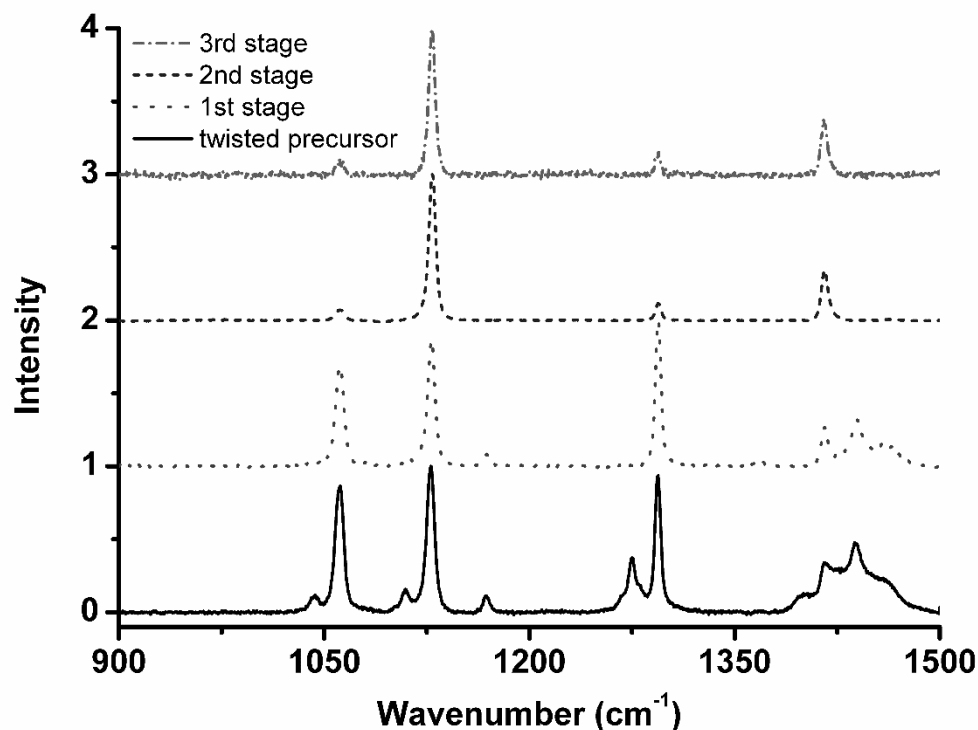


Figure 3.14. Raman spectra of UHMWPE monofilaments at various drawing stages

3.4 Conclusions

In this work, a noval twist-film gel spinning process was introduced for large-size and high performance UHMWPE monofilaments. Using a slot die, uniform films can be spun with optimized spin dope concentration and extruding conditions, which were determined based on DSC and rheological measurements. Mechanical twisting was used to remove spin solvents from the films. It was demonstrated as an effective way to remove as much as 70% of the spin solvent without consumption of extraction solvents. To obtain high strength final filaments, three stages of hot drawing were developed for the twisted-

film precursors. Based on optimal hot-drawing conditions, the effect of twisting on final fiber diameter, drawability, tensile strength and Young's Modulus was quantitatively investigated. It is found with TPMM of 1, PE monofilaments with strength of 3.2 GPa and diameter of 80 μm can be obtained, which have wide potential applications such as dental floss and fish line etc. WAXD and Raman were used to study the fiber structure change from twisted-film precursor to the final hot-drawn filament. The results show that orientation and crystallization of the filaments mainly occur in the first and second stage. It is also demonstrated that the effect of twisting on fiber structure is gradually eliminated in the hot-drawing stages. The monoclinic crystalline phase induced by twisting will be transformed to orthorhombic crystals by hot drawing.

3.5 References

1. Barham, I.P. and A. Keller, *High-strength polyethylene fibres from solution and gel spinning*. Journal of materials science, 1985. **20**(7): p. 2281-2302.
2. Kobayashi, S., et al., *Process for the continuous production of high-strength and high-modulus polyethylene material*, 1992, U.S. Patent No. 5,106,555.
3. Zachariades, A.E. and P. Shukla, *Process for obtaining ultra-high modulus line products with enhanced mechanical properties*, 1995, U.S. Patent No. 5,407,623.
4. Hine, P., et al., *A comparison of the hot-compaction behavior of oriented, high-modulus, polyethylene fibers and tapes**. Journal of Macromolecular Science, Part B, 2001. **40**(5): p. 959-989.
5. Rastogi, S., et al., *Unprecedented high-modulus high-strength tapes and films of ultrahigh molecular weight polyethylene via solvent-free route*. Macromolecules, 2011. **44**(14): p. 5558-5568.
6. Cook, R.B., *Manufacture of polyolefin fishing line*, 2000, U.S. Patent No. 6,148,597.
7. Samler, L.F., *Polyethylene tape extrusion*, 1950, U.S. Patent No. 2,499,421. 7
8. Heeley, E., et al., *Effect of processing parameters on the morphology development during extrusion of polyethylene tape: An in-line small-angle X-ray scattering (SAXS) study*. Polymer, 2013. **54**(24): p. 6580-6588.
9. Weedon, G.C., C.P. Weber Jr, and K.C. Harding, *Ultra high molecular weight polyethylene ballistic structures*, 2008, Google Patents.

10. Fang, X., et al., *Gel spinning of UHMWPE fibers with polybutene as a new spin solvent*. Polymer Engineering & Science, 2016.
11. Kavesh, S. and D.C. Prevorsek, *Producing high tenacity, high modulus crystalline article such as fiber or film*, 1985, U.S. Patent No. 4,551,296. .
12. Zachariades, A.E., *Ultra-high-molecular-weight polyethylene products including vascular prosthesis devices and methods relating thereto and employing pseudo-gel states*, 1987, U.S. Patent No. 4,655,769.
13. Hikmet, R., P. Lemstra, and A. Keller, *X-linked ultra high strength polyethylene fibres*. Colloid and Polymer Science, 1987. **265**(3): p. 185-192.
14. Lemstra, P.J., *Novel irradiated polyethylene filaments tapes and films and process therefor*, 1991, U.S. Patent No. 5,066,755.
15. Kakiage, M., et al., *Hierarchical constraint distribution of ultra-high molecular weight polyethylene fibers with different preparation methods*. Journal of materials science, 2010. **45**(10): p. 2574-2579.
16. Ohta, Y., H. Murase, and T. Hashimoto, *Structural development of ultra-high strength polyethylene fibers: Transformation from kebabs to shishs through hot-drawing process of gel-spun fibers*. Journal of Polymer Science Part B: Polymer Physics, 2010. **48**(17): p. 1861-1872.
17. Motooka, M., H. Mantoku, and T. Ohno, *Process for producing stretched articles of ultrahigh-molecular-weight polyethylene*, 1985, Google Patents.

18. Van Unen, L.H., P.B. Pluyter, and W.M. Pontenagel, *Process for the production of thin stretched films from polyolefin of ultrahigh molecular weight*, 1990, U.S. Patent No. 4,948,544.
19. Ward, I.M., P.J. Hine, and K. Norris, *Process for producing polymeric materials*, 1997, U.S. Patent No. 5,628,946.
20. Tam, T., et al., *High strength ultra-high molecular weight polyethylene tape articles*, 2012, U.S. Patent No. 8,236,119.
21. Wilchinsky, Z.W., *On crystal orientation in polycrystalline materials*. Journal of applied physics, 1959. **30**(5): p. 792-792.
22. Wilchinsky, Z.W., *Determination of orientation of the crystalline and amorphous phases in polyethylene by X-ray diffraction*. Journal of Polymer Science Part A-2: Polymer Physics, 1968. **6**(1): p. 281-288.
23. Ohta, Y., H. Murase, and T. Hashimoto, *Effects of spinning conditions on the mechanical properties of ultrahigh-molecular-weight polyethylene fibers*. Journal of Polymer Science Part B: Polymer Physics, 2005. **43**(19): p. 2639-2652.
24. Smith, P., et al., *Ultrahigh-strength polyethylene filaments by solution spinning and hot drawing*. Polymer Bulletin, 1979. **1**(11): p. 733-736.
25. Lemstra, P., et al., *Fibres based on ultra-high molecular weight polyethylene: processing and applications*. Solid phase processing of polymers/Ed. IM Ward, PD Coates, MM Dumoulin, KS Hyun, 2000: p. 172.

26. Smith, P. and P.J. Lemstra, *Ultrahigh-strength polyethylene filaments by solution spinning/drawing, 2. Influence of solvent on the drawability*. Die Makromolekulare Chemie, 1979. **180**(12): p. 2983-2986.
27. Maghsoud, Z. and H. Moaddel, *Gel spinning characteristics of ultra-high molecular weight polyethylene and study on fibre structure before drawing*. Iranian Polymer Journal, 2007. **16**(6): p. 363-373.
28. Xiao, M., et al., *Effect of UHMWPE concentration on the extracting, drawing, and crystallizing properties of gel fibers*. Journal of materials science, 2011. **46**(17): p. 5690-5697.
29. Wyatt, T., et al., *Direct drawing of gel fibers enabled by twist-gel spinning process*. Polymer Engineering & Science, 2015. **55**(6): p. 1389-1395.
30. Sze, G.M., J.E. Spruiell, and J.L. White, *The influence of drawing, twisting, heat setting, and untwisting on the structure and mechanical properties of melt-spun high-density polyethylene fiber*. Journal of Applied Polymer Science, 1976. **20**(7): p. 1823-1847.
31. Wyatt, T.P., et al., *Development of a gel spinning process for high-strength poly (ethylene oxide) fibers*. Polymer Engineering & Science, 2014. **54**(12): p. 2839-2847.
32. Hoogsteen, W., G. Ten Brinke, and A. Pennings, *The influence of the extraction process and spinning conditions on morphology and ultimate properties of gel-spun polyethylene fibres*. Polymer, 1987. **28**(6): p. 923-928.

33. Harding, K.C. and G.C. Weedon, *Multiple calender process for forming non-fibrous high modulus ultra high molecular weight polyethylene tape*, 2010, U.S. Patent No. 7,740,779. 22.
34. Weedon, G.C., C.P. Weber Jr, and K.C. Harding, *Ultra high molecular weight polyethylene fibers*, 2005, Google Patents.
35. Eichhorn, S.J., et al., *Handbook of Textile Fibre Structure, Volume 1 - Fundamentals and Manufactured Polymer Fibres*, Woodhead Publishing. p. 84.
36. Tasumi, M. and T. Shimanouchi, *Crystal vibrations and intermolecular forces of polymethylene crystals*. The Journal of Chemical Physics, 1965. **43**(4): p. 1245-1258.
37. Painter, P.C., M.M. Coleman, and J.L. Koenig, *Theory of vibrational spectroscopy and its application to polymeric materials*. 1982: Wiley.
38. Luu, D.V., L. Cambon, and C. Lapeyre, *Caractérisation des phases dans le polyéthylène par effet Raman*. Journal of Raman Spectroscopy, 1980. **9**(3): p. 172-175.
39. Strobl, G. and W. Hagedorn, *Raman spectroscopic method for determining the crystallinity of polyethylene*. Journal of Polymer Science: Polymer Physics Edition, 1978. **16**(7): p. 1181-1193.
40. Rull, F., et al., *Estimation of crystallinity in polyethylene by Raman spectroscopy*. Journal of Raman spectroscopy, 1993. **24**(8): p. 545-550.

41. Galitsyn, V., et al., *Change in the structure of a polyethylene fiber, obtained by the gel-formation method, during its orientational drawing*. Fibre Chemistry, 2011. **43**(1): p. 33-40.
42. Kiho, H., A. Peterlin, and P. Geil, *Polymer deformation. VI. Twinning and phase transformation of polyethylene single crystals as a function of stretching direction*. Journal of Applied Physics, 1964. **35**(5): p. 1599-1605.

4 Gel Spinning of High Strength Polyoxymethylene Fibers

ABSTRACT

A novel gel spinning process is introduced for producing high strength polyoxymethylene (POM) fibers in this work. The POM gel-spinning process was enabled through an oligomer-polymer blend instead of conventional organic solvents, and the gelation properties were investigated. An 80/20 wt. % caprolactam/POM gel exhibited a melting temperature about 145°C and was highly stretchable by hot drawing. Some outstanding features of a gel-spun POM fiber with a draw ratio of 40 are that tensile strength at break is 2.01 ± 0.11 GPa, Young's modulus is 40.60 ± 0.69 GPa. The drawability and tensile strength are significantly improved compared to those previously reported. Wide-Angle X-ray Diffraction and Raman Spectroscopy were used to show good molecular orientation along the fiber direction and high crystallinity. The results also demonstrate the mechanical properties can be further improved with this gel spinning process.

Keywords: gel spinning, POM, fiber, caprolactam, high strength

4.1 Introduction

Polyoxymethylene (POM), also known as polyacetal and polyformaldehyde, is a widely used engineering thermoplastic polymer. The bulk mechanical properties of POM are comparable to those of nylon 6 or nylon 66, but POM has much better chemical resistant properties [1]. Since the start of its commercial production in the 1960s the use of POM has spread rapidly in the polymer industry, and various processes including injection molding, extrusion, blow molding and roll milling have been successfully developed for processing POM [2]. Nowadays, molded and extruded POM parts and components with high stiffness, low friction and excellent dimensional stability are used extensively in appliances, machinery, instruments, automobile, marine, aviation, building, and agriculture.

In contrast to its success in molding and extrusion applications, POM has experienced rather slow progress in fiber spinning even though strong fibers with superior chemical resistance are highly demanded in numerous fiber and textile applications [3]. To some extent, POM does meet the basic requirements for fiber formation in melt spinning. It has sufficiently high molecular weight and flexible macromolecules without branches or transverse chemical bonds. It can also be melted at a moderately high melting temperature to transit into a spinnable liquid [4]. However, because of its high crystallization rate, in-fibril voids may occur and formed fibers can easily break during spinning and stretching processes. As a result, long fibers with high strength are difficult to be obtained from melt spinning techniques [5]; melt spun POM fibers typically have much lower mechanical strength than nylon 6 or 6,6 fibers. Moreover, POM can undergo significant thermal degradation above its melting

temperature and, therefore, special measures must be taken to develop a stable spin dope for melt spinning [6].

Besides melt spinning, other methods have also been attempted to obtain high strength or high modulus POM fibers. Hot drawing of melt extrudates or injection-molded specimens was developed in the 1970s. Originally, dumbbell-shaped POM samples were hot-drawn in two stages on a tensile testing machine to obtain filaments [7]. The tensile strength of such filaments reached 1.7 GPa and Young's modulus was about 35 GPa. Afterwards, more follow-up research was done, particularly to improve the heating efficacy during hot drawing. For example, dielectric heating was applied to selectively heat noncrystalline regions to orientate molecular chains during drawing [8]. The highest Young's modulus of 60 GPa was obtained for tube samples. Microwave heating was also attempted during drawing of POM tubes to achieve high strength and modulus [9]. Even though the production of high strength and high modulus POM prototypes was demonstrated, the processes based on hot drawing of extruded or molded specimens was not successfully commercialized due to drawing instability and low production rate. The stretch became unstable when draw ratio exceeded about 10. The low stretchability is related to breakage of crystals and generation of micro-voids during hot drawing [10]. Furthermore, the collected samples had too large cross-sectional size and cannot be used in desired fiber applications.

To mitigate the problem of drawing instability, a pressurized drawing process was developed [11, 12]. POM samples like tubes and rods were drawn in a vessel pressurized by a heated liquid. The application of high pressure was reported to have the effects of reducing drawing tension to reduce sample breakage frequency and preventing formation

of micro-voids [10, 12, 13]. Particularly for cylindrical extrudates, POM filaments with Young's modulus of 50 GPa and tensile strength of 2 GPa can be produced. Nevertheless, like the aforementioned processes, this process lacked productivity and the filaments obtained were quite rigid with diameter in the range of millimeters [5]. The produced filaments were mainly used as geo-textiles. Finer and more uniform fibers are difficult to be obtained with this process.

One latest development about spinning of POM fiber was by synthesis of new POM copolymers. By controlling the half-crystallization time, the modified POM can be melt-spun and then drawn in hot atmosphere to obtain fibers [5]. The reported tensile strength reached 1.4 GPa. Even so, the strength needs further improvement to meet requirements of various high-performance applications.

Among different fiber spinning techniques, gel spinning is a possible way to obtain superstrong polymer fibers, which has potential to be used for POM. This process has been successfully applied to several polymers including polyethylene (PE), polypropylene (PP), and poly (vinyl alcohol) (PVA), generally producing fibers markedly stronger than their corresponding melt or solution spun ones [14-16]. In the melt or solution state, shorter molecular relaxation time makes the macromolecules prefer entropically favorable random-coil conformation, which hinders orientation for high strength. Instead, in the solid or gel state, orientation of the polymers can be kept as the relaxation time is much longer due to the extremely high viscosity of the solid phase or gel-network [17]. However, to the authors' best knowledge, gel spinning has not been tried for POM fibers as no suitable solvents have yet been found to form a gel with POM. It was reported that several types of organic solvents were used for solution spinning of

POM at elevated temperature, but none of them can form a gel network with POM [18]. Thus, to gel spin POM fiber, the first challenge is to find a suitable solvent that can form a thermally reversal gel with POM.

In this study, a gel spinning process for producing high-strength, continuous POM fibers was developed with caprolactam as a spin ‘solvent’, or as a compatible phase in a melt blend, to form a stretchable gel. For gel spinning, selection of a suitable solvent based on the concept of ‘oligomer-polymer’ blend is critical [15, 19]. With caprolactam as a spin ‘solvent’, a tensile strength of 2 GPa and a Young’s modulus of 40 GPa were obtained at a gel/solid draw ratio of 40. The strength is 40% higher than that obtained by melt spinning with the specially synthesized POM copolymer. Compared to the fiber produced with ordinary POM, the gel-spun fibers in this work is more than twice stronger [20]. This study focused on developing a suitable processing receipt for POM gel spinning and investigating the effect of processing on fiber orientation.

The orientation of the gel fiber was completed through three stages of hot drawing. DSC, WAXD and Raman spectroscopy were used to examine thermal properties and structural changes with increase of draw ratio.

4.2 Experimental

4.2.1 Materials

DuPont Delrin[®] POM (polyacetal) homopolymer resin was obtained from DuPont Performance Polymers. The Delrin[®] POM used was an experimental grade resin with a reported density of 1.42 g/cm³ and average molecular weight, $M_n \approx 80,000$ Da. As a

reference, the commercially available Delrin[®] 100P NC010 resin has a reported $M_n \approx 66,000$ Da. Caprolactam was obtained from Brüggemann Chemical. All chemicals were used as received. Municipal water was used for the extraction process. Spin dopes were prepared with two steps. First, mixing POM pellets at 200°C in a C.W. Brabender Prep-Center fitted with twin roller blades until a uniform melt was obtained (approximately 8 minutes). Then caprolactam was slowly added until a uniform solution developed. The concentration of POM in the solution was 20% by weight. Once a uniform solution was obtained, the mixing temperature was reduced to 180°C. The solution was mixed for an additional 3 min before being transferred to the extruder.

4.2.2 Gel Spinning

Fiber spinning was performed through an Alex James and Associates piston extruder with a 2.54 cm bore diameter and 150 mL capacity. The homogenized POM/caprolactam solution was quickly transferred into the bore (preheated to 170 °C) of the extruder and allowed to equilibrate for 30 min. The solution was extruded through a 1 mm die orifice with an aspect ratio of ~15:1 maintained at a temperature of 170 °C. The solution was extruded at a speed of approximately 1.5 m/min. The fiber solution was quenched into a 20 °C water bath 4 cm from the die exit. The quenched gel-fiber was collected onto spools at 15 m/min so as to apply 10 times jet-stretch to the fiber solution as it exited the die. The spools of gel-fiber were stored in a 50% caprolactam/water solution to prevent drying and successive phase separation of caprolactam before extraction and hot-drawing experiments were performed.

4.2.3 Spin Solvent Extraction

Extraction of the spin solvent caprolactam from the gel fiber was completed in warm water. The gel fibers were wound onto a 1 inch diameter polytetrafluoroethylene (PTFE) rod. Both ends of the gel fiber were fixed to maintain unchanged fiber length. The rod as prepared was submerged into an agitated bath of water at $\sim 50\text{ }^{\circ}\text{C}$ for 30 min to fully remove caprolactam. The volume of water was about 5000 times of that of the gel-fiber in order to maintain a maximum concentration gradient throughout the extraction process. The PTFE rod containing the extracted gel-fiber was removed from the water bath and dried under forced air convection while maintaining fixed fiber ends.

4.2.4 Hot-drawing

The extracted precursor fibers were oriented through three stages of hot drawing in a silicon oil bath. The total path length through the hot bath was 0.8 m. The bath temperature was maintained within $\pm 1\text{ }^{\circ}\text{C}$ of the set value. The first stage of hot-drawing was performed at $140\text{ }^{\circ}\text{C}$ with a feeding speed of 1 m/min and a collection speed of 12.5 m/min to obtain a draw ratio of $12.5\times$. The second stage of hot-drawing was performed at $150\text{ }^{\circ}\text{C}$ with a feeding speed of 0.6 m/min and a collection speed of 1.2 m/min to obtain a draw ratio of $2\times$ (total draw ratio $25\times$). The third drawing stage was performed at $160\text{ }^{\circ}\text{C}$ with a feeding speed of 2 m/min and a maximum collection speed of $\sim 3.3\text{ m/min}$, to obtain a draw ratio of $1.65\times$ (total draw ratio ~ 40). Draw ratio used in this work is defined as the ratio of the collection roller speed to the feed roller speed. POM fibers were drawn to the maximum ratio to collect samples at least 10 m long for testing.

4.2.5 Characterization

Differential scanning calorimetry (DSC) data tests were done with a TA Q200 DSC unit (TA Instruments). Samples were sealed in hermetic aluminum pans. Nitrogen atmosphere and a heating rate of 10°C/min were used for all samples. Thermal gravitational analysis (TGA) was performed using a TA TGA5000 (TA Instruments). Samples were heated to 400 °C in nitrogen atmosphere with a heating rate of 20 °C/min to examine weight change. The rheological data were collected with a HAAKE MARS 60 rheometer (Thermo Fisher Scientific). Scanning electron microscopy (SEM) images were collected with a LEO 1550 to inspect the fiber surface and appearance.

Fiber diameter was measured by weighing a known length of fiber and calculating the cross-sectional area assuming a density of 1.42 g/cm³. Before weighing, the hot-drawn fibers were briefly rinsed with hexane to remove residual silicone oil from the hot-drawing stage and dried with forced air convection.

The tensile properties of fibers were measured using an Instron 5566 universal testing machine. Fiber samples were wound onto wooden rods approximately 2 mm in diameter and super-glued over the wound fiber ends. Crosshead speed was 100 mm/min with a gauge length of ~10 cm. All tensile tests were performed under ambient conditions (40-60% relative humidity at 20-22 °C). Around 10 samples from each type of fiber were tested and averaged.

Wide angle x-ray diffraction (WAXD) data were collected on a Rigaku Micro Max 002 (Cu K α radiation, λ =0.154 nm) operating at 45 kV and 0.65 mA using an R-axis IV++ detector. Exposure time was 120 min for all samples. Diffraction patterns were analyzed with AreaMax V1.00 and MDI Jade 6.1. The crystalline orientation factor was calculated

with the method developed by Wilchinsky [21]. The 100 azimuthal diffractions was used to determine the orientation factor based on the hexagonal POM unit cell [22].

Raman spectra of the extracted precursor and fibers obtained in the three drawing stages were obtained using a 785 nm laser on a Raman microscope system from HORIBA Scientific. For Raman spectroscopy, the fiber samples were mounted onto metal tabs and fixed with cyanoacrylate adhesive at both ends. Raman spectra were taken in the VV mode, and the fiber samples were aligned parallel to the polarizer and analyzer. PeakFit software was used to analyze the acquired Raman spectra with Gaussian-Lorentzian curve fitting.

4.3 Results and Discussion

4.3.1 Selection of Solvent for Gel Spinning

The solvent selected is critical for gel spinning process. As is known, gel spinning is only suitable for several types of polymers including PE, PP and PVA. The reason is that suitable solvents can be found to form thermal-reversible gels with the polymers. POM has not been gel-spun due to none suitable solvents discovered. In the gel spinning process, the spin dope prepared by the selected solvent and the polymer should be partially crystallized directly after being extruded to form a solid-like polymer network (gel), but most of the spin-solvent is still maintained inside. The crystallization behavior is critical as it preserves the disentanglements of polymer chains in the spin dope, which is a semi-dilute solution before extrusion. With formation of the gel network, the disentanglement morphology can be maintained in the fiber even after the spin solvent is completely removed. The maintenance of disentanglements is the root reason for high strength and high modulus of gel-spun fiber. Drawing of the disentangled solid-like

precursor fiber can reach a large ratio for high orientation and crystallinity. By comparison, melt-spun fibers of the same polymer, which are also drawn under solid stage, cannot reach high draw ratio and high strength comparable to the gel-spun fibers. The reason is high concentration of entanglements available in the melt-spun fibers [17]. Compared to the conventional solution spinning, the benefit of gel spinning is that the relaxation time of polymer molecules in the gel network is much longer so that orientation of the polymer chains during drawing should not be relaxed to the entropically favorable random coils [19]. With preservation of the orientation, the polymer chains can be aligned to obtain high performance fibers.

To obtain an appropriate spin-solvent for formation of a thermal-revisable gel, a concept of ‘oligomer-polymer’ blend system can be used. In the system, oligomer and polymer have identical or similar chemical repeat units, but vary in number of repeat units. They are intrinsically favorable to each other due to the same or similar repeat units. At elevated temperature, they are possible to be miscible with low Gibbs free energy of mixing. Thus, the feature of this system is that it shows solution-like behavior when temperature is above the melting point of the polymer. While the blend is quenched below the crystallization point of the polymer, distinct gelation can be obtained. With preservation of disentangled morphology in the gel which allows large ratio of drawing in the solid stage, high strength and high modulus fibers can be obtained. This concept has been successfully used for discovering spin-solvents for gel spinning of ultra-high molecular weight polyethylene (UHMWPE), poly(ethylene oxide) (PEO) etc. [15, 19]. As the repeat units of POM are quite close to UHMWPE and PEO, it has high probability to obtain solvents that can form a gel with POM by using this concept.

Caprolactam was selected as such a solvent based on the ‘oligomer-polymer’ blend system and thermal stability of POM. The monomers and comonomers used for POM include formaldehyde, trioxane, ethylene oxide, 1, 2-propylene oxide, tetrahydrofuran, 1, 3-dioxane, 1, 4-dioxane, 1, 3-dioxolane and 1, 3-dioxepane. According to the oligomers that can be formed from the monomers, several types were proposed for forming gels with POM. Paraformaldehyde ($n=10$) was initially attempted to blend with POM. It had a relatively high boiling point but was not stable, and decomposed to formaldehyde when heated. A second oligomer used was polyethylene glycol (PEG) ($n\approx 9$). A relatively stable solution with POM can be formed at 170°C for fiber spinning. When the solution was quenched to ambient temperature, gels can be formed and continuous fiber can be collected. However, one issue was the relatively narrow processing window. The POM would decompose and bubbles generated in the spin dope would greatly decrease the property of the fiber spun after a certain time. To address the stability issue of the solution, addition of amine groups to the oligomers was considered. According to the reports in the literature, the thermal stability of POM can be significantly improved by addition of polyamide [23, 24]. The amide groups provide active hydrogen to absorb formaldehyde generated from decomposition of POM so that the decomposition reaction can be suppressed [25, 26]. Three types of oligomers with addition of amine groups were examined including formamide, acetamide and caprolactam. Compared to the other two oligomers, caprolactam is more stable at elevated temperature up to 270°C. Additionally, it is a low-cost material with production over billion kilograms per year. It was demonstrated with experiments that stable

solutions of caprolactam with POM can be formed at high temperature, which will become gels when quenched to room temperature.

4.3.2 POM/Caprolactam Blend Properties

It was demonstrated that caprolactam can form a gel with POM. However, little information is available about the properties of the gel of POM with caprolactam. In this study, the thermal properties and rheological properties of POM/caprolactam blend was investigated. As shown in Figure 4.1 (A), DSC of a 20% wt. POM/caprolactam blend shows a single melting peak at reduced temperature (144°C) relative to the neat POM (175°C), suggesting complete compatibility and similarity to the UHMWPE/polybutene and PEO/PEG blends [15, 19]. The melting point of POM is suppressed by 31°C with addition of caprolactam. For the crystallization behavior, it shows similar trend that the crystallization peak is reduced from ~148°C to ~124°C after mixing 20% wt. POM in caprolactam.

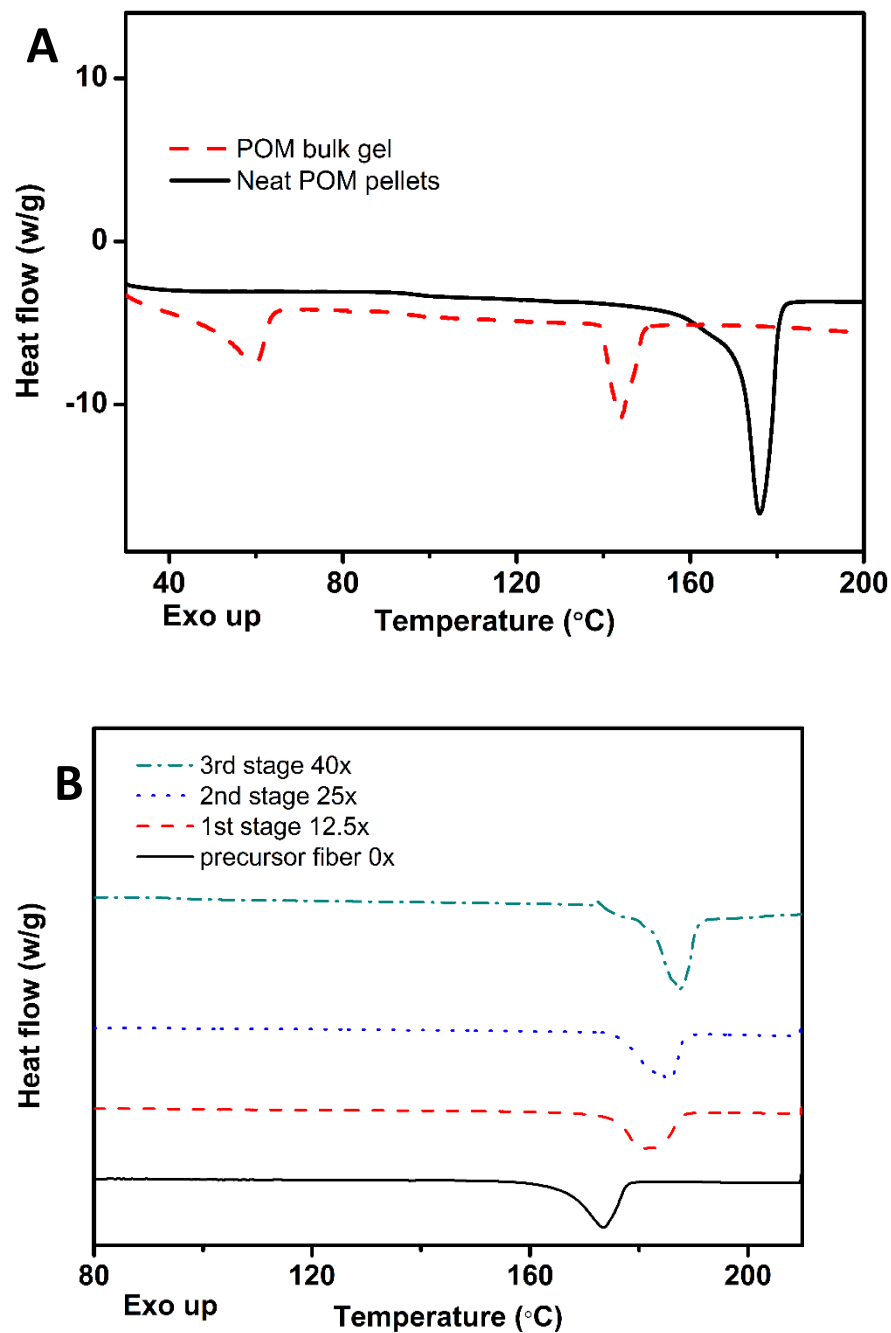


Figure 4.1. DSC heating endotherms of (A) neat POM pellets and 20% POM/caprolactam blend and (B) gel-spun POM fiber at various stages of drawing. The DSC scans were conducted at 10 °C/min in nitrogen atmosphere.

The dynamics of gel formation when POM/caprolactam blends are quenched to low temperature was explored. As has been characterized with UHMWPE and PEO [19, 27], the transition from viscous solution to solid gel can be inferred from a sharp increase of viscosity approaching infinity as measured by parallel-plate rheometry with a temperature sweep from above the melting peak of the neat POM pellets down to the gel transition temperature. Figure 4.2 shows the complex viscosity of the 20/80 POM/caprolactam solution gradually increases when the solution is cooled from $\sim 170^{\circ}\text{C}$ to $\sim 148^{\circ}\text{C}$. At $\sim 148^{\circ}\text{C}$, the viscosity suddenly increases indicating a transition from solution to solid gel. Another method for determination of the gelation temperature is the crossover point of storage modulus with loss modulus in temperature sweep with a parallel-plate rheometry [28]. As shown in Figure 4.2, the crossover point of storage modulus with loss modulus is at $\sim 147.5^{\circ}\text{C}$, which is very close to the value determined from the abrupt change of complex viscosity. The gelation temperature ($\sim 147.5^{\circ}\text{C}$) is very close to the normal crystallization temperature of the POM pellets ($\sim 148^{\circ}\text{C}$) as measured by DSC. These findings are in general agreement with those of the UHMWPE/paraffin oil and UHMWPE/decahydronaphthalene gels [29], indicating that they may have similar thermomechanical behavior. They share the same mechanism that gelation is attributed to liquid-liquid phase separation driven by concentration fluctuations caused by crystallization of the polymer when the solution is quenched. The gels formed are a network of polymer molecules swollen by the oligomer and physically reinforced by crystalline regions.

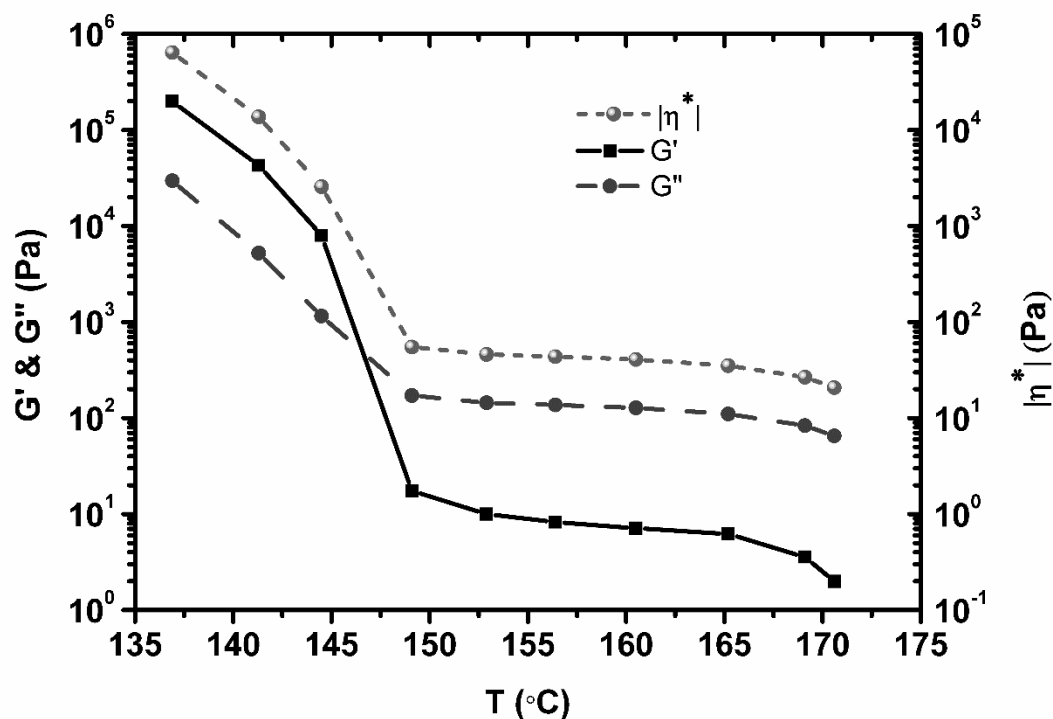


Figure 4.2. Temperature sweep of the POM/caprolactam blend cooling from 170°C by parallel plate rheometry

Viscoelasticity of the POM/caprolactam blend was also investigated to provide support for determination of spinning parameters. In this work, the spinning temperature was set to 170°C. At this temperature, viscoelastic properties of the blend was studied by parallel-plate rheometry to assist in selection of appropriate spinning speed so that die swell and defects in the gel fiber can be reduced. The strain range suitable for linear viscoelasticity study was determined by strain sweep and the data are shown in Figure 4.3(A). It can be seen that the storage modulus (G') and loss modulus (G'') are almost constant in the strain range of 2~ 10%, which was chosen as the targeted region. In this region, frequency sweep was done for the 20% POM/caprolactam solution at 170°C to

examine changes of storage modulus (G'), loss modulus (G'') and complex viscosity ($|\eta^*|$), as shown in Figure 4.3(B). It can be observed that the complex viscosity shows only a slight decrease when frequency is swept from 0.1 to 100 Hz. The storage modulus is always smaller than the loss modulus in the whole frequency zone, which means the solution is dominated by viscous behavior. Using the Cox-Merz rule [15], one may map the frequency behavior to the shear rate space. The upper limit of the spinning speed is determined by the crossover point of the storage modulus with loss modulus.

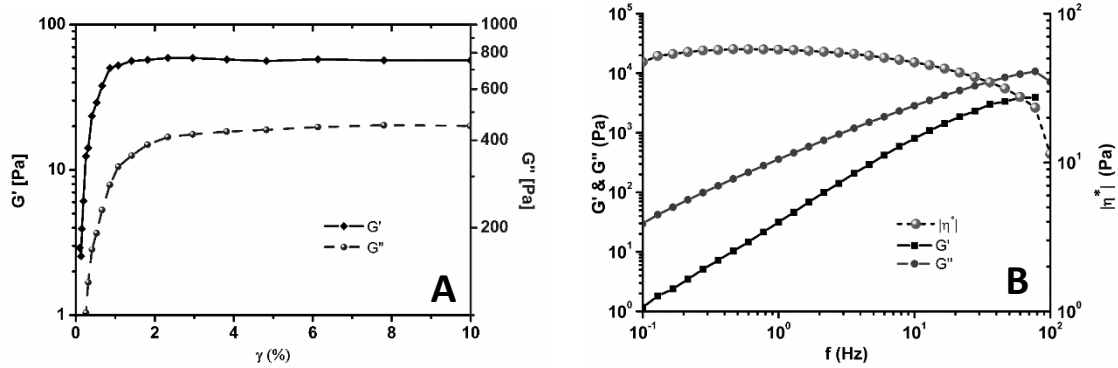


Figure 4.3. Viscoelastic properties of the 20% POM/caprolactam blend at 170°C: (A) linear viscoelastic region determination with strain sweep; (B) frequency sweep with strain of 2.5%

4.3.3 Gel Spinning of POM Fiber

In this work, a 20/80 POM/caprolactam blend was used as a spin dope for spinning POM fibers. Fiber properties can be affected by several parameters including spinning temperature, spinning speed and jet stretch ratio. As caprolactam has high

boiling temperature (270°C), the extrusion temperature was allowed to be manipulated over a broad range so that uniform extrudates can be obtained. This is quite different from conventional solvents, like hexafluoroisopropanol (HFIP), which have significantly low boiling points [30, 31]. An extrusion temperature of 170°C was used throughout this study. The extrusion speed, which is related to viscoelasticity of the spin dope, was set to 1.5 m/min with the collected rheological data as a reference to obtain continuous fibers with smooth surface. Another important parameter to be determined in the extrusion stage is jet stretch ratio. According to the literature about UHMWPE gel spinning, too much jet stretch can be detrimental to the fiber property [14]. Thus, generally, little jet stretch is applied to UHMWPE fiber to reach high strength. However, for POM, a jet stretch ratio of 10 was applied. As the melting point of caprolactam is about 69°C, the extrudate turned to a rigid rod without applying jet stretch after coming out from the 1 mm spinneret. A 10-time jet stretch was found to be adequate for reducing diameter of the fiber so that it can be flexible to wind onto spools. A significant difference of this process from gel spinning of UHMWPE and PEO is that the oligomer used is solid at room temperature. Thus for the extruded POM fibers, besides applying jet stretch to increase flexibility, they need to be stored in the mixture of caprolactam with water. The purpose is to decrease phase separation and segregation of caprolactam plates in the fiber. If the fiber was left in the air to dry and crystallized caprolactam on the fiber surface was removed by mechanical force, the fiber property would be greatly decreased due to increase of defects.

4.3.4 Spin-Solvent Extraction

It was necessary to extract caprolactam before hot drawing to allow high-strength final fiber to be obtained. As learned from drawing of UHMWPE precursor fibers, tensile strength of the final fiber would be significantly lower if drawing is conducted at lower temperature with spin solvents inside [32]. Thus, caprolactam in the gel-fiber was extracted in warm water at ~50°C and then dried with forced air convection before hot drawing. To assure caprolactam is fully removed from the gel fiber, TGA was performed on pure caprolactam, and the POM/caprolactam gel-fiber before and after extraction, as shown in Figure 4.4. The pure caprolactam evaporates almost completely after 10 min at 200°C in nitrogen atmosphere. A similar TGA test on the solvent-rich gel fiber showed a weight reduction of 40% at 200°C which was assumed to be caused by evaporation of the caprolactam component; therefore, the composition of the solvent-rich gel fiber was estimated to be 60% POM and 40% caprolactam. A caprolactam content of about 40% differed from the initial concentration of 80% in the spin dope. The reduced caprolactam content in the gel-fiber probably resulted from phase separation and extraction that occurred between extrusion and actual testing of the gel-fiber [15]. From the concentration difference between the spin dope and the gel-fiber, it can be observed that caprolactam is efficiently separated from the gel-fiber between extrusion and collection with rollers, which means the solvent removal is not an issue for gel spinning of POM. The spin-solvent separation is more significant than that in gel spinning of UHMWPE [33, 34], making this POM process highly potential for continuous production. As predicted previously, the caprolactam content measured by TGA became minimal after extraction in warm water for 30 min, ~0.2% as shown in Figure 4.4, indicating that the

extraction process was sufficient to obtain a POM precursor fiber. The precursor should be almost free of the caprolactam spin-solvent. Morphology of the POM precursor fiber is shown in Figure 4.5(A). Relatively smooth surface can be obtained after extraction of caprolactam with water.

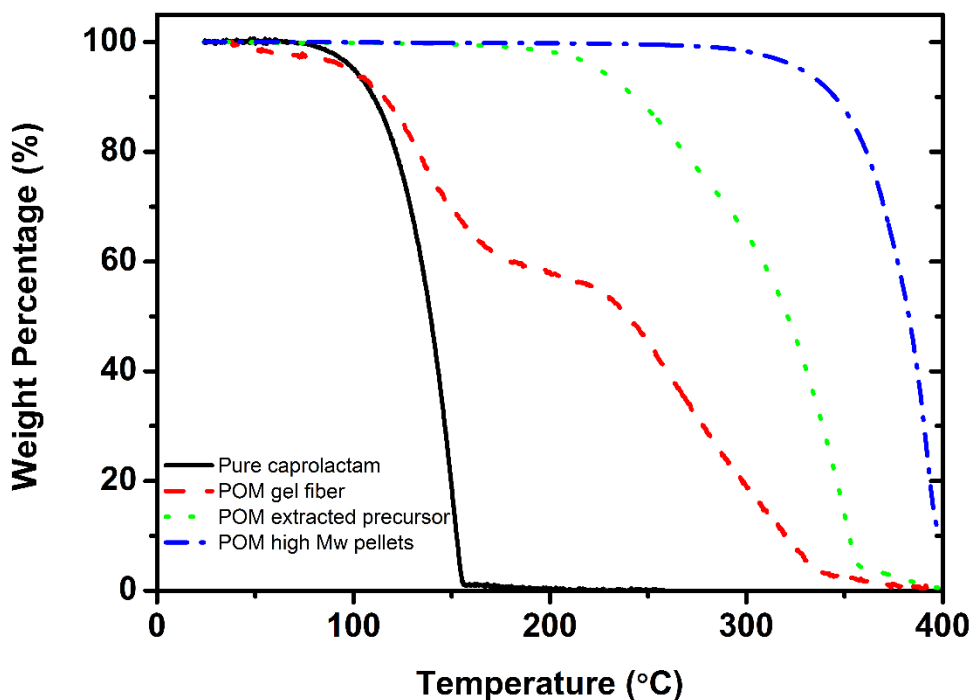


Figure 4.4. TGA curves of POM/caprolactam gel-fiber before and after extraction. TGA of pure caprolactam and neat POM pellets were included for reference. The samples were heated in nitrogen atmosphere to 400°C with rate of 20°C/min.

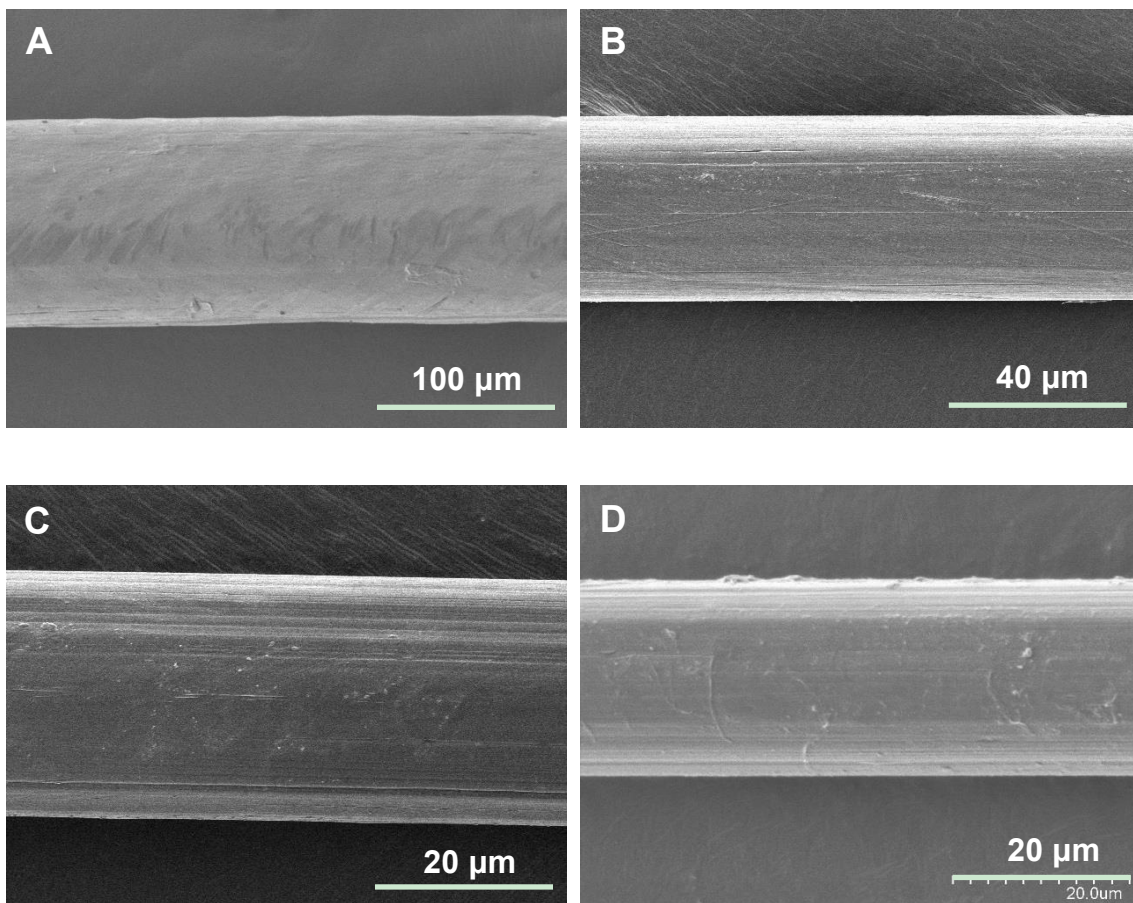


Figure 4.5. SEM images of gel-spun POM fibers at various stages: (A) precursor after fully extraction; (B) 12.5× drawn first stage fiber; (C) 25× drawn second stage fiber; (D) ~40× drawn third stage fiber.

4.3.5 Hot Drawing

As described in the preparation of superstrong UHMWPE and PEO gel-spun fiber, hot drawing is a necessary step to orientate the fibers to reach high strength [19, 32]. Selection of suitable drawing conditions is critical. Significant changes in tensile properties with change of drawing conditions (particularly drawing temperature and

drawing ratio) have been reported for gel-spun PEO and PE fibers. At low temperature, the molecular mobility is limited to achieve high draw ratios, while at too high temperature, the fiber may melt. For hot drawing of POM to obtain oriented products, plenty of studies have been done [7, 35, 36]. However, almost all of them were about orientation of rods or tubes obtained by extrusion or molding from POM melt. No conclusive drawing temperature and drawing rate can be obtained from the previous reports. One useful hint from the previous studies is that the temperature about 30°C below the melting point may be associated with an alpha transition in the crystal, which can be used as a reference for hot drawing [7]. Besides, it can be found a majority of the drawing tests for POM were completed in the temperature range of 108-165°C [36]. Thus, in this study, the POM fibers were subject to a three stage drawing process by utilizing the aforementioned information.

Drawing temperature for the first stage was set to 140°C to allow sufficient molecular mobility to reach high draw ratios. A draw ratio of 12.5× was proved to be stable and robust fibers can be obtained. By comparison, final fiber obtained with several other draw ratios (either smaller or larger) showed decreased tensile properties. Therefore, in this work, the first stage drawing was conducted with a constant draw ratio of 12.5×. With tensile stress induced orientation, the fiber property and structure showed significant changes compared to the precursors. As shown in Figure 4.5(B), the fiber diameter is much smaller after drawing for 12.5 times compared to that of the precursor in Figure 4.5(A). After hot drawing, small wrinkles on the fiber surface were removed. The disappearance of the wrinkle is probably due to the transformation of large-scale shish-kebab structure to small shish-kebabs with a serious deformation due to 12.5× hot

drawing [37]. POM molecules in the kebabs were forced to orientate under strong external drawing and the oriented molecules transformed into secondary shish structures.

WAXD patterns of the precursor and the first stage fiber are shown in Figure 4.6, which can provide more information about orientation of the fiber by drawing. As shown in Figure 4.6 (A), the precursor fiber shows diffractions along the meridian indicating crystalline orientation perpendicular to the fiber axis. The diffraction is similar to that of polyethylene gel fibers spun and extracted with solvents [34]. For the 12.5× drawn first stage fiber, as shown in Figure 4.6 (B), two strong circular spots are present on the equator and four ellipsoid spots are symmetrically distributed in the pattern. The spots on the equator originate from the diffractions of the (100) crystal plane of the POM hexagonal crystals. The corresponding 2θ of the diffraction of (100) is 22.9° . The four ellipsoid spots represent the diffraction of the (105) crystal plane and the corresponding 2θ is 34.6° . One-dimensional X-ray diffraction curve corresponding to the two-dimensional diffraction patterns is shown in Figure 4.7. The relative intensity of the diffraction peaks represent the degree of the order in the material including crystallization and orientation. It can be observed that the diffraction peak at 22.9° is higher, and a new peak appears at $2\theta=34.6^\circ$. The change of intensity indicates crystallization and orientation of POM by hot stretching. The orientation and crystallization can also be validated by DSC thermograms of the precursor and the first stage fiber as shown in Figure 4.1 (B). The peak melting temperature of the 12.5× drawn fiber slightly increases from 173.5 to 180.9°C.

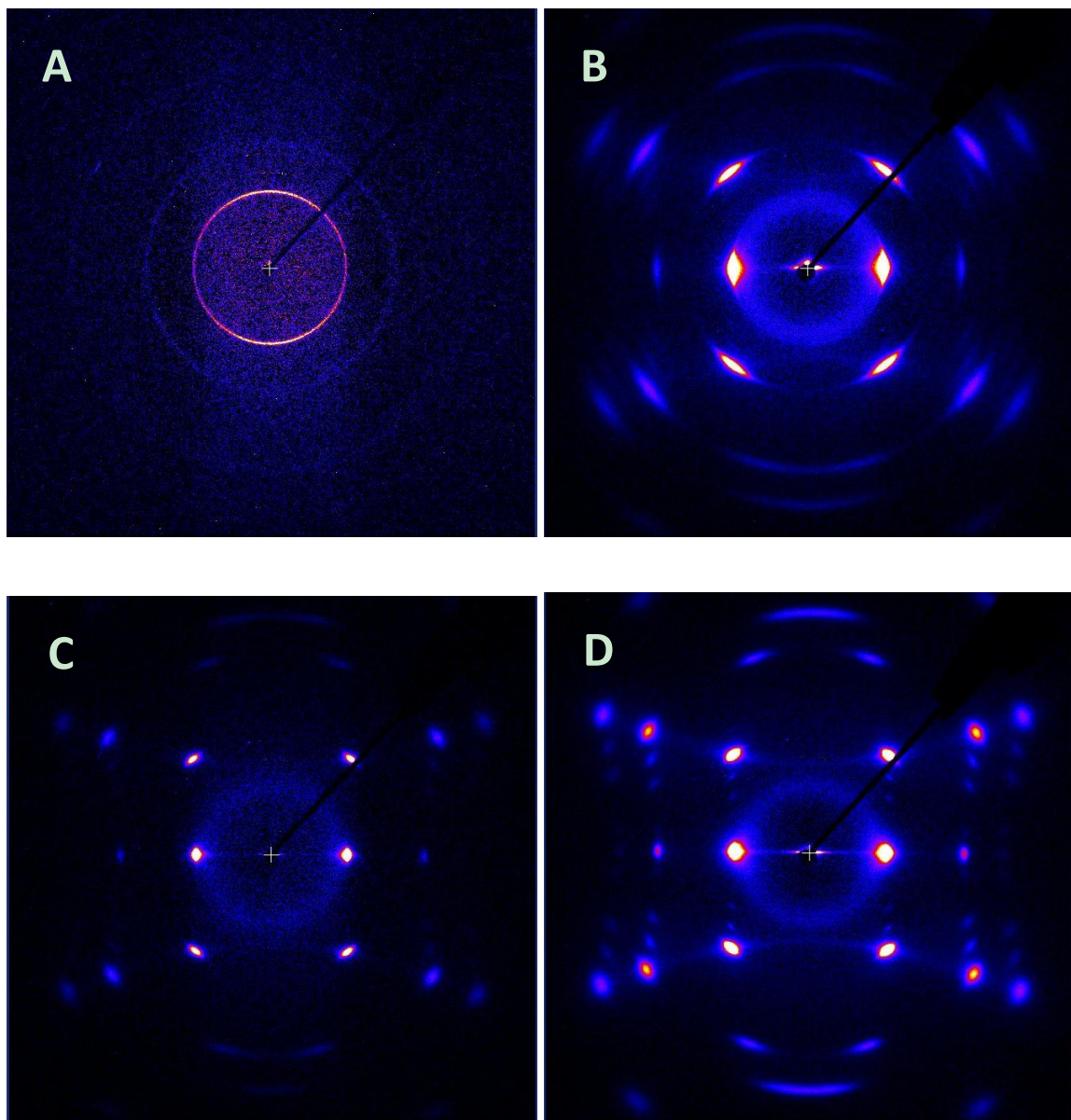


Figure 4.6. WAXD patterns of gel-spun POM fiber at various drawing stages: (A) precursor after solvent extraction; (B) 12.5 \times drawn first stage fiber; (C) 25 \times drawn second stage fiber; (D) ~40 \times drawn third stage fiber.

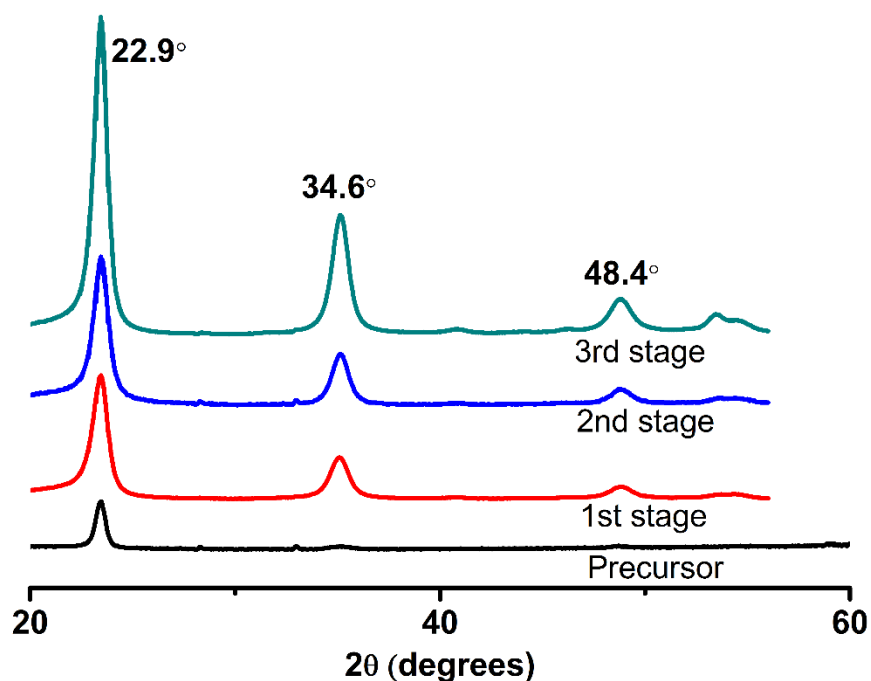


Figure 4.7. WAXD curves of gel-spun POM fibers at various stages

The second stage and the third stage hot drawing were conducted at 150 and 160°C, respectively. The draw ratios were 2 and 1.65, correspondingly. With continuous drawing at each stage, the melting peak of the fibers measured by DSC shifted to a higher temperature as shown in Figure 4.1(B). This indicates increase of crystallinity, which is in consistence with hot drawing of the UHMWPE and PEO [19, 32]. The high-temperature endotherm indicates melting of the highly chain-extended (melting point of 187°C) and the highly oriented crystalline blocks formed by hot drawing [39]. SEM images of the 25× and 40× drawn fiber are shown in Figure 4.5 (C) and (D). It can be observed that smoother surface and smaller size can be obtained by drawing. The

diameter of the final fiber is about 20 μm . WAXD patterns of the POM fibers drawn to 25 \times and 40 \times are shown in Figure 4.6 (C) and (D). It can be observed that highly oriented, crystalline structure was developed with hot drawing. Figure 4.7 shows that in such two drawing stages, the relative intensity of the peak at 48.4° corresponding to the diffraction plane (115) and the peak at 34.6° representing (105) increases fast. It infers crystallization and orientation of the POM fiber should be significantly improved. Meanwhile, it can be observed the diffraction peak positions under different draw ratios had no change, indicating hot drawing did not affect the crystal type.

To quantitatively examine orientation of the fiber during hot drawing, azimuthal integrations of the (100) diffraction at various drawing stages were obtained as shown in Figure 4.8. For hexagonal POM unit cell, the orientation factors at different drawing stages were calculated with Herman's orientation model, as shown in Table 4.1. The orientation factor increases during the drawing stages with a maximum value of 0.875 at 40 \times drawing. It can be found that a majority of the orientation was completed in the first stage, which emphasized the importance of the first stage drawing. It also shows that the mechanical property has potential to be further improved by optimizing the drawing conditions. With a total draw ratio of 40, high tensile strength and high modulus fibers were obtained. Figure 4.9 shows representative tensile stress-strain curves of gel-spun POM fibers. The tensile strength and Young's modulus are 2.01 ± 0.11 GPa and 40.60 ± 0.69 GPa, respectively. The strain at maximum load is about 10%.

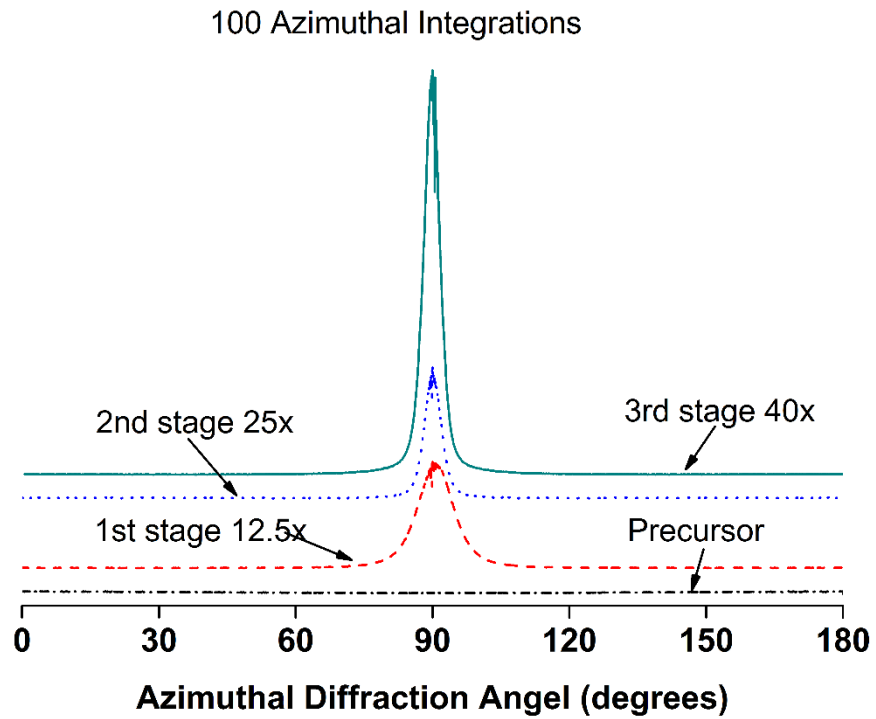


Figure 4.8. Relative intensity of the 100 as a function of the azimuthal diffraction angle for gel-spun POM fibers at various stages

Table 4.1. Orientation factors of POM fibers

Fiber type	Orientation factor
Precursor	-0.2734
1 st stage 12.5×	0.7654
2 nd stage 25×	0.8103
3 rd stage 40×	0.8752

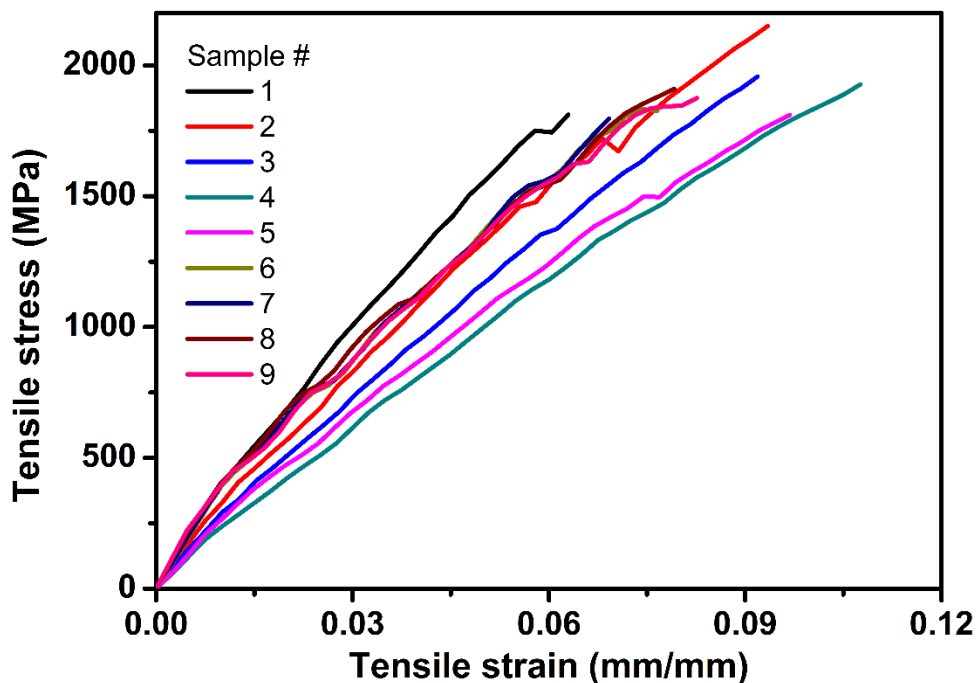


Figure 4.9. Representative stress-strain curves of gel-spun POM fibers with total draw ratio of 40.

Raman spectroscopy was also used to examine the orientation of the POM fibers during hot drawing stages, as shown in Figure 4.10. As is known, POM has two types of crystalline forms: an orthorhombic with a 2/1 helical conformation and a hexagonal unit structure with a 9/5 helical conformation. It can be confirmed from the Raman spectra that the crystalline structure is hexagonal with the peaks at 542 cm^{-1} , 921 cm^{-1} , 1339 cm^{-1} and 1493 cm^{-1} [40]. Meanwhile, the elimination of the peak at 1130 cm^{-1} demonstrates the transformation of noncrystalline region to crystalline region in the first stage of drawing. It can also be observed that the width of the peak becomes narrower and the

intensity of each peak increases, indicating the degree of crystallinity and orientation is higher with progress of hot drawing.

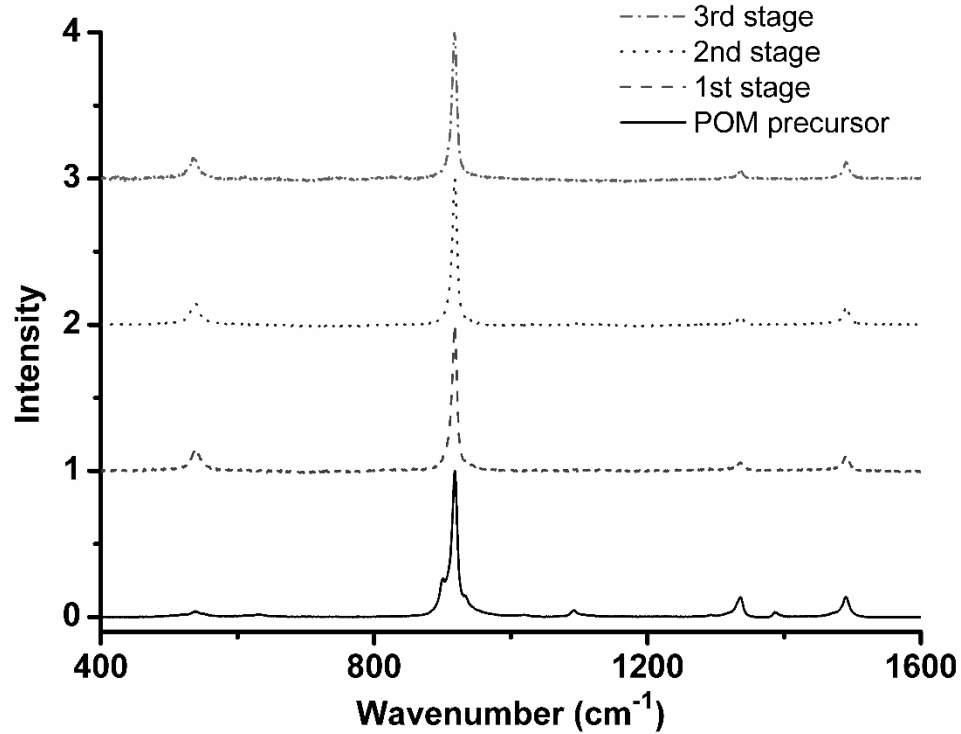


Figure 4.10. Raman spectroscopy of the gel-spun POM fibers at various drawing stages

The oriented fiber may have two types of morphological structure in the crystalline region: extended-chain crystal (ECC) and folded-chain crystal (FCC). The FCCs may be considered as imperfect crystals with stems shorter than ECCs and with folded-chain segments on two opposite sites [39]. Thus, to obtain highly oriented fiber, the ECCs need to be increased. For the gel-spun POM fiber, as observed from SEM image, the shish-kebab structure is a hybrid structure of ECC and FCC [41]. This particular structure is also found for polyethylene, consisting of a pile of lamellar

crystallinities grown around a single polymer crystal with an extended chain structure [42]. However, it is hard to identify the two types of phases of hexagonal from the Raman spectra, as the vibrational spectra of the two crystal structures are identical. Similarly, no significant difference exists between the WAXD patterns of the two crystal structures. DSC of the pellets and the fibers in Figure 4.1 provides a solution for identifying the components of ECC and FCC in the oriented fiber. As the melting point of ECC is 187 °C and the melting point of FCC is 175 °C [39], it can be deduced that the final fiber is mainly composed of ECC. Thus, with combination of WAXD, Raman and DSC, it can be obtained that a major composition of the gel-spun POM fiber is highly oriented extended-chain hexagonal crystal after hot drawing.

4.4 Recommendations and Outlook

A novel gel spinning process for producing strong POM continuous fibers was introduced. The POM gel-spinning process utilized similar techniques to UHMWPE gel-spinning, which enabled efficient fiber spinning and solvent extraction. The concept of “oligomer-polymer” blend system was used to assist determination of an optimal spin-solvent. The spin-solvent selected shared similar repeating units with POM with addition of an amine group to increase stability of POM. Thus, when selecting spin-solvents using the “oligomer-polymer” blend system, addition of other short functional groups can also be considered to improve certain types of properties.

For the gel spinning of POM fibers or films, more work can be done. For example, the processing conditions including extruding temperature, jet stretch ratio and the hot drawing conditions can be optimized to further improve the mechanical properties

of the fiber. The rheological properties and thermal properties of the POM/caprolactam blends can further be investigated to provide guidance for fiber spinning.

4.5 Conclusion

In this work, a gel spinning process for producing high-strength, high-modulus and continuous POM fibers was developed and investigated. Particularly, caprolactam was used as a spin solvent for POM with guidance of the “oligomer-polymer” blend system. The results showed that the POM/caprolactam blend was compatible and had a single melting peak at 144°C. The gelation temperature of the blend was about 147°C, which is consistent with mechanism of the gel formation. Gelation of the blend occurred because of liquid-liquid phase separation resulting from concentration fluctuation. These fluctuations were caused by crystallization of the polymer when the solution was quenched.

A spin dope with 20% POM and 80% caprolactam was used for spinning gel-fibers. After solvent extraction, the gel fibers were hot drawn for three stages in a silicone oil bath. The total draw ratio was about 40. The highly drawn, gel-spun POM fibers showed remarkably high tensile strength and Young’s modulus. Such fibers showed a highly oriented crystalline structure as measured with x-ray diffraction and Raman spectroscopy. All the results indicated that the selected spin solvent (caprolactam) was effective for gel spinning high-performance POM fibers. The “oligomer-polymer” blend system can be used for gel-spinning of other polymers.

4.6 References

1. Kikutani, T., *Formation and structure of high mechanical performance fibers. II. Flexible polymers*. Journal of applied polymer science, 2002. **83**(3): p. 559-571.
2. Tadokoro, H., et al., *Molecular configuration of polyoxymethylene*. Journal of Polymer Science, 1960. **44**(143): p. 266-269.
3. Gezovich, D. and P. Geil, *Deformation of polyoxymethylene by rolling*. Journal of Materials Science, 1971. **6**(6): p. 509-530.
4. KUCHINKA, M., et al., *Effect of structural changes on the sorption properties of polyformaldehyde fibers(Heat stretching-induced changes effect on strength, sorption and structural properties of polyformaldehyde fibers, noting structural orientation enhancement and porosity growth)*. Mekhanika Polimerov, 1971. **7**: p. 1103-1106.
5. Kase, S. and T. Matsuo, *Studies on melt spinning. I. Fundamental equations on the dynamics of melt spinning*. Journal of Polymer Science Part A: General Papers, 1965. **3**(7): p. 2541-2554.
6. Kikutani, T. and H. Okawa, *Polyoxymethylene fiber and method for production thereof*, 2004, U.S. Patent No. 6,818,294.
7. Samon, J.M., et al., *Structure development during the melt spinning of poly (oxymethylene) fiber*. Polymer, 2001. **42**(4): p. 1547-1559.
8. Clark, E. and L. Scott, *Superdrawn crystalline polymers: A new class of high-strength fiber*. Polymer Engineering & Science, 1974. **14**(10): p. 682-686.

9. Nakagawa, K., T. Konaka, and S. Yamakawa, *Production of ultrahigh modulus polyoxymethylene by drawing under dielectric heating*. Polymer, 1985. **26**(1): p. 84-88.
10. Konaka, T., K. Nakagawa, and S. Yamakawa, *Mechanical and physical properties of ultraoriented polyoxymethylene produced by microwave heating drawing*. Polymer, 1985. **26**(3): p. 462-468.
11. Komatsu, T., S. Enoki, and A. Aoshima, *The effects of pressure on drawing polyoxymethylene: 2. Drawn fibre properties and structure*. Polymer, 1991. **32**(11): p. 1988-1993.
12. Komatsu, T., S. Enoki, and A. Aoshima, *The effects of pressure on drawing polyoxymethylene: 1. Processing*. Polymer, 1991. **32**(11): p. 1983-1987.
13. Komatsu, T., S. Enoki, and A. Aoshima, *Effect of pressure on drawing poly(oxymethylene) fibres: 4. Heat shrinkage of annealed superdrawn fibres*. Polymer, 1991. **32**(16): p. 2992-2994.
14. Barham, I.P. and A. Keller, *High-strength polyethylene fibres from solution and gel spinning*. Journal of materials science, 1985. **20**(7): p. 2281-2302.
15. Fang, X., et al., *Gel spinning of UHMWPE fibers with polybutene as a new spin solvent*. Polymer Engineering & Science, 2016.
16. Zhang, X., et al., *Gel spinning of PVA/SWNT composite fiber*. Polymer, 2004. **45**(26): p. 8801-8807.
17. Smith, P. and P.J. Lemstra, *Ultra-high-strength polyethylene filaments by solution spinning/drawing*. Journal of Materials Science, 1980. **15**(2): p. 505-514.

18. Moelter, G.M., *A method of making crimped polyoxymethylene filaments*, 1967, U.S. Patent No. 3,347,969.
19. Zhao, X. and L. Ye, *Structure and properties of highly oriented polyoxymethylene produced by hot stretching*. Materials Science and Engineering: A, 2011. **528**(13): p. 4585-4591.
20. Wyatt, T.P., et al., *Development of a gel spinning process for high-strength poly(ethylene oxide) fibers*. Polymer Engineering & Science, 2014. **54**(12): p. 2839-2847.
21. Wilchinsky, Z.W., *On crystal orientation in polycrystalline materials*. Journal of applied physics, 1959. **30**(5): p. 792-792.
22. Wilchinsky, Z.W., *Determination of orientation of the crystalline and amorphous phases in polyethylene by X-ray diffraction*. Journal of Polymer Science Part A-2: Polymer Physics, 1968. **6**(1): p. 281-288.
23. Hu, Y. and L. Ye, *Study on the Thermal Stabilization Effect of Polyamide on Polyoxymethylene **. Polymer-Plastics Technology and Engineering, 2006. **45**(7): p. 839-844.
24. Gur'yanova, V., et al., *Accelerated degradation of the polyformaldehyde chain on oxidation*. Polymer Science USSR, 1966. **8**(10): p. 1968-1972.
25. Alishoyev, V., et al., *Thermal-oxidative degradation and stabilization of polyformaldehyde*. Polymer Science USSR, 1963. **4**(6): p. 1340-1346.
26. Shi, J., et al., *Investigation on thermo-stabilization effect and nonisothermal degradation kinetics of the new compound additives on polyoxymethylene*. Journal of materials science, 2009. **44**(5): p. 1251-1257.

27. Chiu, H.T. and J.H. Wang, *Characterization of the rheological behavior of UHMWPE gels using parallel plate rheometry*. Journal of applied polymer science, 1998. **70**(5): p. 1009-1016.
28. Fang, X., et al., *Rapid Vacuum Infusion and Curing of Epoxy Composites with a Rubber-Cushioned Mold Design*. Polymer-Plastics Technology and Engineering, 2016(just-accepted).
29. Shi, X., et al., *Gelation/crystallization mechanisms of UHMWPE solutions and structures of ultradrawn gel films*. Polymer journal, 2014. **46**(1): p. 21-35.
30. Kongklang, T., et al., *Electrospun polyoxymethylene: spinning conditions and its consequent nanoporous nanofiber*. Macromolecules, 2008. **41**(13): p. 4746-4752.
31. Kongklang, T., et al., *Electrospinning as a new technique to control the crystal morphology and molecular orientation of polyoxymethylene nanofibers*. Journal of the American Chemical Society, 2008. **130**(46): p. 15460-15466.
32. Smook, J. and J. Pennings, *Influence of draw ratio on morphological and structural changes in hot-drawing of UHMW polyethylene fibres as revealed by DSC*. Colloid and Polymer Science, 1984. **262**(9): p. 712-722.
33. Wyatt, T., et al., *Direct drawing of gel fibers enabled by twist-gel spinning process*. Polymer Engineering & Science, 2015. **55**(6): p. 1389-1395.
34. Xiao, M., et al., *Effect of UHMWPE concentration on the extracting, drawing, and crystallizing properties of gel fibers*. Journal of materials science, 2011. **46**(17): p. 5690-5697.

35. Schweizer, T. and G. Vancso, *The mechanism of orientation in cold-drawn polyoxymethylene as revealed by crystallographic pole figures*. Die Angewandte Makromolekulare Chemie, 1989. **173**(1): p. 85-100.
36. Brew, B. and I. Ward, *Study of the production of ultra-high modulus polyoxymethylene by tensile drawing at high temperatures*. Polymer, 1978. **19**(11): p. 1338-1344.
37. Li, L., et al., *Formation of a large-scale shish-kebab structure of polyoxymethylene in the melt spinning and the crystalline morphology evolution after hot stretching*. Polymers for Advanced Technologies, 2015. **26**(1): p. 77-84.
38. Hoogsteen, W., G. Ten Brinke, and A. Pennings, *The influence of the extraction process and spinning conditions on morphology and ultimate properties of gel-spun polyethylene fibres*. Polymer, 1987. **28**(6): p. 923-928.
39. Kobayashi, M., et al., *Vibrational spectroscopic study on the solid-state phase transition of poly (oxymethylene) single crystals from the orthorhombic to the trigonal phase*. Macromolecules, 1987. **20**(10): p. 2453-2456.
40. Shimomura, M., M. Iguchi, and M. Kobayashi, *Vibrational spectroscopic study on trigonal polyoxymethylene and polyoxymethylene-d 2 crystals*. Polymer, 1988. **29**(2): p. 351-357.
41. Iguchi, M. and I. Murase, *"Shish kebab" structures formed on needle-like polyoxymethylene crystals*. Journal of Polymer Science: Polymer Physics Edition, 1975. **13**(7): p. 1461-1465.

42. Iguchi, M. and Y. Watanabe, *Oriented overgrowth crystallization on needle shaped polyoxymethylene single crystals from molten polymers*. Polymer, 1977. **18**(3): p. 265-268.

5 Conclusions, Recommendations and Outlook

5.1 Conclusions

In this thesis, an ‘oligomer-polymer’ blend system was used to gel spin high performance fibers. Based on this system, new spin solvents and extraction methods were discovered for improving process efficiency and reducing manufacturing cost. Besides, with this system, a new polymer was gel spun to obtain high performance fibers. The major work was covered from chapter 2 to chapter 4. UHMWPE was used as a representative case of high performance fibers to optimize the gel-spinning process. In chapter 2, polybutene was found to be a new spin solvent for UHMWPE, which can significantly improve extraction efficiency and reduce consumption of extraction solvents. The major contribution resulted from strong phase separation of the UHMWPE/PB blend. To further improve the extraction efficiency and reduce consumption of extraction solvents, in the work shown in chapter 3, a mechanical twisting method was developed to remove spin solvents. This was completed by utilizing the strong phase separation behavior of the ‘oligomer-polymer’ blend at ambient temperature. It was demonstrated that as much as 70% spin solvents can be removed with applied twisting while maintaining mechanical properties of the final fiber. Large-size and high-strength UHMWPE fibers were obtained with a developed twist-film gel spinning process. Compared to conventional strong PE fibers, these fibers had noticeable features of diameter about 80 μm and strength of 3.2 GPa, which can be used as fish line and dental floss. Besides addressing the extraction issue of gel spinning, the ‘oligomer-polymer’ blend system was also useful for exploring new polymers that can be gel-spun.

As presented in chapter 4, POM gel-spun fibers were successfully obtained with a selected oligomer caprolactam. Specific results of each of the three chapters are recapitulated as follows.

In chapter 2, a low molecular weight polybutene was used as a new spin solvent for gel spinning of UHMWPE fibers. A 98/2 wt. % UHMWPE/PB gel exhibits a melting temperature about 115°C and shows large-scale phase separation upon cooling the solution to room temperature. The resulting precursor fiber from this gel was hot-drawn to a ratio of 120 yielding a fiber with tensile strength of 4 GPa and Young's modulus of over 150 GPa. Wide-angle x-ray diffraction indicates good molecular orientation along the fiber axis. The results also demonstrate the potential to further improve the mechanical properties. With respect to the gel spinning industry, this new solvent has a number of advantages over paraffin oil and decahydronaphthalene, and holds a promise of greatly improving the process efficiency. Phase diagrams of PE/PB blend and PE/paraffin oil were built based on Flory-Huggins theory to compare phase separation at room temperature. The simulated results were consistent with the experimental data that PE/PB shows stronger phase separation when quenched to room temperature. PB is more effective for improving efficiency and reducing cost in the extraction stage.

In chapter 3, to further improve extraction efficiency and reduce usage of extraction solvents, a novel twist-film gel spinning process was developed for large-size and high performance ultra-high molecular weight polyethylene (UHMWPE) monofilaments. In this process, twisting is demonstrated as an effective way to significantly reduce consumption of extraction solvent by more than 70%. Applying twisting to the gel film makes conventional solvent extraction proceed significantly

faster. Besides solvent extraction efficiency is greatly improved, UHMWPE monofilaments can be obtained with diameter about 80 μm while tensile strength is still over 3.2 GPa, which cannot be completed with conventional processes. Compared to the conventional ones, this process is more efficient and cost-effective for commercialization of high performance and large-size UHMWPE monofilaments. It is expected to promote broad expansion of such monofilaments into various applications.

In chapter 4, a novel gel spinning process was introduced for producing high strength polyoxymethylene (POM) fibers. The POM gel-spinning process was enabled through an oligomer-polymer blend instead of conventional organic solvents, and the gelation properties were investigated. An 80/20 wt. % caprolactam/POM gel exhibited a melting temperature about 145°C and was highly stretchable by hot drawing. Some outstanding features of a gel-spun POM fiber with a draw ratio of 40 are that tensile strength at break is 2.01 ± 0.11 GPa, Young's modulus is 40.60 ± 0.69 GPa. The drawability and tensile strength are significantly improved compared to those previously reported. Wide-Angle X-ray Diffraction and Raman Spectroscopy were used to show high crystallinity and good molecular orientation along the fiber direction. The results also demonstrate that the mechanical properties can be further improved by optimizing the process parameters.

5.2. Recommendations

The following recommendations can be made based on the results of the research work presented in this thesis.

First, it is expected that some other oligomers can be found for gel spinning of UHMWPE fibers based on the ‘oligomer-polymer’ blend system. With such oligomers, the blends may have even stronger phase separation at room temperature. If high extraction rate can also be achieved, such oligomers have high potential to be applied in industry. For gel spinning of polymer fibers, the ultimate goal is to obtain high strength fibers while maintaining low manufacturing cost. The application of ‘oligomer-polymer’ blend system to gel spinning may significantly affect the industry.

Second, some other mechanical methods have potential to be developed for removing spin-solvents, such as compression. A majority of the spin-solvents are trapped in the gel network after phase separation, which can be removed by twisting and squeezing. In this work, twisting was demonstrated as an effective way to remove solvents while maintaining excellent mechanical properties of the fiber. Little work has been completed about compressing the gel to remove solvents. It is possible to develop a new extraction method based on compression, which can make continuous fibers in a simple way.

Third, for the twist-film gel spinning process, the film size and drawing conditions can be further optimized to improve fiber properties. It should have an optimized group of processing parameters. With such parameters, it is highly possible to obtain high-strength fibers in various sizes to meet requirements of increasing applications.

Finally, the gel spinning process for POM fibers should be further investigated so that it can be scaled up for large-scale production. As demonstrated in this work, the tensile strength of gel-spun POM fibers can reach 2 GPa, which is higher than almost all

corresponding data reported on POM fibers. Meanwhile, equipment and procedures of the conventional gel spinning process can be adapted to POM gel spinning. Thus, the method developed in this thesis for gel spinning of POM can likely be scaled up for volume production.

5.3 Outlook

Some future work may be followed after this thesis work to further investigate the ‘oligomer-polymer’ blend system and its application in gel spinning.

First, more work should be completed to study the effect of processing conditions on properties of the final fibers. For UHMWPE fibers obtained with polybutene as the spin solvent, the effect of spin dope concentration and molecular weight of oligomer should be investigated. Besides, in the hot-drawing stages, drawing temperature, draw ratio and extension rate should also be studied to improve orientation of molecular chains. A series of processing parameters can affect fiber properties. Thus, the ultimate goal is to build a model to quantitatively analyze the effect of these parameters.

Second, more theoretical work should be completed to assist in understanding of fundamental mechanism of the ‘oligomer-polymer’ blend system. In this thesis work, a phase diagram for the blend was built based on Flory-Huggins theory to explain strong phase separation behavior at room temperature. Several assumptions were made to simplify the model. In fact, more conditions should be considered in analysis of the blend, such as dependence of the interaction parameter on volume fraction.

Third, theoretical modeling is needed for the solvent removal by the mechanical twisting process. It is demonstrated with experimental results that twisting is an effective way to remove spin solvent. A key parameter that determines the effect of twisting is TPMM (twist per millimeter). An optimized value should be found to remove the maximum amount of solvent while maintaining mechanical property of the final fiber. It is hard to obtain this value with trials. Thus, a model for predicting the TPMM should be built based on the fiber geometry and properties of the spin solvent. With this model, the twisting process can be quantitatively described so that spin-solvent can be removed to the upper limit.

Fourth, the relationship between processing and structure should be further investigated. Particularly, the effect of twisting on WAXD patterns and Raman spectra should be studied. Few reports in the literature can explain the effect of twisting on crystal structure. As shown in chapter 3, a peak with high density is observed in the azimuthal integrations, which is significantly different from that of PE fibers without twisting. It is still not clear how twisting induces this peak and the corresponding crystal structure.

Finally, more work can be done for gel spinning of POM fibers. With the ‘oligomer-polymer’ system, three oligomers were proposed. Experimental results demonstrated that two of them worked and high strength fibers can be obtained. Some other oligomers may also work and fibers with higher tensile strength may be obtained. When selecting oligomers, the stability of the blend should also be considered. For the POM fibers prepared with caprolactam in this work, more work can be done to optimize the hot drawing conditions. For example, drawing ratio and temperature at each stage can

be changed to check the effect on fiber property. The focus of this work was mechanical properties of the fiber at room temperature. In fact, other properties of the gel-spun POM fibers should also be investigated, such as electrical properties, creep and relaxation at elevated temperature and wear resistance.